

**POTENTIAL USE OF CARBON
NANOTUBES AS A NANOFILLER
FOR NATURAL RUBBER LATEX
CONDOMS**

V.C. AGBAKOBA

215161440

2018

**POTENTIAL USE OF CARBON NANOTUBES AS A
NANOFILLER FOR NATURAL RUBBER LATEX
CONDOMS**

By

VICTOR CHIKE AGBAKOBA

**Submitted in fulfilment of the requirements for the degree of *Magister Scientiae* in
the Faculty of Science at the Nelson Mandela University, Port Elizabeth, South Africa**

April 2018


Supervisor: Dr S.P. Hlangothi

Co-supervisor: Assoc. Prof. G. S. Simate

Co-supervisor: Dr C. Yah

DECLARATION

I, Victor Chike Agbakoba (215161440), hereby declare that the research in this dissertation for the award of Magister Scientiae is my original work, and has not been submitted for assessment or completion of any postgraduate qualification in another University.

A handwritten signature in black ink, appearing to read 'Victor Chike Agbakoba', written over a horizontal line.

Victor Chike Agbakoba (Mr)

ACKNOWLEDGEMENTS

I to appreciate the support and contributions of the following people and institutions for the role they played towards the completion of this research study.

- Dr S.P. Hlangothi, for been an astute supervisor and for given me the opportunity to. Thank you for accommodating those countless impromptu meetings and for handling all the inconveniences with a cheerful attitude.
- Assoc. Prof G.S. Simate, for your critical suggestions and resolute personality.
- Dr C. Yah, for always showing great optimism. I really wish to appreciate the energy you brought in towards the execution of this research.
- Sincere gratitude is expressed to CRST and PGRS-Nelson Mandela University for financial support.
- To the Department of Civil Engineering, Belinda van der Wat and Ernest Kaboka, for the access granted me to conduct Flow behaviour studies at the North campus bitumen laboratory section.
- Mr Len Compton for the great job done towards the construction and assembling of the customized latex dipping unit.
- For the team at eNtsa who assisted in assembling a customized latex cutter and dipping tanks.
- Dr James Carson, Dr Rekha Neglur, Dr Eric Hosten, Mr Henk Schalekamp, Ms Pumza Fibi, and Mr Bolo Lukanyo for all the prompt advice and assistance offered.
- To the entire Centre for Rubber Science and Technology (CRST) team, for the invaluable contribution towards the success of this research. Especially my good friends and colleagues, Keith Nare, Phuti Tsipa, Stuart von Berg, Sendibitiyosi Gandidzanwa and Jabulani Gumede, cheers to our friendship and the amazing support you offered.
- To my church family, for the selfless love you showed me. Thanks for the invaluable food-support you showed during the long periods of laboratory works and dissertation writing.
- To my siblings, Azubuike, Obiageli and Nneka Agbakoba, for your immeasurable love and support.

DEDICATION

In the loving memory of my father, Augustine Nnamdi Agbakoba (late), who initiated this journey but never lived to see it.

This research is equally dedicated to every mind that dares to dare, for the love of science and humanity.

SUMMARY

The recent advancement in the field of nano-technology has raised much interest in the area of natural rubber latex (NRL) processing. This interest stems from the exceptional properties of nano-material and the promising results obtained by several researchers. Studies have shown that very low loadings of inorganic nanomaterials such as carbon nanotube (CNT) in NRL matrix leads to enhanced tensile strength, tensile modulus, tear resistance and aberration resistance. Thus providing a great prospect for reinforcement of thin film NRL articles such as condom.

In this research, prevulcanised natural rubber latex (PvNRL) composite blends containing single walled carbon nanotubes (SWCNTs) were prepared via direct mixing. A progressive discolouration of PvNRL was observed with increased loadings of CNTs. Thermal analysis revealed faster drying rates for the composite blends containing SWCNT. Results from equilibrium swelling experiments also suggested a slight increase in crosslink density in the presence of SWCNT.

There was a significant influence on flow behaviour of PvNRL as a result of varying loadings of SWCNT suspension. This was reflected as a change in pseudoplasticity and apparent viscosity. For Instance, apparent viscosity at a shear rate of $1\ s^{-1}$ at 25°C for PvNRL with $\sim 0.08\%$ SWCNT was $2.5\ \text{Pa}\cdot\text{s}$, compared to $0.49\ \text{Pa}\cdot\text{s}$ for the blends with 0.02% SWCNT.

Condoms were moulded via the straight dipping technique using custom made glass formers. A series of dilutions was performed to correct the viscosity differences. This also ensured good consistency and promoted uniform deposition of PvNRL on the glass former. The average dimensions of the condoms produced in terms of length and width were $\sim 191.17 \pm 5.17\ \text{mm}$ and $52.67 \pm 5.17\ \text{mm}$ respectively. Thickness measurement varied slightly according to the method of determination. The water leakage test suggested the absence of holes in the condoms produced. However, results from electrical leakage test contradicted those from water leak test.

The results from infrared spectroscopy (FTIR) did not confirm the presence of chemical interactions between the SWCNT and PvNRL matrix. Glass transition temperature (T_g) was also unaffected across the blends. The stiffness (or modulus) was unaffected in all the condoms, as revealed by results from indentation hardness analysis.

The SWCNT showed no significant influence on thermal decomposition temperatures of the condoms. Nonetheless, images from optical microscopy revealed increased surface roughness corresponding to higher loadings of SWCNT. Results from stress relaxation studies revealed improved retention of modulus under constant strain for condom samples containing SWCNT.

PRESENTATIONS AND COMPETITIONS

2017 March 10th, the Twenty Third National Rubber Conference (Parys, Free State Province.)

Oral Presentation Titled: A study of the Effect of using carbon nanotubes as a nanofiller for natural rubber latex condom:

Part A: Characterization and viscosity study of prevulcanised natural rubber latex

Part B: Electrical pinhole detection on natural rubber latex condom

2017 June 23rd, IOM3 Young Person's Lecture Competition (University of Witwatersrand)

Oral presentation Titled: A study of the flow behaviour of natural rubber latex nanoblends using rotational viscometry and power law equation.

2017 August 16th, Annual Karbochem Student Evening (Port Elizabeth)

Oral Presentation Titled: Potential use of carbon nanotubes as a nanofiller for natural rubber latex condoms.

2017 November 9th, Inaugural Nelson Mandela University 3-Minute Thesis Competition

Oral Presentation Titled: Carbon nanotubes as a nanofiller for natural rubber latex condoms: an exciting prospect!

Final position: First Runner-up in the MSc. Science, Engineering and Technology (SET) Disciplines

WORKSHOPS AND TRAININGS ATTENDED

2017 June 20th, Malvern Instruments Rheology Seminar (Johannesburg)

Content(s): Introduction to viscosity and oscillation
Using rheology to test the stability of a product
Benchmarking products with rheology
Practical demonstration of the Kinexus rheometer.

2016 November, Data Analysis with Excel for Analysts, Scientists and Engineers

Short course offered by InnoVenton, Nelson Mandela University, Port Elizabeth. (Passed with Distinction)

2016 September, 6th Southern African Conference on Rheology. (Pretoria).

Attended as: Student delegate

TABLE OF CONTENT

<u>DECLARATION.....</u>	<u>II</u>
<u>ACKNOWLEDGEMENTS</u>	<u>III</u>
<u>DEDICATION</u>	<u>IV</u>
<u>SUMMARY</u>	<u>V</u>
<u>PRESENTATIONS AND COMPETITIONS</u>	<u>VII</u>
<u>WORKSHOPS AND TRAININGS ATTENDED</u>	<u>VII</u>
<u>TABLE OF CONTENT</u>	<u>IX</u>
<u>LIST OF FIGURES</u>	<u>XIV</u>
<u>LIST OF ABBRIVIATIONS</u>	<u>XVII</u>
<u>CHAPTER ONE.....</u>	<u>1</u>
INTRODUCTION AND LITERATURE REVIEW	1
1.0: INTRODUCTION	2
1.1 Motivation	2
1.2 RESEARCH QUESTIONS	3
1.2.1 Problem statement	3
1.2.2 Hypotheses	3
1.2.3 Key research questions	3
1.2.4 Research Aims and Objectives	3
1.3: REVIEW OF LITERATURES	4
1.3.1: THE MALE CONDOM.....	4
1.3.1.1: A brief History	4
1.3.1.2: Natural rubber latex male condom	4
1.3.1.3: Condoms as prophylactic and contraceptive method	6
1.3.1.4: Condom related problems.....	7
1.3.1.5: Alternatives to natural rubber latex condoms.....	9
1.3.2: NATURAL RUBBER NANOCOMPOSITES	10
1.3.2.1: Brief overview	10

1.3.2.2: Carbon nanotubes (CNT).....	10
1.3.2.3: Synthesis of carbon nanotubes	11
1.3.2.4: Preparation of natural rubber latex/carbon nanotube composite	11
1.3.2.5: Physio-Mechanical properties of NRL/CNT composites.....	12
1.4: RESEARCH RATIONALE	13
1.5: PROJECT SCOPE AND LIMITATIONS.....	14
1.6: DISSERTATION OUTLINE	15
REFERENCES	15
<u>CHAPTER TWO.....</u>	<u>21</u>
A BRIEF BACKGROUND ON MATERIALS AND INSTRUMENTATIONS	21
2.1: CHAPTER OVERVIEW.....	22
2.2: MATERIALS	22
2.2.1: Prevulcanised Natural rubber latex (PvNRL)	22
Table 2.1: specifications of PvNRL according to suppliers	22
2.2.2: Single walled carbon nanotube (SWCNT) suspension	22
Table 2.2: Composition and Properties of the SWCNT suspension	23
2.2.3: Chemicals and solvents	23
2.3: BRIEF BACKGROUND ON INSTRUMENTATIONS.....	23
2.3.1: Mass measurements.....	23
2.3.2: Mixing Set-up.....	23
2.3.3: Ultraviolet-visible spectroscopy (UV-vis) Analysis	24
2.3.4: Fourier-transform infrared spectroscopy (FTIR)	25
2.3.5: Differential scanning calorimetry (DSC) Analysis	26
2.3.6: Dynamic mechanical analysis (DMA)	27
2.3.7: Thermogravimetric analysis (TGA).....	28
2.3.8: Flow behaviour Analysis.....	29
REFERENCES	30
<u>CHAPTER THREE.....</u>	<u>31</u>
SECTION A:	31
PHYSIOCHEMICAL ANALYSIS OF SINGLE-WALL CARBON NANOTUBES/PRE-VULCANISED NATURAL RUBBER LATEX COMPOSITES	31
3.1 INTRODUCTION.....	32

3.2	EXPERIMENTALS	33
3.2.1	Materials	33
3.2.2	ANALYSIS OF TUBALL™ SWCNT SUSPENSION	33
3.2.2.1	Ultraviolet-visible spectroscopy (UV-vis).....	33
3.2.2.2	Fourier-transform infrared spectroscopy (FTIR).....	33
3.2.3	ANALYSIS OF PRE-VULCANISED NATURAL RUBBER LATEX (PvNRL) .	34
3.2.3.1	Sampling and determination of pH of PvNRL	34
3.2.3.2	Determination of total solid content (TSC)	35
3.2.3.3	Determination of dry rubber content (DRC)	35
3.2.4	ANALYSIS OF PvNRL NANO-BLENDS	36
3.2.4.1	Preparation of Blends	36
	Table 3.1: Description of the four Nano-blends.....	36
3.2.4.2	Thermogravimetric Analysis (TGA)	37
3.2.4.3	Determination of swelling ratio and crosslink density	37
3.3	RESULTS AND DISCUSSION.....	39
3.3.1	UV-vis analysis of TUBALL™ SWCNT suspension.....	39
3.3.2	ATR-FTIR analysis of TUBALL™ SWCNT suspension.....	40
3.3.3:	Analysis of the concentration of PvNRL.....	42
3.3.4:	TGA analysis of PvNRL and SWCNT reinforced PvNRL.....	42
3.3.5:	Effect of SWCNT suspension on swelling index and crosslink density of PvNRL films	45
	Table 3.2: Swelling index, Gel and Sol content	46
3.4	SUMMARY OF OBSERVATIONS	47
	REFERENCES	47
	SECTION B:.....	52
	FLOW BEHAVIOUR OF PRE-VULCANISED NATURAL RUBBER LATEX AND ITS NANO-BLENDS USING ROTATIONAL VISCOMETRY AND POWER LAW MODEL	52
3.5:	INTRODUCTION.....	53
3.6:	EXPERIMENTAL	54
3.6.1:	Materials and sample preparation.....	54
3.6.2:	Flow behaviour measurements	55
3.6.3:	Power law model.....	57
3.7:	RESULTS AND DISCUSSION.....	58

3.7.1: Effect of shear rate and Temperature on viscosity of PvNRL	58
3.7.2: Effect of TUBALL™ SWCNTs suspension on viscosity of PvNRL	60
3.7.3: Effect of low shear rates on the flow behaviour of PvNRL and its nanoblends	65
3.7.4 Fitting the power law model for viscosity measurements at 25°C	66
Table 3.3: A summary of the fitting parameters of the power law model for Pv-NRL and its nano-blends.....	68
3.8: SUMMARY OF OBSERVATIONS	69
REFERENCES	69
SECTION C:.....	72
SINGLE WALLED CARBON NANOTUBES REINFORCED MALE LATEX	
CONDOMS: PRODUCTION AND DETERMINATION OF DIMENSIONS.....	
3.9: INTRODUCTION.....	73
3.10: EXPERIMENTAL	74
3.10.1: List of chemicals.....	74
3.10.2: Formulation of blends.....	74
Table 3.4: Specifications of Blend Formulation.....	75
3.10.3: Dilutions	75
3.10.4: Moulding	77
3.10.5: Vulcanisation, leaching and stripping	78
3.10.6: Determination of length and width.....	80
3.10.7: Determination of thickness.....	80
3.10.7.1: Comparison of results from thickness measurements	82
3.11: SUMMARY OF OBSERVATIONS	84
REFERENCES	84
SECTION D.....	87
PHYSIOMECHANICAL ANALYSIS OF SINGLE WALLED CARBON NANOTUBES	
REINFORCED MALE LATEX CONDOMS	
3.12: INTRODUCTION.....	88
3.13: EXPERIMENTAL	89
3.13.1: Condom production and description.	89
Table 3.5: Description of condoms	90
3.13.2: Fourier-transform infrared spectroscopy (FTIR).....	90
3.13.3: Differential scanning calorimetry (DSC)	90
3.13.4: Thermogravimetric analysis (TGA)	91

3.13.5: Testing for holes	91
3.13.5.1: Water Leak test	91
3.13.5.2: Electrical test	91
Table 3.6: Calibration table	93
3.13.6: Optical microscopy	94
3.13.7: Hardness test.....	94
3.13.8: Stress relaxation analysis.....	94
3.13.8.1: Sampling	94
3.13.8.1: Test method	95
3.14: RESULTS AND DISCUSSION	95
3.14.1: ATR-FTIR analysis of PvNRL and Pv-NB condoms	95
3.14.2: Effect of SWCNT on thermal stability	97
3.14.3: Effect of SWCNT on the calorimetric glass transition temperature (T_g)	98
3.14.4: Surface morphology of MLC films	100
3.14.5: Effect of SWCNT on the occurrence of holes.....	100
Table 3.7: Table showing results of the water leak and electric tests	101
3.14.6: Effect of SWCNT on Shore A hardness.....	102
Table 3.8: Result from Shore A hardness analysis.....	102
3.14.7: Stress relaxation analysis of PvNRL and Pv-NB condoms.....	103
Table 3.9: Results from Stress Relaxation analysis of PvNRL and Pv-NB condoms under a 25% constant strain.....	105
3.15: SUMMARY OF OBSERVATIONS	106
REFERENCES	106
<u>CHAPTER FOUR</u>	110
OVERALL SUMMARY AND RECOMMENDED FUTURE WORK	110
SECTION A:	111
SECTION B:.....	111
SECTION C:.....	112
SECTION D:	113
RECOMMENDED FUTURE WORKS	114

LIST OF FIGURES

Figure 1.1: general chemical structure of natural rubber (showing cis-1,4-poly(isoprene) configuration) ^[13]	5
Figure 1.2: behavioural indicators amongst women aged 15-44 years in south africa. (a.) ≥ 2 partners within 12 months, (b.) Used a condom and (c.) Tested for hiv within 12 months. ^[22]	7
Figure 1.3: a schematic showing open-ended single-walled carbon nanotube (SWCNT) and multi-walled carbon nanotube (MWCNT).	10
Figure 2.1: a schematic showing the dimensions of the gate-impeller design spindle. (dimensions included).	24
Figure 2.2: schematic of a typical dual beam spectrophotometer. ^{[2] [3]}	25
Figure 2.3: schematic of a multiple reflection atr system ^[4]	26
Figure 2.4: a schematic of a typical heat flux dsc cell: (s) sample pan, (r) reference pan, (δt) thermocouple system. ^[5]	27
Figure 2.5: a schematic of film tension analysis set-up for q800 showing a combined motor and transducer; (a) mounted sample. (b) displacement sensor and (c) force motor. ^[6]	28
Figure 2.6: schematic of a typical sdt: (a) thermobalance, (b) sample holder. ^[7]	29
Figure 2.7: (a) a typical schematic of the concentric cylinder measuring system (cc-ms), (b) cross-sectional view of the of cc-ms showing t narrow shear gap. ^[8]	29
Figure 3.1: evolution of UV-vis spectra of 0.1 wt% tuball™ SWCNT suspension: the suspension was diluted 1000 (solid line) and 500 times (dashed lines).	40
Figure 3.2: ATR-FTIR spectra of nacmc (a), tuball™ SWCNT suspension (b), d-tuball™ SWCNT (c) and p-tuball™ SWCNT (d).	41
Figure 3.3: bar graphs showing the average total solid content (tsc) and dry rubber content (drc) of PvNRL.	42
Figure 3.4: tga (solid line) and dta (dashed line) curves showing the evaporation of the volatile components of PvNRL.	43
Figure 3.5: plots of the drying behaviour of pvnrl containing varying loadings of tuball™ swent: (a) comparison of TGA curves, (b) comparison of DTG curves.	44
Figure 3.6: plot showing the comparison of crosslink density.	46
Figure 3.7: viscosity versus shear rate of PvNRL at 25 and 35°c showing the overlay of run1 and run2.....	56

Figure 3.8: plot showing the relationship between shear stress and apparent viscosity of pvnrl under varying shear rates.	56
Figure 3.9: an idealised flow curve showing the power law region, zero shear and infinite shear viscosity regions; adopted from the article “malvern instruments ltd” ^[17]	57
Figure 3.1.1: viscosity versus shear rate of PvNRL at 25, 30 and 35°C showing shear thinning behaviour.....	59
Figure 3.1.2: plot of viscosity versus shear rate at 25°C of pvnrl, tuball™ SWCNT and the four nanoblends.	60
Figure 3.1.3: chemical structure of sodium carboxymethyl cellulose showing 1 degree of substitution ^[21]	61
Figure 3.1.4: a schematic showing proposed interaction between surfactant (NaCMC) stabilized SWCNT and a solvated rubber particle (note that sizes are exaggerated for clarity). 62	
Figure 3.1.5: viscosity versus shear rate at 25, 30 and 35°C showing shear thinning behaviour. A) pv-nb/1, b) pv-nb/2, c) pv-nb/3 and d) pv-nb/4.....	64
Figure 3.1.6: viscosity versus shear rate 25°C showing the flow behaviour of pvnrl and the various nano-blends at low shear rates;.....	65
Figure 3.1.7: shear stress [pa/s] versus shear rate [1/s] of pvnrl and the four nano-blends at 25°C. The red-line shows the fitting of the power law model.	67
Figure 3.1.8: interpretation of consistency (k) versus power law index (n) for all the samples studied. 68	
Figure 3.1.9: image showing the discolouration of pvnrl with increasing loadings of swcnt suspension: (a). PvNRL, (b) pv-nb/1 (c) pv-nb/2, (d) pv-nb/3, (e) pv-nb/4	75
Figure 3.1.1.1: image showing the effect of dilution on viscosity. From left to right: pvnrl, pv-nb/1, pv-nb/2, pv-nb/3 and pv-nb/4.....	76
Figure 3.1.1.2: dipping set-up: (a) glass former, (b) former attachment, (c) wooden guide, (d) hollow steel pipe, (e) dipping chamber, (f) water jacket.	78
Figure 3.1.1.3: schematic showing various production steps; (1) vulcanisation, (2) leaching, (3) drying (4) dry stripping.....	79
Figure 3.1.1.4: samples of mlc produced using the different latex blends. From left to right: pvnrl, pv-nb/1, pv-nb/2, PvNB/3 and PvNB/4.	80
Figure 3.1.1.5: materials for thickness determination. (a) vernier caliper (inside jaws), (b) rectangular test-specimens, (c) anvil (micrometre), (d) spindle and (e) ratchet.....	82
Figure 3.1.1.6: a plot of method versus average thickness.	83

Figure 3.1.1.7: electrical conductivity set-up: (a) condom support, (b) condom filled with electrolyte, (c) electrode, (d) trough with electrolyte, (e) electrode, (f) 10 k ω resistor, (g) 10 v constant dc supply.....	92
Figure 3.1.1.8: condom sampling description: (a) the area 25 \pm 5 mm away from the open end, (b) mid-region, (c) the area 25 \pm 5 mm away from the closed tip, (d) overall condom length \sim 191.2 \pm 5.2 mm.....	95
Figure 3.1.1.9: FTIR spectra of PvNRL and PvNB condoms: (a.) PvNRL condom, (b.) PvNB1 condom, (c.) PvNB2 condom, (d.) PvNB3 condom, and (e.) PvNB2 condom.	96
Figure 3.1.1.1.1: (a) TGA and (b) DTA plots of PvNRL and Pv-NB condoms: (1) onset temperature, (2) and (3) two staged decomposition of the rubber matrix, (3) complete decomposition.....	98
Figure 3.1.1.1.2: DSC thermograms showing the glass transition of PvNRL and Pv-NB condoms: (a) rigid and glassy region, (b) glass transition region, (c) and (d) soft rubbery region.	99
Figure 3.1.1.1.3: optical micrographs of condoms specimens at 6.5 \times magnification; (a) PvNRL condom, (b) PvNB1 condom, (c) pvnb2 condom, (d) Pv-NB3 condom, and (e) PvNB2 condom.	101
Figure 3.1.1.1.4: (a) stress relaxation behaviour of PvNRL condoms over 30 minutes of constant 25% strain, with error bars; (b) plot truncated in the y-axis to show min and max relaxation modulus.	103
Figure 3.1.1.1.5: (a) an overlay of the stress relaxation analysis of PvNRL and Pv-NB condoms; (b) insert shows a truncated y-axis of the plot.....	104

LIST OF ABBRIVIATIONS

STDs	Sexually transmittable diseases
HIV	Human immunodeficiency virus
CNTs	Carbon nanotubes
SWCNT	Single-walled carbon nanotubes
MWCNT	Multi-walled carbon nanotubes
NRL	Natural rubber latex
PvNRL	Prevulcanised natural rubber latex
Pv-NB	Prevulcanised rubber containing varying amount of SWCNT
CVD	Carbon vapour deposition
CCVD	Catalytic carbon vapour deposition
HPV	Human papillomavirus
USAID	United States Agency for International Development
MSM	Men having sex with men
MLC	Male latex condoms
USFDA	United States food and drugs administration
HLB	Hydrophile-Lyphophlye Balance
VDW	Van der Waals
UV-vis	Ultraviolet-visible
ATR-FTIR	Attenuated Total Reflectance Fourier-transform infrared
DSC	Differential scanning calorimeter
DMA	Dynamic mechanical analyser
TGA	Thermogravimetric analyser
DTG	Derivative thermogravimetric

SDT analyser	Simultaneous differential scanning calorimeter and thermogravimetric analyser
MCR	Modular compact Rheometer
CC-MS	Concentric cylinder measuring system
DRC	Dry rubber content
TSC	Total solid contents
NaCMC	Sodium carboxymethyl cellulose
XLD	Crosslink density
VFA	Volatile fatty acids
EDL	Electrical double layer
MMSG	Micrometer screw guage
VCp	Vernier caliper
Fmlr	Formula for calculating volume of a rectangle
ANOVA	Analysis of variance
ISO	International standards organization
ASTM	American society for testing and materials
SANS	South African national standards
RQTS	Rheological quality test systems
T _g	Glass transition temperature
Δc _p	Heat capacity change at constant pressure

CHAPTER ONE

INTRODUCTION AND LITERATURE REVIEW

1.0: INTRODUCTION

1.1 Motivation

Physical barrier materials such as latex condoms play a major role in curtailing the spread of most sexually transmittable diseases (STDs) including the human immunodeficiency virus (HIV) and also as serves as a form of contraception as they are able to prevent exchange of coital fluids^{[1] [2]}. Studies has shown that the consistent and correct use of condoms is known to offer more than 85% risk reduction of HIV^{[1] [2]}.

Currently, most male condoms are made from natural rubber latex (NRL)^[3]; which are relatively easy to use and serves as a good physical barrier^{[1] [2] [3]}. However, the decrease in strength at maximum stretch, low lubricity, poor heat transfer characteristics, and deleterious effects of oil based lubricants and oxidation are amongst the greatest shortcomings^{[1] [3]}. Some of the alternatives includes synthetic and lambskin condoms amongst others^[1]. Nevertheless, literature have reported higher failure rates for some synthetic condoms in comparison to their NR-latex counterparts^[4]. Whereas, lambskin condoms are known to be permeable due to larger pore sizes^[4].

Interestingly, the “rediscovery” of carbon nanotubes (CNTs) by Iijima^[5] presents a new unique material. The CNTs as nanofillers are currently known to improve the properties of NR and other polymer materials due to their excellent flexibility, low density, high thermal and electrical conductivity, modulus and large aspect ratio^[6]. The CNTs can be single, double or multi-walled long cylindrical graphene sheets containing sp^2 - hybridized carbon atoms and are often synthesized through one of these techniques; electrical arc discharge method, laser ablation and carbon vapour deposition (CVD)^{[6] [7]}.

However, not much has been reported to show specifically the impact of CNTs on male NRL condoms. Consequently, the approach of this study was designed to elucidate the consequence of the incorporation of CNTs on the pre- and post-production processes of male NRL condoms. In this regard, several physio-chemical and mechanical analysis techniques were adopted and executed. The overall aim of this study is to determine the potential reinforcement of male NRL condoms using CNT. It is envisaged that the resulting NRL/CNT condoms would show superior physical, chemical and mechanical properties

1.2 RESEARCH QUESTIONS

1.2.1 Problem statement

A review of literature shows that single walled carbon nanotubes (SWCNTs) as a reinforcing filler can be used to improve the physio-mechanical properties of thin-film articles such as male natural rubber latex condoms. Nonetheless, functionalised SWCNTs is required towards ensuring adequate dispersibility in prevulcanised natural rubber latex (PvNRL) and promote polymer-filler interactions.

1.2.2 Hypotheses

- The incorporation of SWCNT into NRL would reinforce NRL condoms and result in significant of physio-mechanical properties.

1.2.3 Key research questions

- Can reinforcement of NRL be achieve at low loadings of functionalised SWCNT?
- To what extent would SWCNT modify the flow behaviour of natural rubber latex?
- Will the incorporation of SWCNT into NRL affect the condom production?
- How will the physio-mechanical properties of SWCNT-reinforced NRL condoms compare to that of non-reinforced condoms?

1.2.4 Research Aims and Objectives

The overall research aim is to;

- To study the potential reinforcement of NRL using SWCNT, in a bid to fabricate NRL-latex condoms with superior mechanical integrity.

The research objectives are therefore as outlined below:

- Analyse the physio-chemical characteristics of SWCNT/NRL composite blends.
- Investigated the effect of varying loadings of SWCNT on the flow behaviour of PvNRL.
- Design and execute laboratory scale condom production process.
- Perform Analysis on the physio-mechanical characteristics of SWCNT/NRL composite condoms and compare them to condoms without SWCNT.

1.3: REVIEW OF LITERATURES

1.3.1: THE MALE CONDOM

1.3.1.1: A brief History

The male condom can be defined as any sheath of material donned over a male sex organ to prevent the exchange of coital fluids^[1]. The history of male condoms can be traced as far back as the 1350 BC Egypt where an art murals was found to depict a sort of barrier material used to cover the tip of the penis^[8]. Animal tissues are thought to have been used during the medieval times^[9] ^[2]. A Popular legend suggest that the name “condom” was a corruption of the name “Quondam”. The reason behind this legend is, a British army physician named Colonel Quondam once prescribed gut condoms to King Charles 1 (1660-1685) as a contraceptive tool^[10]. However, the word “condom” have been reported to have only appeared first in a poem written by Lord Belhaven around 1706^[10].

The Italian anatomist and syphilis expert, Fallopius is credited with the first written description of condom as presented in his book titled *De morbo gallico*^[8]. Fallopius’s condom featured a linen sheath used to cover the head of the penis to prevent syphilis infection^[8]. Condoms use towards contraceptive purpose only picked-up towards the end of the 18th century England. This era saw the famous Giacomo Casanova referred to condoms as “The English riding coat”, “assurance caps” and preservative sheaths” in his autobiography titled *Histoire de ma vie* (story of my life)^[8] ^[2].

1.3.1.2: Natural rubber latex male condom

The male natural rubber latex (NRL) condom is a hollow-cylindrical thin film material that is open ended on one side and closed on the other. The primary raw material used in the production NRL condoms is the complex colloidal dispersion of naturally occurring rubber particles in aqueous serum; which is composed of mainly cis-1,4-polyisoprene polymer chains (Figure 1.1). Commercial quantities of NRL is mainly obtained from the sap of *Hevea brasiliensis* tree^[11]. Dried NRL films on its own exhibits poor tensile properties, thus, it requires some form of chemical modification, to effect drastic improvements in the physical and mechanical properties^[11] ^[12].

The modification of NRL follows a process referred to as vulcanisation, which involves the formation of chemically crosslinks between long hydrocarbon chains^[14]. The advent of the sulphur vulcanisation of natural rubber latex (NRL) by Charles Goodyear and Thomas

Hancock in 1843-1844 provided a major shift in the production and quality of condoms^[2]^[9]. Till this day, sulphur vulcanisation still remains the most prominent way of converting NRL into durable products^[12].

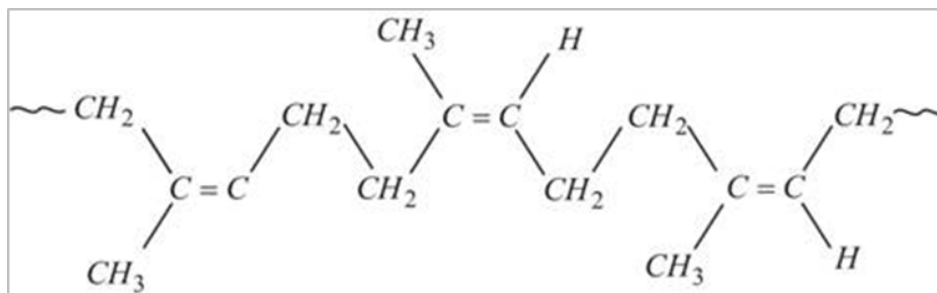


Figure 1.1: *General chemical structure of natural rubber (showing cis-1,4-poly(isoprene) configuration)^[13].*

The exact history of NRL condoms is unclear but has been speculated to date as far back as 1876^[9]. Earlier designs of NRL condoms featured a seam running its entire length, however, seamless condoms became popular towards the late 19th century^[9]. Goodyear received a U.S. patent for the production of hollow rubber articles in the year 1848, Hancock on the other hand was awarded a British patent in the same year for the production of glass mould used with the crystalline percha-latex^[9].

The male NRL condoms were initially made by dipping a suitable mould into solvent dissolved NRL, which is subsequently vulcanised via exposure to sulphur dioxide^[9]. Alexander patented this method of treating rubber using sulphur dioxide in 1846^[9]. This early dipping process was not feasible because it was time-consuming and the solvents used posed a constant fire hazard due to their high flammability^[9]. The modern design and production process of NRL condoms is still based on the techniques developed during the late 18th century^{[11][2]}.

Presently, an optimised combination of chemical additives such as sulphur, accelerators and activators are used to hasten the rate of the vulcanisation^[12]. NRL condoms are commonly moulded via the vertical dipping process; which involves immersion and slow withdrawal of a solid mould/former into a trough filled with pre-vulcanised natural rubber latex (PvNRL)^{[12][11][15]}. Nevertheless, these modern methods require a high level of skill and the quality of the finished product is highly dependent on process variables^{[15][16]}. The present global production capacity is estimated to be ~15 billion units/year^[17].

1.3.1.3: Condoms as prophylactic and contraceptive method

When used as a prophylactic, quality condoms are impermeable to numerous microorganisms including the HIV virus^{[18][19]}. Studies on condom use amongst sero-discordant relationships (where one partner is HIV-positive) suggested that the HIV-negative partners were 80% less likely to become infected compared to couples who do not use condoms in similar relationship settings^[20].

Increase in Condom use has been linked to observed decline in the new cases of HIV as seen in South Africa between 2002 and 2008, recording about 34% decline in new HIV infections^{[1][19][21]}. In contrast, the recent report released by the Human Sciences Research Council (HSRC) of South Africa in 2014 showed an increase in people living with HIV/AIDS from an estimated 5.2 million (10.6%) in 2008 to about 6.4 million (12.2%) in 2012^[21]. The 2012 report by HSRC sights notable increase in risky behaviours which included decline in condom use^[21]. Figure 1.2 shows the behavioural trend between amongst a group of South African women from a survey conducted by Rehle *et al*^[22].

Another great example attribute to successful condom use was as recorded in Thailand between 1989 until 1994^[1]. The fight against the spread of STDs saw a decline from over 400,000 known cases in 1987 to ~29,000 cases in 1994^[1]. Wald *et al* reported in a 2005 article, that consistent condom use can cut the risk of contracting genital herpes by half^[23]. However, herpes infection rarely show any symptoms^[23], thus it is quite problematic to really conclude about condom effectiveness in preventing the spread of genital herpes.

Epidemiological studies on the role of condoms in preventing sexually transmitted infections (STIs) has shown that its overall effectiveness as a barrier varies with the type of infection^[19]. For example, the condom fact sheet^[19] released by the U.S Agency for International Development (USAID) in 2015 claimed that condoms can offer about 71% protection for gonorrhoea, 75% for Chlamydia and about 66% for syphilis^{[24][25]}. Research has shown that transmission of human papillomavirus (HPV) can be considerably curtailed through proper condom use^[26].

Condoms are so far the only reversible male contraceptive method that are available. Male condoms have been reported to be as high as 87% effective for pregnancy control. However, one underlining factor for success is the consistent correct use and condom quality. Studies on the effectiveness of male latex condoms as a contraceptive have been published^{[2][27][4]}.

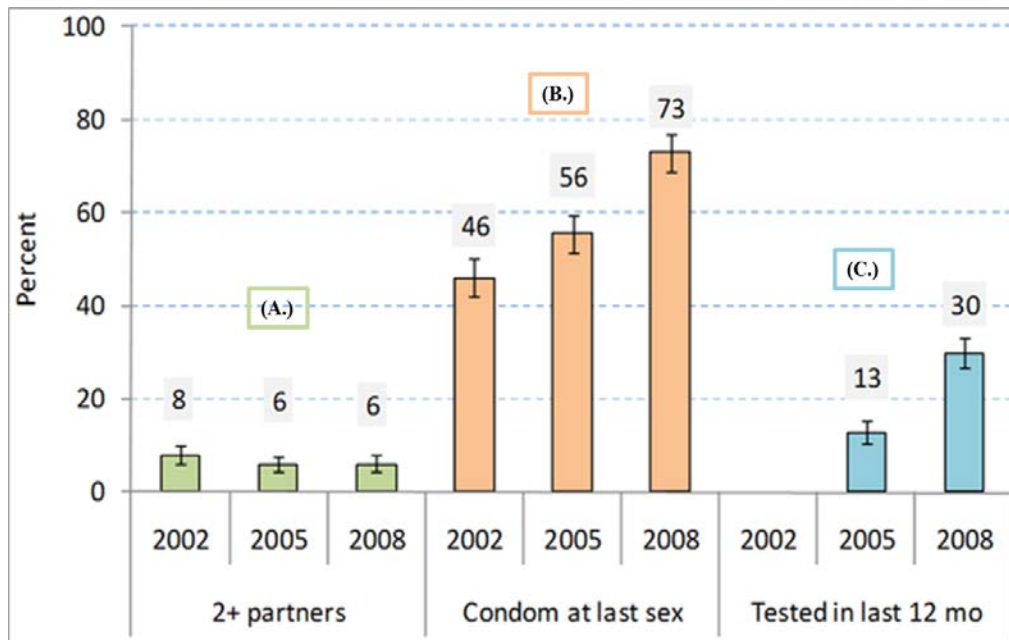


Figure 1.2: Behavioural indicators amongst women aged 15-44 years in South Africa. (A.) ≥ 2 partners within 12 months, (B.) Used a condom and (C.) Tested for HIV within 12 months.^[22]

1.3.1.4: Condom related problems

The frequency of condom related problems amounting to slippages and breakages during use vary amongst various available reports and is often associated with user errors and less often to material failure^{[28] [29]}. However, there are limited research and published papers that addresses the mechanism of condom breakages. This is mainly because such catastrophic failures of condoms are quite rare or go unreported. The failure rate associated with breakage of NRL condoms during use is typically reported as 0.1 – 0.2%^{[30] [31]}, and 0.6 – 6% for synthetic condoms^{[30] [31]}.

The report by White *et al*^[32] proposed a mechanism that could explain condom failure in the absence of user error. The study identified distensions around the holes present in failed polyurethane condoms. White *et al*^[32] concluded that the repeated, progressive and localized straining of the condom film resulted in it rupturing.

The result from Reece *et al* investigation on condom sizing, revealed that the failure rate of well-fitted condoms (0.7%) were significantly less than those of standard-sized condoms (1.4%)^[33]. Bekinska *et al*^[34] reported about 41% men and 37% women experienced condom failure in a study conducted at some STI clinics in South Africa. In a similar study by Goodall *et al*^[35] through a Scottish male condom postal distributing scheme reported that 27% experienced breakage and 40% slippage. Pickles *et al*^[36] reported about 16.7% condom

breakage in their study amongst female sex workers and Men having sex with men (MSM) in India. A higher failure pattern has been reported amongst adolescents and inexperienced users^[37].

Slightly higher failure rates have been reported for anogenital coital activities compared to vaginal^[38]. At some point, a few European countries had adopted thicker (stronger) condoms for anogenital coitus. However, the decision was based on the assumption that anogenital intercourse involved “greater friction”^[39]. Golombok *et al*^[40] argued that there is no correlation between failure rate and condom thickness amongst MSM. The same study also identified several risk factors leading to the incidence of condom breakage, some of which include, longer duration of coitus, inappropriate lubricant, tightly fitted condoms and inadequate lubrication^[40]. However, Extra lubrication has been suggested for anogenital coitus^{[19] [35] [40]}. Choice of lubrication is paramount in ensuring NRL condom effectiveness^[1]. Water and silicon based lubricants are known to be suitable lubricants.

Reports have revealed that saliva increases the rate of breakage, low molecular weight oils are also known to quickly compromise the mechanical integrity of NR-latex condoms as a result of excessive swelling of the rubber matrix^{[1] [3]}. Smith *et al*^[41] reported that the site of lubricant application contributes to condom failure. On contrary, the results from Das *et al*^[3] investigation contradicts these findings. Gabby & Gibbs^[42] reported no correlation between excess application of lubricants and condom failure. Nevertheless, the significant swelling action by any lubricant would most likely result to a rapid stress relaxation in the rubber matrix of condoms; and as a result, it would lead to loss of seal pressure which could lead to a higher chance of breakage and slippage^[3].

A growing number of the global population are allergic to NRL. Literature suggests that latex allergy is caused by the naturally occurring proteins dissolved in the latex serum or adsorbed onto rubber particles^[43]. According to Meade *et al*^[43] there are over 100 types of proteins in NRL, of which only a few with allergens have been identified. Reports on the removal of proteins from latex have been published^[44]. However, removal of proteins is detrimental to the overall latex colloidal stability. Meade *et al*^[43] report stated that the United States food and drugs administration (USFDA) registered over a 1000 cases allergic reactions to latex products and about 15 deaths resulting from protein-induced anaphylaxis between 1989 and 1992. Several chemicals used during the processing and manufacturing of NRL articles have been identified as potential allergens^[43].

1.3.1.5: Alternatives to natural rubber latex condoms

Technological advancements in the latex industry has resulted in the production of condoms from synthetic lattices. These condoms are often claimed to be stronger and better than NRL condoms. Some of the advantages often raised are; tasteless, odourless, allow more sensitivity, durable and free from allergens. Examples the synthetic condoms includes; the polyvinyl (plastic) polyurethane condoms^[45] and synthetic elastomers condoms. Several comparison studies between natural latex and synthetic condoms have been reported^[28] ^[46] ^[30].

Porter and Villemeur^[30] reported a similar clinical failure rate between high-quality latex condoms and a brand of polyurethane condoms. This was similar to observations reported by Callahan *et al*^[31], in a study that compared slippage and breakage rates between 3 different types of Tactylon™ polyurethane condoms to a standard latex condom. Cook *et al* also reported a slightly higher clinical breakage rate for a brand of polyurethane condom (eZ.on™ condoms) in comparison to latex condoms^[47].

Gallo *et al*^[4] concluded that although non-latex condoms have higher clinical breakage rates in comparison to natural latex condoms; they proffer an alternative option for people with latex allergies and sensitivity. This agreed with conclusions from both Callahan *et al*^[31] and Cook *et al*^[47], as results from each study indicated a higher preference and acceptability of non-latex condoms amongst the studied population. The outcomes from a study that looked into the acceptability of non-latex condoms in Thailand and South Africa have been reported by Niruthisard *et al*^[46]. Again, these condoms are more expensive compared to natural latex condoms^[45].

Another alternative condom that is available are those made from natural membranes; commonly sheaths of lamb cecum^[45]. Again, natural membrane condoms are reported to proffer a more natural sensation during coitus and can also function as a contraceptive, since they do not allow the passage of sperm^[24] ^[45]. However, these are not effective in prevention of STDs, for they are known to have pore large as 1,500 nm in diameter. To put that in perspective, the pores are 10 times the diameter of HIV and over 25 times that of HBV^[24] ^[45] ^[48].

1.3.2: NATURAL RUBBER NANOCOMPOSITES

1.3.2.1: Brief overview

There has been a great move towards the utilization of nano-fillers in the field of natural rubber latex processing. This desire is majorly fuelled by unsuccessful reinforcement of NRL using bulk inorganic fillers such as carbon black, clays and silicates^[13]. Conversely, studies have shown promising reinforcement of NRL containing very low loadings of nano-fillers such as carbon nanotubes (CNT)^[13]. The result of successful reinforcement is as seen in improved physicochemical and mechanical properties.

1.3.2.2: Carbon nanotubes (CNT)

Carbon nanotubes (CNTs) are long cylindrical sp² hybridized allotropic forms of carbon, and are visualised as graphene sheets rolled into cylindrical tubes^[6] (Figure 1.3). CNTs were first discovered by M. Endo in 1978 at the University of Orleans (France), however the interest CNTs only picked-up after its re-discovery by Iijima in 1991^[6].

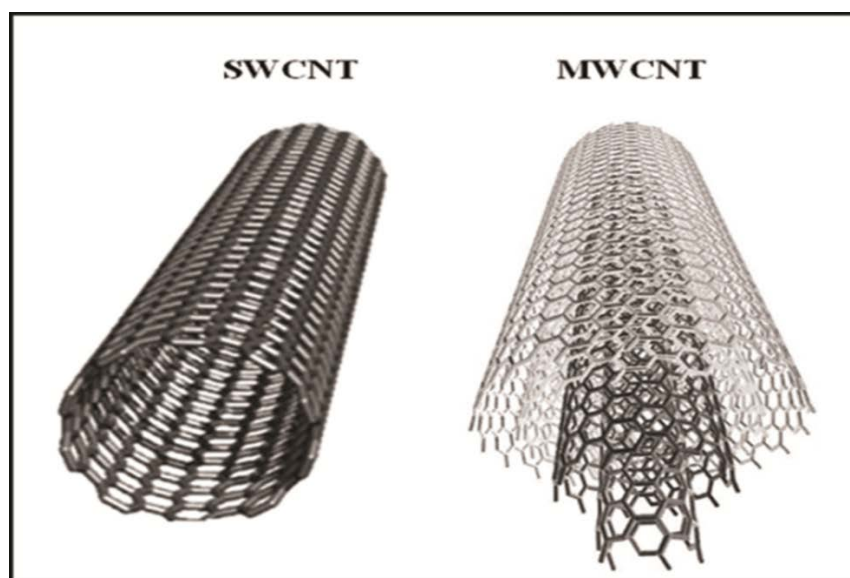


Figure 1.3: A schematic showing open-ended single-walled carbon nanotube (SWCNT) and multi-walled carbon nanotube (MWCT).

Generally, CNTs are classified as; Single-walled carbon nanotubes (SWCNT) which consist of just a single-cylindrical graphene structure and multi-walled carbon nanotubes (MWCNT) which consist sets of concentric SWCNT (Figure). CNTs are just a few nanometres in diameter, however the diameter of MWCNTs are generally larger compared

to SWCNT. The excellent characteristics of CNT is particularly dependent on the type, degree of graphitization, chirality and diameter.

1.3.2.3: Synthesis of carbon nanotubes

The three main methods of synthesising CNT includes arc-discharge, laser ablation and catalytic carbon vapour deposition (CCVD) ^{[6] [7]}. The overall quality and characteristics of CNTs is largely dependent on the method and conditions during synthesis. SWCNTs are often the principal products under catalytic growth conditions, whereas non-catalytic growth conditions mostly yields MWCNTs. Literature reports show that CCVD technique is a more preferred synthesis technique as it offers better control of the final nanomaterial unlike the laser ablation and arc discharge methods ^{[6] [7]}.

Synthesizing CNTs through the catalytic carbon vapour deposition (CCVD) technique involves the decomposition of hydrocarbon gases on a suitable transition metal catalyst at elevated temperatures (800 – 1100⁰C) performed in a reactor^[7]. The resulting CNTs formed largely depends on various process variable like temperature, pressure, flow rate, catalyst and catalyst support^{[6] [7]}. Colomer *et al*^[49] synthesized SWCNTs using methane gas as carbon source and various transition metal salts (Ni, Co and Fe) supported on magnesium oxide as catalyst. Kong *et al*^[50] account on the CCVD synthesis of SWCNTs showed that using ferric oxide (Fe₂O₃) as catalyst on crystalline alumina support resulted to largely individual SWCNTs whereas amorphous silica support yielded bundles of SWCNTs. Inert support materials like alumina and silica are difficult to separate from the synthesized SWCNTs. Alternatively, gasified catalyst can be passed through the reactor^{[50] [7]}.

1.3.2.4: Preparation of natural rubber latex/carbon nanotube composite

The preparation of NRL/CNT films requires the direct mixing of CNT into NRL during the compounding process. This requires the dispersion of CNT in an aqueous medium, preferable distilled water. However, the enormous surface area and high flexibility of CNT favours the close packing and entanglement, which results in poor dispersibility. The dispersibility of CNTs are usually improved via two main approaches summarised as follows^{[6] [51]}.

- The first approach utilises mechanical actions such as high shear mixing and ultrasonication. However, this approach if uncontrolled can lead to a reduction in aspect ratio due to the fragmentation of CNT^{[6] [51]}.
- The second approach involves the modification of the surface free energy of CNTs. This has been achieved either via non-covalent (physical) treatments or covalent (chemical) treatments^[6].

The chemical method involves the introduction of hydrophilic functional groups along the surfaces of the CNT to improve dispersibility. However, the consequence chemical treatment could also include the introduction of surface defects which is detrimental to the properties CNTS^[6].

Non-covalent treatments involves the adsorption or wrapping of surfactants onto the surface of CNTs. The preferred surfactant systems are those with a relatively high Hydrophile-Lyphophlye Balance (HLB)^[51]. Controlled ultrasonication is frequently used to promote the exfoliation of individual CNTs^[6].

1.3.2.5: Physio-Mechanical properties of NRL/CNT composites

The overall performance of CNT as a nano-filler is largely dependent on the extent of dispersion and the nature of the interaction within the NRL matrix. A good interfacial bonding is critical towards effective load transfer. The consequence of high interfacial shear stress is thought to result in the transfer of load from the NRL matrix to the CNT over a short distance^[6]. This is however not the outcome for poor interfacial, as shear stress would instead require a long distance. The load transfer between NRL matrix and the CNT can result from the individual or the combination of these three mechanisms, listed as follows^[6]:

- Mechanical interlocking; this is less likely due to the smooth surface of CNTs. However, surface irregularities or defects could promote interlocking.
- Chemical bonding; establishing either ionic or covalent bond is the ideal type of interfacial interaction towards achieving good mechanical properties.
- Van der Waals (VDW) attraction; this could occur as a result of molecular proximity, and can be significant due to the large surface area of CNTs. However, VDW interactions are not as strong as chemical bonds, hence result in inferior reinforcement properties.

Anoop *et al*^[52] reported 53% increase in tensile strength of NRL/CNT composite films resulting from adding just 2.0 phr CNTs (modulus = 1 - 1.8 TPa). The CNT used in that particular study was dispersed in water using surfactant and controlled ultrasonication. Sui *et al*^[53] reported improved thermal stability, rebound resilience, dynamic compression properties and storage modulus of natural rubber.

Bhattacharyya *et al*^[54] also achieved significant reinforcement of NRL which was reflected as improved tensile and storage modulus. In that particular work, they dispersed carboxylated MWCNT using surfactants and sonication. In a similar fashion, Ngoy *et al*^[55] also successfully functionalised MWCNT. Peng *et al*^[56] reported improved thermal stability and tensile strength of NR/CNT composite films. They attributed the improved properties of the composites to strong interfacial adhesion between the CNT and NRL matrix.

Nonetheless, increasing loading of CNTs is known to result in increase in material stiffness, which is not desirable for this study. Polymers like NR have very poor heat transfer properties (0.13 - 0.14 W/m.K), whereas CNTs are known to have very high thermal conductivity (>2000W/m.K)^{[57] [58]}. However, thermal conductivity of polymer/CNTs composite has shown lower thermal conductivities than estimated ^{[57] [58]} often due to poor dispersion and interfacial thermal resistance resulting from interfacial phonon mismatch between CNTs and polymer matrix^[57]. Nevertheless, any significant increase in heat transfer properties of NRL condoms as a result of CNTs would amount to a great positive outcome.

1.4: RESEARCH RATIONALE

The review literature has clearly show that the significance of male NRL condoms cannot be over-emphasised. It was prominent that the acceptability and desirability of condoms are dependent on its performance and user satisfaction. Thinner condoms are required to promote better coital sensation which could ultimately encourage condom use. Unfortunately, the desire for thinner male NRL condoms increases the risk of mechanical failure ^{[2] [4]}.

Taking into consideration the cyclic tangential shear and circumferential exposed to during coitus, thin condoms would require less force to break. Mostly as a result of the definite reduction in the modulus of NRL condom under deformation/stain. However, for CNTs reinforced condoms, decrease in modulus can be compensated if adequate interfacial interaction is established.

There has been very little technological advancement in the condom industry despite the role they play. The Bill and Melinda Gates Foundation in March 2013 challenged the scientific community to reinvent and re-innovate the condom^[17]. One of the winning designs of the \$100,000 grant, proposed the use of graphene to reinforce NRL condoms. This research also intends to consolidate on the recent successes that have been recorded from the exploitation of the intrinsic properties of carbon nanotubes (CNTs) in the fabrication of modified NRL composite materials.

1.5: PROJECT SCOPE AND LIMITATIONS

The areas covered within this present scope of study includes;

- Characterization of NRL and CNTs suspension
- NRL/CNT composite blend preparation and physio-chemical analysis
- Flow behaviour studies of NRL/CNT composite blends
- Condom production and determination of dimensions
- Physio-mechanical analysis of condoms

On the choice of natural rubber latex:

For this study, commercially available fully prevulcanised natural rubber latex (PvNRL) was utilised. PvNRL serve as a good alternative since they eliminate the rigorous yet sensitive NR latex compounding process. However, slight dilutions and adjustments can still be carried out on the PvNRL to further alter the extent of prevulcanisation. Hence, PvNRL was used in this research in an attempt to eliminate the possible discrepancies that could arise from repeated compounding procedures. PvNRL are very popular in the rubber dipped-goods industry, including for the production of condoms and other prophylactics.^{[12] [59]}

On the Choice of Carbon nanotubes:

Non-covalently functionalised single-walled carbon nanotubes (SWCNTs) were specifically employed for this study. This was based on two rationales; firstly, in comparison to multi-walled nanotubes (MWCNTs), SWCNTs are easily dispersed, offer more surface area and are less likely to cause excessive material stiffness. Furthermore, the non-covalent functionalisation ensures the preservation of intrinsic properties of the SWCNT.

1.6: DISSERTATION OUTLINE

The outline given here provides an overview of this four chaptered dissertation; as follows:

Chapter 1: Introduction and literature review

Chapter 2: a brief background on materials and instrumentations

Chapter 3: SECTION A

Physiochemical analysis of single-wall carbon nanotubes/pre-vulcanised natural rubber latex composites

SECTION B

Flow behaviour of pre-vulcanised natural rubber latex and its nano-blends using rotational viscometry and power law model

SECTION C

Single walled carbon nanotubes reinforced male latex condoms: production and determination of dimensions

SECTION D

Physio-mechanical analysis of single walled carbon nanotubes reinforced male latex condoms

Chapter 4: Overall summary and recommended future work

REFERENCES

- [1] UNAIDS, "THE MALE LATEX CONDOM: 10 condom programming fact sheets," ed: WHO library, 2001, pp. http://data.unaids.org/publications/irc-pub01/jc003-malecondom-factsheets_en.pdf. Access Date: 28/10/2017
- [2] A. Samuel, "FDA Regulation of Condoms: Minimal Scientific Uncertainty Fuels the Moral Conservative Plea to Rip a Large Hole in the Public's Perception of Contraception," 2005.
- [3] S. S. Das, J. C. Coburn, C. Tack, M. R. Schwerin, and D. C. Richardson, "Exposure of natural rubber to personal lubricants—swelling and stress relaxation as potential indicators

of reduced seal integrity of non-lubricated male condoms," *Contraception*, vol. 90, pp. 86-93, 2014.

[4] M. F. Gallo, D. A. Grimes, L. M. Lopez, and K. F. Schulz, "Nonlatex versus latex male condoms for contraception," *The Cochrane Library*, 2006.

[5] M. Monthioux and V. L. Kuznetsov, "Who should be given the credit for the discovery of carbon nanotubes?," *Carbon*, vol. 44, pp. 1621-1623, 2006.

[6] V. Choudhary and A. Gupta, "Polymer/carbon nanotube nanocomposites," in *Carbon nanotubes-Polymer nanocomposites*, ed: Intech, 2011.

[7] N. J. Coville, S. D. Mhlanga, E. N. Nxumalo, and A. Shaikjee, "A review of shaped carbon nanomaterials," *South African Journal of Science*, vol. 107, pp. 01-15, 2011.

[8] N. E. Himes, C. Tietze, and R. L. Dickinson, *Medical history of contraception vol. 657: Gamut Press New York*, 1963.

[9] V. L. Bullough, "A brief note on rubber technology and contraception: the diaphragm and the condom," *Technology and Culture*, vol. 22, pp. 104-111, 1981.

[10] Y. Marfatia, I. Pandya, and K. Mehta, "Condoms: Past, present, and future," *Indian journal of sexually transmitted diseases*, vol. 36, p. 133, 2015.

[11] NOCIL LIMITED., "Technical Note : NR-Latex & Latex Products," pp. 1-56, 2010.

[12] K. O. Calvert, *Polymer Latices and Their Applications*. Essex, England.: APPLIED SCIENCE PUBLISHERS LTD, 1982.

[13] O. S. N. Ghosh, S. Gayathri, P. Sudhakara, S. Misra, and J. Jayaramudu, "Natural Rubber Nanoblends: Preparation, Characterization and Applications," in *Rubber Nano Blends*, ed: Springer, 2017, pp. 15-65.

[14] D. C. Blackley, *Polymer Latices: Science and Technology Volume 3: Applications of Latices: Springer Science & Business Media*, 2012.

[15] M. Jasmin and N. Mathew, "Influence of compounding and process variables on quality of condoms made from natural rubber latex," *Cochin University of Science and Technology*, 1996.

[16] S. Rapra, *Latex and Synthetic Polymer Dispersions 2013: Smithers Rapra*, 2013.

- [17] Bill & Melinda Gates foundation. (2013). Develop the Next Generation of Condom (Round 11) (Date accessed: 11th December 2017 ed.). Available: <https://gcgh.grandchallenges.org/challenge/develop-next-generation-condom-round-11>
- [18] National Institute of Allergy and Infectious Diseases., "Scientific Evidence on Condom Effectiveness for Sexually Transmitted Disease (STD) prevention," NIAID, 2001.
- [19] United States Agency for International Development., "CONDOM FACT SHEET," USAID.,2015.
- [20] S. C. Weller and K. Davis-Beatty, "Condom effectiveness in reducing heterosexual HIV transmission," The Cochrane Library, 2002.
- [21] O. Shisana, T. Rehle, L. Simbayi, K. Zuma, S. Jooste, N. Zungu, et al., "South African national HIV prevalence, incidence and behaviour survey, 2012," 2014.
- [22] T. M. Rehle, T. B. Hallett, O. Shisana, V. Pillay-van Wyk, K. Zuma, H. Carrara, et al., "A decline in new HIV infections in South Africa: estimating HIV incidence from three national HIV surveys in 2002, 2005 and 2008," PloS one, vol. 5, p. e11094, 2010.
- [23] A. Wald, A. G. Langenberg, E. Krantz, J. M. Douglas, H. H. Handsfield, R. P. DiCarlo, et al., "The relationship between condom use and herpes simplex virus acquisition," Annals of internal medicine, vol. 143, pp. 707-713, 2005.
- [24] N. I. o. Health, "Workshop summary: scientific evidence on condom effectiveness for sexually transmitted disease (STD) prevention," 2001.
- [25] J. Hocking and C. K. Fairley, "Associations between condom use and rectal or urethral chlamydia infection in men," Sexually transmitted diseases, vol. 33, pp. 256-258, 2006.
- [26] R. L. Winer, J. P. Hughes, Q. Feng, S. O'reilly, N. B. Kiviat, K. K. Holmes, et al., "Condom use and the risk of genital human papillomavirus infection in young women," New England Journal of Medicine, vol. 354, pp. 2645-2654, 2006.
- [27] T. L. Walsh, R. G. Freziers, K. Peacock, A. L. Nelson, V. A. Clark, L. Bernstein, et al., "Effectiveness of the male latex condom: combined results for three popular condom brands used as controls in randomized clinical trials," Contraception, vol. 70, pp. 407-413, 2004.

- [28] R. G. Frezieres and T. L. Walsh, "Acceptability evaluation of a natural rubber latex, a polyurethane, and a new non-latex condom," *Contraception*, vol. 61, pp. 369-377, 2000.
- [29] R. Crosby, S. Sanders, W. L. Yarber, and C. A. Graham, "Condom-use errors and problems: a neglected aspect of studies assessing condom effectiveness," *American journal of preventive medicine*, vol. 24, pp. 367-370, 2003.
- [30] W. Potter and M. de Villemeur, "Clinical breakage, slippage and acceptability of a new commercial polyurethane condom: a randomized, controlled study," *Contraception*, vol. 68, pp. 39-45, 2003.
- [31] M. Callahan, C. Mauck, D. Taylor, R. Frezieres, T. Walsh, and M. Martens, "Comparative evaluation of three Tactylon TM condoms and a latex condom during vaginal intercourse: breakage and slippage," *Contraception*, vol. 61, pp. 205-215, 2000.
- [32] N. D. White, D. M. Hill, and S. Bodemeier, "Male condoms that break in use do so mostly by a "blunt puncture" mechanism," *Contraception*, vol. 77, pp. 360-365, 2008.
- [33] M. Reece, D. Herbenick, S. Sanders, P. Monahan, M. h. Temkit, and W. L. Yarber, "Breakage, slippage and acceptability outcomes of a condom fitted to penile dimensions," *Sexually transmitted infections*, vol. 84, pp. 143-149, 2008.
- [34] M. E. Beksinska, J. A. Smit, and J. E. Mantell, "Progress and challenges to male and female condom use in South Africa," *Sexual health*, vol. 9, pp. 51-58, 2012.
- [35] L. Goodall, D. Clutterbuck, and P. Flowers, "Towards condom skills: a cross-sectional study of the association between condom proficiency, condom problems and STI risk amongst MSM," *BMC public health*, vol. 12, p. 747, 2012.
- [36] M. Pickles, R. Adhikary, M. Mainkar, K. Deering, S. Verma, M. Boily, et al., "P1-S5. 16 Investigating self-reported level of condom use and condom use in last act among high-risk groups in Southern India," *Sex Transm Infect*, vol. 87, pp. A180-A181, 2011.
- [37] R. A. Crosby, R. J. DiClemente, G. M. Wingood, L. F. Salazar, E. Rose, D. Levine, et al., "Condom failure among adolescents: implications for STD prevention," *Journal of Adolescent Health*, vol. 36, pp. 534-536, 2005.
- [38] S. O. Aral and J. M. Douglas, *Behavioural Interventions for Prevention and Control of Sexually Transmitted Diseases*: Springer Science Business media, 2007.

- [39] G. Magnani, G. F. Elia, M. M. McNeil, J. M. Brown, M. Gabrielli, C. Chezzi, et al., "The success and failure of condom use by homosexual men in San Francisco," *JAIDS Journal of Acquired Immune Deficiency Syndromes*, vol. 6, p. 430, 1993.
- [40] S. Golombok, R. Harding, and J. Sheldon, "An evaluation of a thicker versus a standard condom with gay men," *Aids*, vol. 15, pp. 245-250, 2001.
- [41] A. M. Smith, D. Jolley, J. Hocking, K. Benton, and J. Gerofi, "Does additional lubrication affect condom slippage and breakage?," *International journal of STD & AIDS*, vol. 9, pp. 330-335, 1998.
- [42] M. Gabbay and A. Gibbs, "Does additional lubrication reduce condom failure?," *Contraception*, vol. 53, pp. 155-158, 1996.
- [43] B. J. Meade, D. N. Weissman, and D. H. Beezhold, "Latex allergy: past and present," *International immunopharmacology*, vol. 2, pp. 225-238, 2002.
- [44] Y. Yamamoto, P. T. Nghia, W. Klinklai, T. Saito, and S. Kawahara, "Removal of proteins from natural rubber with urea and its application to continuous processes," *Journal of Applied Polymer Science*, vol. 107, pp. 2329-2332, 2008.
- [45] K. A. Workowski and S. Berman, "Sexually transmitted diseases treatment guidelines, 2010," ed: Centers for Disease Control and Prevention, 2010.
- [46] S. Niruthisard, I. Shah, I. Warriner, and M. Beksinka, "The latex versus the non-latex male condom: Perspectives from contrasting populations," in *International Union for the Scientific Study of Population seminar, Taking Stock of the Condom in the Era of HIV/AIDS*, Gaborone, Botswana, 2003, pp. 13-17.
- [47] L. Cook, K. Nanda, and D. Taylor, "Randomized crossover trial comparing the eZ-on™ plastic condom and a latex condom," *Contraception*, vol. 63, pp. 25-31, 2001.
- [48] C. D. Lytle, P. G. Carney, S. Vohra, W. H. Cyr, and L. E. Bockstahler, "Virus leakage through natural membrane condoms," *Sexually transmitted diseases*, vol. 17, pp. 58-62, 1990.
- [49] J.-F. Colomer, C. Stephan, S. Lefrant, G. Van Tendeloo, I. Willems, Z. Konya, et al., "Large-scale synthesis of single-wall carbon nanotubes by catalytic chemical vapor deposition (CCVD) method," *Chemical Physics Letters*, vol. 317, pp. 83-89, 2000.

- [50] J. Kong, A. M. Cassell, and H. Dai, "Chemical vapor deposition of methane for single-walled carbon nanotubes," *Chemical Physics Letters*, vol. 292, pp. 567-574, 1998.
- [51] L. Vaisman, H. D. Wagner, and G. Marom, "The role of surfactants in dispersion of carbon nanotubes," *Advances in colloid and interface science*, vol. 128, pp. 37-46, 2006.
- [52] A. Anand K, S. Jose T, R. Alex, and R. Joseph, "Natural rubber-carbon nanotube composites through latex compounding," *International Journal of Polymeric Materials*, vol. 59, pp. 33-44, 2009.
- [53] G. Sui, W. Zhong, X. Yang, and Y. Yu, "Curing kinetics and mechanical behavior of natural rubber reinforced with pretreated carbon nanotubes," *Materials Science and Engineering: A*, vol. 485, pp. 524-531, 2008.
- [54] S. Bhattacharyya, C. Sinturel, O. Bahloul, M.-L. Saboungi, S. Thomas, and J.-P. Salvétat, "Improving reinforcement of natural rubber by networking of activated carbon nanotubes," *Carbon*, vol. 46, pp. 1037-1045, 2008.
- [55] J. M. Ngoy, S. E. Iyuke, W. E. Neuse, and C. S. Yah, "Covalent functionalization for multi-walled carbon nanotube (f-MWCNT)-folic acid bound bioconjugate," *Journal of Applied Sciences*, vol. 11, pp. 2700-2711, 2011.
- [56] Z. Peng, C. Feng, Y. Luo, Y. Li, and L. Kong, "Self-assembled natural rubber/multi-walled carbon nanotube composites using latex compounding techniques," *Carbon*, vol. 48, pp. 4497-4503, 2010.
- [57] Z. Han and A. Fina, "Thermal conductivity of carbon nanotubes and their polymer nanocomposites: a review," *Progress in polymer science*, vol. 36, pp. 914-944, 2011.
- [58] M. Martin-Gallego, R. Verdejo, M. Khayet, J. M. O. de Zarate, M. Essalhi, and M. A. Lopez-Manchado, "Thermal conductivity of carbon nanotubes and graphene in epoxy nanofluids and nanocomposites," *Nanoscale research letters*, vol. 6, p. 610, 2011.
- [59] John Woon. (2013). *Practical latex technology: Over 100 Questions Answered plus Many Useful Tips and Ideas* (Kindle Edition ed.). 2. Available: <http://latexconsultants.blogspot.com>

CHAPTER TWO

A BRIEF BACKGROUND ON MATERIALS AND INSTRUMENTATIONS

2.1: CHAPTER OVERVIEW

This chapter contains an overview of materials and a brief background of various instrumentations used in the cause of this study. Experimental methodologies are clearly stated within the respective sections in CHAPTER 3.

2.2: MATERIALS

2.2.1: Pre vulcanised Natural rubber latex (PvNRL)

Medium modulus type pre vulcanised natural rubber latex (PvNRL) with trade name GIVUL MR, a product of GETAHINDUS (M) SDN BHD (Tangkak, Malaysia) was supplied by Carst & Walker (South Africa). The specifications of the PvNRL used in this study were determined in accordance with the Malaysian standard (MS 281), as listed in Table 2.1.

Table 2.1: specifications of PvNRL according to suppliers

Properties/units	Specification
Total Solid Content (%)	60.42
Alkalinity (%)	0.71
Mechanical stability time at 55% TSC (sec.)	1450
Viscosity B/F LVT at 26±2°C (cps)	78
pH	10.73
Coagulum content (ppm)	49

2.2.2: Single walled carbon nanotube (SWCNT) suspension

Surfactant stabilised Single walled carbon nanotubes (SWCNTs) suspension with trademark TUBALL™ LATEX H₂O was supplied by OCSiAl (Grand-Duche de Luxembourg) and was used as received. The SWCNT suspension was prepared via non-covalent functionalisation through the aid of the anionic hydrocolloid surfactant, sodium carboxymethyl cellulose (NaCMC) which also served as a stabilizer.

Table 2.2: Composition and Properties of the SWCNT suspension

COMPOSITION		PROPERTIES	
Component	Concentration (Wt. %)	Appearance	Black liquid
Water	99.7	Density, g/cm ³ at 25°C	1.01
SWCNT	0.1	Viscosity, mPas.s at 20rpm	<30
Sodium Carboxymethyl cellulose	0.2	pH	~9

2.2.3: Chemicals and solvents

The chemicals and reagents used in this study were obtained from Sigma Aldrich (St Louis, MI, USA) and Emplura® Merck (Darmstadt, Germany). All chemicals are of reagent grade and were used as supplied. The lists of chemicals are shown under the respective sections in CHAPTER 3.

2.3: BRIEF BACKGROUND ON INSTRUMENTATIONS

2.3.1: Mass measurements.

PvNRL samples were weighed using an EJ-4100 (A&D, Newton EJ) top pan balance; with 4100 g maximum load and 0.1 g resolution.

A Sartorius AB204-5 (Mettler Toledo, Switzerland) analytic balance with 220 g maximum load and 0.1 mg resolution, was used for mass measurements during crosslink density and swelling ratio determinations. The SWCNT suspension was weighed using the AB204-5.

Samples for thermal analysis (DSC and TGA) experiments were weighed using a MX5 UMT2 (Mettler Toledo, Switzerland) microbalance; with 5.1 g maximum load and 0.1 µg resolution.

2.3.2: Mixing Set-up

The blends of PvNRL and SWCNT suspension were thoroughly mixed using a Heidolph RZR1 (Heidolph, Germany) overhead stirrer. RZR1 features a split pole motor and a minimum speed range of 35- 250 min⁻¹.

The spindle used features a gate-geometry impeller (Figure 2.1); this impeller design is known to be suitable for low-shear mixing of viscous liquids.^[1]

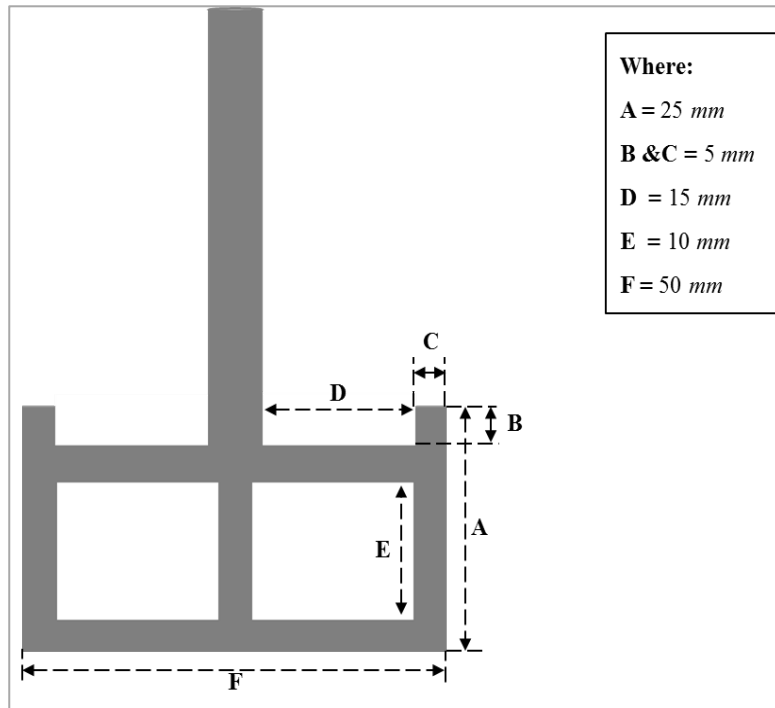


Figure 2.1: A Schematic showing the dimensions of the gate-impeller design spindle. (Dimensions included).

2.3.3: Ultraviolet-visible spectroscopy (UV-vis) Analysis

Lamda™ 35 UV-vis spectrophotometer from PerkinElmer (Waltham, USA) was used to investigate the absorbance spectra of TUBALL™ SWCNT suspension. Test sequence were programmed into the UV™ WinLab control software. The instruments scanning range covers wavelength between 190 – 1100nm, using pre-aligned deuterium and tungsten lamps. It is also equipped to perform a true double-beam operation; this enables the measurement of reference absorbance and perform corrections in real time. The dual beam compensates for the short term variations of the intensities of the light sources and the efficiency of similar optical components of the both light source^[2]. A sealed quartz-coated high-throughput optics ensures consistent performance^[3]. The schematic representation of a dual beam spectrophotometer showing the optical path is as illustrated in Figure 2.2.

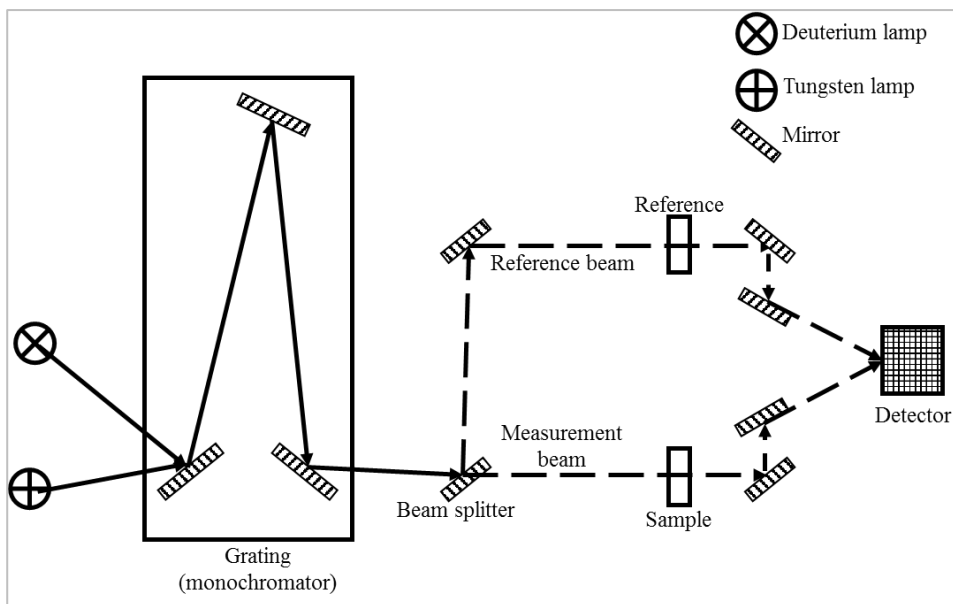


Figure 2.4: Schematic of a typical dual beam spectrophotometer. ^{[2] [3]}

The UV-vis spectroscopy is one of the most versatile techniques used in the qualitative and quantitative analysis of single walled carbon nanotube (SWCNT) dispersions. This technique elucidates a materials property through its interaction with a light of known wavelength. A material is said to have absorbed light if the incident photons results to charge or atomic movements within the material. The correlation between the height of the absorption signal and the concentration of SWCNT is determined via the Beer Lambert’s law as follows:

$$A = \epsilon lc \dots \dots \dots (2.1)$$

Where, ϵ is the molar absorptivity of the solution; l is the path length; and c is concentration.

2.3.4: Fourier-transform infrared spectroscopy (FTIR)

TENSOR II FTIR spectrophotometer from BRUKER (Billerica, MA. USA) fitted with a Platinum Attenuated Total Reflectance (ATR) accessory was used to fingerprint the functional groups present in TUBALL™ SWCNT suspension. The TENSOR II is fitted with a pure diamond crystal, and can perform measurements in the near, mid- and far infrared. It is pertinent for the refractive index of the crystal to be significantly greater than that of the sample to ensure an internal reflectance.

The ATR-FTIR operates by directing an infrared (IR) beam onto the optically dense crystal at a specified angle. An evanescent wave is created stemming from the resultant internal

reflectance, which is then extended beyond the surface unto the test material held in contact with the crystal. The evanescent waves produced only extends a few microns beyond the crystal surface to make contact with the sample. Hence, it is important that the sample makes direct contact with the ATR crystal. The evanescent wave is altered or attenuated in the IR regions where the sample absorbs energy. Subsequently, the attenuated energy for each of the evanescent wave is relayed back to the IR beam, before exiting the reverse end of the crystal into the detector which generates an IR spectrum (Figure 2.3)^[4].

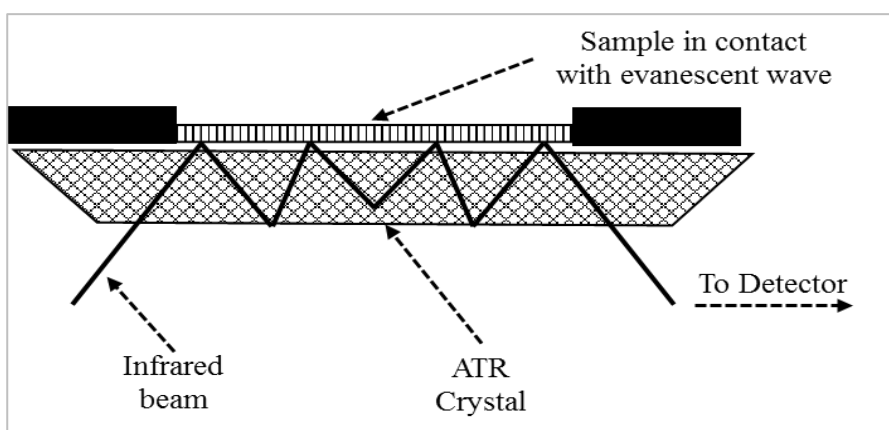


Figure 2.3: Schematic of a multiple reflection ATR system^[4]

2.3.5: Differential scanning calorimetry (DSC) Analysis

A Q200 differential scanning calorimeter (DSC) fitted with a Refrigerated Cooling System (RCS 90) from TA instruments (New Castle, USA) was used to study glass transition temperatures. The Q200 DSC is equipped with a heat flux cell capable of measuring the differential heat flow between a specimen and a reference material as a function of time and temperature (Figure 2.4). Test specimens were encapsulated in a specialised aluminium pan, and placed on the sample thermoelectric disk. Specialised heat flow sensors fitted to Q200 DSC enables it to account for the effect of cell resistance and capacitance.^[5]

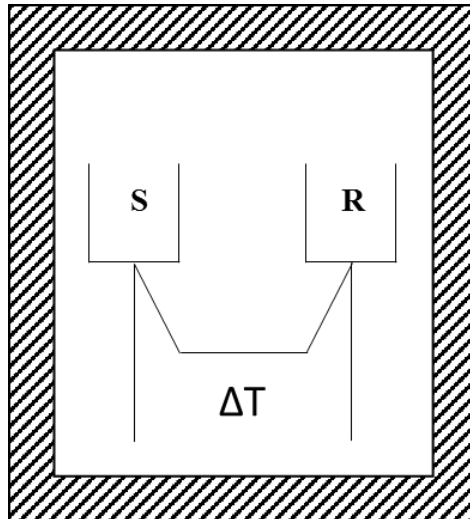


Figure 2.5: A schematic of a typical heat flux DSC cell: (S) sample pan, (R) reference pan, (ΔT) thermocouple system.^[5]

2.3.6: Dynamic mechanical analysis (DMA)

A TA instruments Q800 (New Castle, USA) Dynamic mechanical analyser (DMA) was used to conduct stress relaxation behaviour of condom specimens. The Q800 uses a non-contact direct drive motor that transmit force directly to a rectangular air bearing slide. The frictionless surface of the bearings is maintained using pressurized air. The Q800 uses a high-resolution linear optical encoder to measure sample displacement; this is based on diffraction patterns of light directed through a stationary and moveable gratings. Q800 also features an automated bifilar wound furnace, designed to provide efficient temperature control.

In this present work, transient testing on the Q800 was conducted in the Stress Relaxation mode. Samples were analysed in the tension mode using a film tension clamp measuring system (Figure 2.5). Film tension and clamp compliance calibration were performed. The specimen was subjected to a fixed strain, and stress monitored as a function of time. The ratio between the time dependent stress and strain was obtained and expressed as Stress Relaxation Modulus, as expressed in Equation 2.2.^[6]

$$G(t) = \sigma(t)/\gamma \dots\dots\dots 2.2$$

Where: $G(t)$ is the Stress Relaxation modulus, $\sigma(t)$ is the time-dependent stress, and γ is the applied strain.

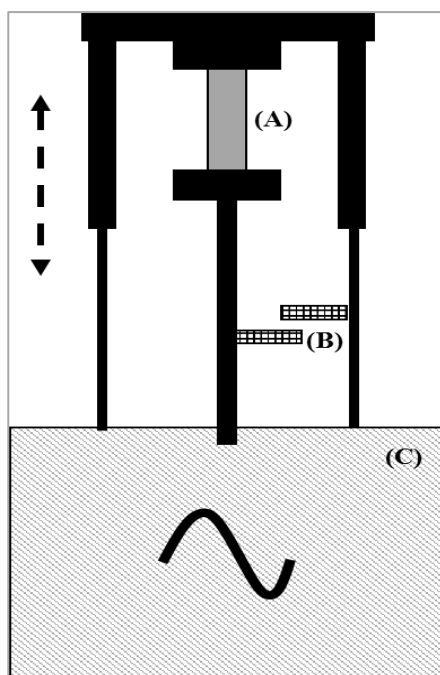


Figure 2.6: *A schematic of film tension analysis set-up for Q800 showing a Combined Motor and transducer; (A) mounted sample. (B) Displacement sensor and (C) Force motor. [6]*

2.3.7: Thermogravimetric analysis (TGA)

Thermal stability experiments was performed on a TA instruments Q600 (New Castle, USA) simultaneous differential scanning calorimeter and thermogravimetric analyser (SDT). The Q600 SDT employs a horizontal dual beam-balance, platinum thermocouple, horizontal purge gas system and a horizontal furnace^[7] (see Figure2.6). The SDT measures mass change as a function of temperature; the mass and temperature difference is compared with that of a known reference pan. High grade platinum sample and reference pans during sample analysis. The sample contained in the relevant pan was subjected to a pre-programmed heating rate and the results obtained were presented as a percentage mass change.

Temperature, heat flow and mass calibrations were performed on the SDT. Heat flow was calibrated using the enthalpy of fusion of Indium (28.58 J/g). Mass calibration was performed using reference mass standards. Temperature calibration was done using the melting temperature of pure samples of Indium (In = 156.61C), tin (Sn = 231.88C), lead (Pb = 324.46C) and zinc (Zn = 419.53C).

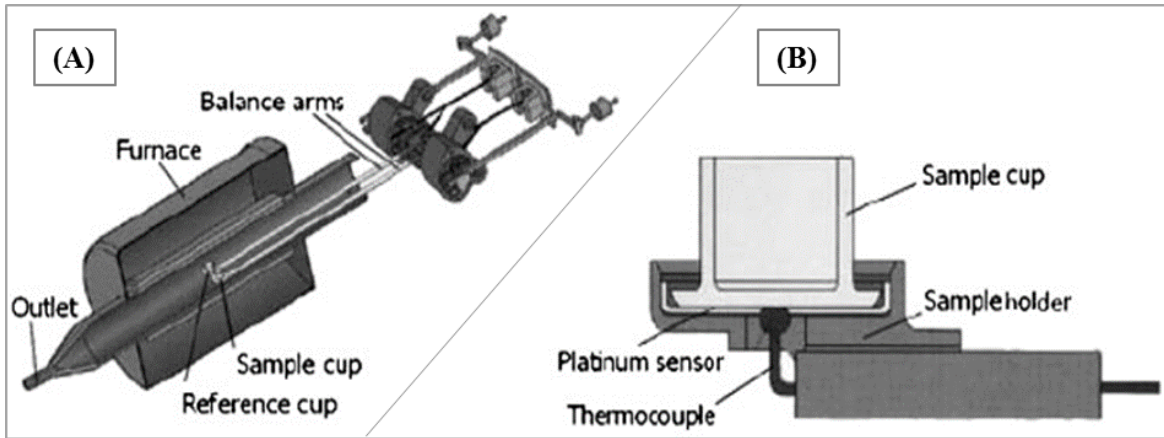


Figure 2.6: Schematic of a typical SDT: (A) thermobalance, (B) sample holder.^[7]

2.3.8: Flow behaviour Analysis

An Anton-paar Modular Compact Rheometer (MCR-502) was used to study the effect of shear rate and temperature on the flow behaviour of the latex samples. The fully digitised MCR-502 is a state of the art Rheometer that can perform wide range viscosity measurements. It features an air-bearing synchronous Electrically Cumulated (EC) motor, high resolution optical encoders and two air bearing support motor. The MCR-504 was fitted with a Peltier Modular temperature control accessory.

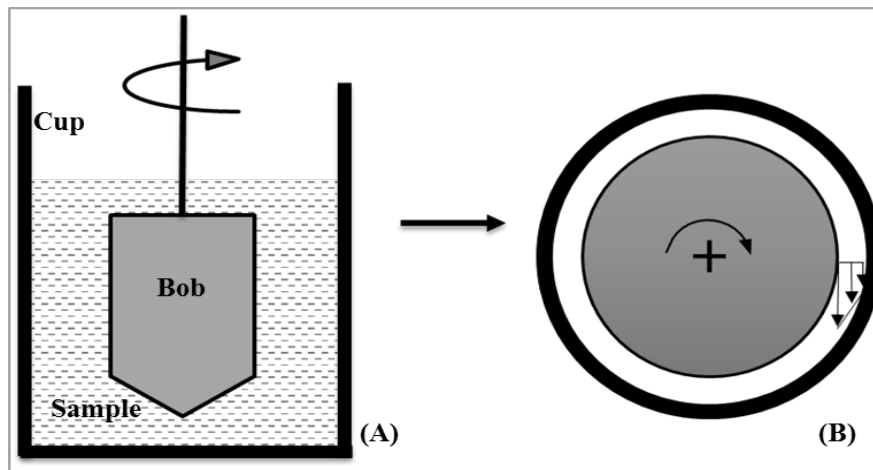


Figure 2.7: (A) A typical schematic of the concentric cylinder measuring system (CC-MS), (B) Cross-sectional view of the of CC-MS showing t narrow shear gap.^[8]

The narrow-gap concentric cylinder measuring system (CC-MS) according to ISO 3219^[9] was employed for this current study. CC-MS consist of an inner cylinder bob (length 39.99 mm and diameter 26.659 mm) and an outer cylinder cup (28.920 internal diameter); rotational analysis was performed according to the Searle method. This method involves a

stationary cup that houses the test sample, and a spinning bob attached to the MCR-504 measuring system, this is as illustrated in Figure 2.7 (A). The narrow gap CC-MS ensures optimal distribution of the circumferential velocity in the shear gap. The cross-section of a CC-MS showing a narrow shear gap is illustrated in Figure 2.7 (B).

REFERENCES

- [1] A. Vicente González, J. Marlen Sanna, A. Galland Andersen, and J. Kanton, "Evaluating and designing systems for mixing water in oil," Universitat Politècnica de Catalunya, 2014.
- [2] J. A. Soares, "Introduction to Optical Characterization of Materials," Practical Materials Characterization, p. 43, 2014.
- [3] S. Upstone and U. Seer Green, "Validating UV/visible spectrophotometers," 2012.
- [4] P. Elmer, "FT-IR Spectroscopy Attenuated Total Reflectance (ATR)," Technical Note, 2005.
- [5] TA instruments., "DSC Differential Scanning Calorimeter," in DSC Q Series Getting Started Guide, ed. New Castle, DE 19720, 2007.
- [6] TA instruments., "Dynamic Mechanical Analysis," in basic Theory & Applications Training, ed. New Castle, DE 19720, 2016.
- [7] A. T. Masiá, B. Buhre, R. Gupta, and T. Wall, "Characterising ash of biomass and waste," Fuel Processing Technology, vol. 88, pp. 1071-1081, 2007.
- [8] Mezgar T. G., The Rheology Handbook, 4 ed. Hanover, Germany: Vincentz Network, 2014.
- [9] ISO 3219:1993, "Plastics (polymers/resins in the liquid state or as emulsions or dispersions)," in Viscosity using a rotational viscometer with a defined shear rate (definition of the concentric cylinder and cone-and plate measuring geometries with a narrow shear gap), ed, 1993.

CHAPTER THREE

SECTION A:

PHYSIOCHEMICAL ANALYSIS OF SINGLE-WALL CARBON NANOTUBES/PRE-VULCANISED NATURAL RUBBER LATEX COMPOSITES

3.1 INTRODUCTION

Generally, prevulcanised natural rubber latex (PvNRL) consists of mainly sulfur crosslinked cis-1,4-polyisoprene rubber chains^[1]. Its stable colloidal nature makes it easy to use; since it requires little or no additional compounding, possesses excellent wet gel strength and requires low drying temperature^{[1] [2]}. The incorporation of reinforcing fillers such as carbon black and silicates into rubber matrices is known to improve their chemical and mechanical properties^{[3] [4]}. However, several attempts towards reinforcing rubber lattices using conventional fillers such as carbon blacks have been largely unsuccessful. This is due to their large size and agglomeration as they are not easy to disperse^{[5] [6]}.

Conversely, recent studies have shown that carbon nanomaterials such as single walled carbon nanotubes (SWCNT) outperforms conventional fillers like carbon black in reinforcing rubber lattices ^{[7] [8] [6]}. This is attributed to the enormous surface area, relative low density and excellent mechanical properties of SWCNT. Depending on intended application, SWCNT may require surface treatment to maximize their potential to achieve reinforcement at even very low loadings^[7]. The ability to chemically functionalize their surfaces aids in achieving the dispersibility and compatibility, especially in rubber lattices through a simple latex mixing technique ^{[7] [9]}.

For example, Anand *et al.*,^[9] achieved over 56% improvement in the tensile strength of natural rubber films after adding about 2phr (parts per hundred rubber) of non-covalently functionalised SWCNT suspension. In that study, a number of surfactants were employed to disperse SWCNT in water under sonication; some of which included sodium dodecylsulfate (SDS), poly vinyl alcohol (PVA) and sodium benzoate^[9]. Other researchers have prepared stable aqueous dispersion of SWCNT using covalent functionalization techniques^{[5] [10]}. Peng *et al.*,^[5] prepared stable dispersion of multi-walled carbon nanotubes (MWCNT); the solubility was achieved after treating the MWCNT using a mixture of nitric acid (HNO₃) and sulphuric acid (H₂SO₄).

In this study, UV Spectroscopy and Attenuated Total Reflectance-Fourier Transform Infrared Spectroscopy- (ATR-FTIR) have been used to characterise aqueous dispersion of SWCNT. The concentration of PvNRL was determined by drying and acetic acid coagulation techniques; this is described as total solid content (TSC) and dry rubber content (DRC). The blends of SWCNT/PvNRL were prepared via the latex mixing technique. Thermogravimetric analyser (TGA) was used to study the drying behaviour of PvNRL and

PvNRL/SWCNT blends. The crosslink density of films casted from PvNRL and PvNRL/SWCNT were studied using the equilibrium swelling technique.

3.2 EXPERIMENTALS

3.2.1 Materials

Single walled carbon nanotubes (SWCNT) suspension with trademark TUBALL™ LATEX H₂O and pristine TUBALL™ SWCNT (75% SWCNT content) was supplied by OCSiAl, (Grand-Duche de Luxembourg). The suspension consists of 1g SWCNT non-covalently dispersed in 1L water. The dispersant/surfactant used is the cellulose derivative, sodium carboxymethyl cellulose (NaCMC). A 218 ± 2 kg drum of Medium modulus pre-vulcanised natural rubber latex, GIVUL MR (GETAHINDUS (M) SDN. BHD, Tangkak, Malaysia) was supplied by Carst & Walker (South Africa).

The chemicals and reagents used in this study include: propan-2-ol (Emplura® Merck, Darmstadt, Germany); glacial acetic acid (assay ≥99.7 %) and Sodium carboxymethyl cellulose (NaCMC, average M_w ~90,000) were sourced from Sigma-Aldrich (St Louis, MI, USA). All chemicals are of reagent grade and were used as supplied.

3.2.2 ANALYSIS OF TUBALL™ SWCNT SUSPENSION

3.2.2.1 Ultraviolet-visible spectroscopy (UV-vis)

About 20 µL of SWCNT suspension was accurately measured using a micropipette (P200, pipetman®) into two clean glass vial bottles labelled as CNT/1 and CNT/2. The samples were diluted by two factors; 1000 times for the content of CNT/1 and 500 times for CNT/2. This was to observe the effect of concentration on the UV-vis adsorption of dispersed SWCNT. Distilled water was used to perform the dilutions and the vials were vigorously agitated before analysis. Baseline corrections were performed using distilled water. The spectra of samples in quartz cuvettes were recorded from 200 – 800 nm on a PerkinElmer Lambda™ 35 UV-vis spectrophotometer (Waltham, USA). The data points were set at 1 nm interval and recorded over 100 cycles.

3.2.2.2 Fourier-transform infrared spectroscopy (FTIR)

The mid-infrared spectra (IR) of SWCNT suspension was recorded using a BRUKER TENSOR II FTIR spectrophotometer (BRUKER, Billerica, MA. USA) equipped with a

platinum Attenuated Total Reflectance (ATR) accessory. The spectrophotometer was operated between 4000 – 400 cm^{-1} range; and was programmed to perform 100 scans at 1 cm^{-1} resolution on an OPUS data collection program.

The diamond crystal of the FTIR was cleaned with propan-2-ol and left to dry for about 1 $min \pm 30 sec$. Subsequently, the background spectrum was measured before loading the sample on the crystal. The nano-suspension was vigorously stirred, and then an aliquot was withdrawn using a pipette. This was carefully spread over the diamond crystal test-area before recording its spectrum.

Further FTIR analysis on NaCMC, p-SWCNT and d-Tuball™ SWCNT was performed following test procedure and conditions as highlighted earlier in this section. The pressure arm of the ATR accessory was used to hold the samples in place before commencing analysis. To obtain dried SWCNT, an aliquot of the suspension was transferred onto a sheet of Teflon and dried in an air oven (50° C for 10 h) to obtain a sheet of approximately 0.04 mm thickness.

3.2.3 ANALYSIS OF PRE-VULCANISED NATURAL RUBBER LATEX (PvNRL)

3.2.3.1 Sampling and determination of pH of PvNRL

The sampling and pH determination were performed in accordance to ASTM D1076-02^[11]. Firstly, the drum of PvNRL was laid on its side and rolled for approximately 15 min \pm 2min to ensure homogeneity of the mixture. Afterwards, the drum was placed on its original position and allowed to stand for another 15 min \pm 2min. This process was repeated one more time before commencement of sampling.

Sampling was performed by gently inserting a clean cylindrical glass tube of 10 mm internal diameter, until it reached the bottom of the drum. The upper open end of the glass tube was closed, followed by gradual withdrawal of the glass tube. The sampled PvNRL was then transferred into a clean stoppered sample bottle.

For pH determination, about 20 mL of PvNRL was transferred into a glass vial and equilibrated to about 23 \pm 1° C in a water bath. A probe pH metre (OHAUS Europe GMBH, Switzerland) was then used to record pH of the PvNRL sample.

3.2.3.2 Determination of total solid content (TSC)

The TSC represents the percentage by weight of the whole non-volatile components of PvNRL at a definite temperature. The determination of TSC was performed in triplicate in accordance with the ASTM D1076-02 specifications^[11].

About $2.5 \text{ g} \pm 0.5 \text{ g}$ sample of PvNRL was weighed (m_0) into a flat-bottom glass dish. The dish was slowly tilted in a clockwise direction to effect even distribution. It was then placed in an air oven set at 70°C and dried for 16 h . After drying, the sample was cooled to room temperature in a desiccator and weighed. The drying and weighing procedure was repeatedly performed until a constant weight (m_1) was obtained. The TSC of the PvNRL sample was calculated as follows:

$$TSC (\%) = \frac{m_1}{m_0} \times 100 \dots\dots\dots (3.1)$$

Where: m_1 = mass after drying; m_0 = mass before drying

3.2.3.3 Determination of dry rubber content (DRC)

The DRC represents the percentage by weight of coagulated dry rubber, precipitated by acetic acid under specified conditions. The determination of DRC was performed in triplicate in accordance with the ASTM D1076-02 specifications^[11].

About $10 \pm 1 \text{ g}$ sample of PvNRL was weighed (m_0) into a flat-bottom glass dish. The weighed sample was then diluted with distilled water to a TSC of $20 \% \pm 1 \% \text{ (m/m)}$. The dish containing the diluted sample was slowly swirled on a smooth surface to achieve homogeneity. About $75 \text{ cm}^3 \pm 5 \text{ cm}^3$ of acetic acid aqueous solution (20 g/dm^3) was slowly poured down the inside edge of the dish over a period of 5 min . the dish was continuously swirled during this process to promote coagulation of rubber, which occurs as acetic acid reacts with the PvNRL.

The dish was then placed on a steam bath and left undisturbed for a period of $15 \text{ min} \pm 2 \text{ min}$ until the serum turned clear. The coagulated PvNRL was then washed with running water. The coagulum was placed on a glass, and pressed using a cylindrical glass rod to expel water and to sheet the coagulum to a thickness of about 2 mm . The sheeted coagulum was then dried in an air oven set at $70 \pm 2^\circ \text{ C}$ over a period of 12 h . The dried sample was cooled to room temperature by placing it in a desiccator and subsequently weighed. The

process of drying and weighing was repeated until a constant weight (m_1) is reached. DRC is calculated as follows:

$$DRC (\%) = \frac{m_1}{m_0} \times 100 \dots\dots\dots (3.2)$$

Where: m_1 = mass after drying; m_0 = mass before drying

3.2.4 ANALYSIS OF PvNRL NANO-BLENDS

3.2.4.1 Preparation of Blends

Currently, there are no existing standards that prescribes the ideal loading of nano-suspensions. However, studies have achieved remarkable reinforcement of rubber lattices using very low loadings of SWCNT^[5]. The prescribed loading of TUBALL™ LATEX H₂O in natural latex as outlined in the supplied usage guidelines manual is 0.03 – 0.1 wt. % (based on wt. % dry rubber content in PvNRL).

Consequently, in this study the loading of SWCNT-suspension in PvNRL follows an arithmetic progression within the recommended loading range. The loading were as follows; 0.02, 0.04, 0.06 and 0.08 wt. % SWCNT. Also, to avoid triggering a pH shock on the PvNRL, the pH of TUBALL™ LATEX H₂O was adjusted to 10.8 using 0.5 M potassium hydroxide solution and was stirred vigorously before use. To simplify the identity of samples, the four nano-blends prepared were assigned the alphanumeric codes; Pv-NB/1, Pv-NB/2, Pv-NB/3 and Pv-NB/4 as listed and described in Table 3.1.

Table 3.1: Description of the four Nano-blends

Sample description	Dry rubber content (g)	SWCNTs (Wt. %)
Pv-NB/1	100	0.02
Pv-NB/2	100	0.04
Pv-NB/3	100	0.06
Pv-NB/4	100	0.08

Predetermined volume of PvNRL was accurately weighed into a 500 mL glass beaker, an overhead stirrer (Heidolph RZR1) fitted with a gate-geometry impeller was used to mix each blend at ambient temperature ($\sim 25^\circ\text{C}$). The mixing procedure was in accordance with the usage guidelines manual provided by OCSiAl, (Grand-Duche de Luxembourg).

Firstly, the overhead stirred was operated at a constant motor speed of 100 rpm during the gradual introduction of the nano-suspension and was left to stir for 25 minutes. The speed was then increased to 250 rpm and maintained for an additional 10 minutes. A good mixing routine is critical towards ensuring effective homogeneity of the blends whilst avoiding any compromise to colloidal stability. PvNRL is known to undergo an irreversible coagulation upon exposure to high shear conditions. The pH of the PvNRL blends was monitored using a probe pH metre (OHAUS Europe GMBH, Switzerland), and maintained at 10.7 using 0.5 M potassium hydroxide solution. The pH measurements were performed at $20 \pm 2^\circ\text{C}$.

3.2.4.2 Thermogravimetric Analysis (TGA)

Thermogravimetric analysis (TGA) was performed on a Q600 (TA instruments, New Castle, USA) simultaneous differential scanning calorimetric and thermogravimetric analyser (SDT). About $50\text{ mL} \pm 3\text{ mL}$ of the latex samples were transferred into open platinum pans. The test samples were placed in the SDT test chamber and desolvated/dehydrated at a heating rate of 3°C min^{-1} from ambient temperature ($\sim 20^\circ\text{C}$) to 200°C . This experiment was conducted under a nitrogen atmosphere at a gas flow rate of 100 mL min^{-1} .

3.2.4.3 Determination of swelling ratio and crosslink density

The determination of swelling ratio was done using the equilibrium swelling technique. Films with thickness of $1\text{ mm} \pm 0.5\text{ mm}$ were cast from PvNRL and PvNRL nanoblends (see Table 3.1) respectively. To cast the films, about 15 mg of the latex samples was evenly spread-out in a flat-bottomed glass container; this was followed by drying at $70 \pm 2^\circ\text{C}$ in an air oven for 1 h.

To determine swelling ratio, approximately $0.3\text{ g} \pm 0.03\text{ g}$ (w_0) of the sample was immersed in 80 ml of toluene for 72 h at room temperature. The glass vials containing the swollen samples were placed away from direct sunlight, and toluene was changed after every 24 hours. Changing toluene was necessary to avoid the saturation of the solvent. The clear

colour of toluene at the end of 72 h swelling exercise signified optimum swelling and extraction of the soluble (sol) contents.

The swollen samples were removed and the excess toluene on the surface was gently dried with a tissue paper. Samples were immediately weighed (W_1) in a closed container and swelling ratio was then was calculated as follows^{[12] [2]}:

$$\text{Swelling ratio (\%)} = \frac{W_1 - W_0}{W_0} \times 100 \dots \dots \dots (3.3)$$

Where; W_0 and W_1 are the weight of dry and swollen rubber sample (g).

The toluene in the swollen samples was then removed by drying in an oven at $50 \pm 2^\circ\text{C}$ in an air oven until a constant weight (W_2) for approximately 12 hours. The sol and gel contents were calculated using the equation 3.4^[13]:

$$\text{sol fraction (\%)} = \frac{W_0 - W_2}{W_0} \times 100 \dots \dots \dots (3.4)$$

Where; W_0 and W_2 are the weight of dry rubber sample before and after solvent exposure.

The crosslink density was calculated using the Flory-Rehner equation (3.5)^[14].

$$XLD = \frac{v_r + \chi v_r^2 + \ln(1 - v_r)}{v_s(Bv_r - A\eta(v_r)^{1/3})} \times 100 \dots \dots \dots (3.5)$$

Where: XLD = crosslink density

v_r = volume fraction of rubber in the swollen gel

χ = Flory-Huggins polymer-solvent interaction parameter

η = ratio of r.m.s length of the chain-end distance in the crosslinked network to free chains. In most situation $\eta = 1$.

A, B = these are theoretical constants. In this study, the commonly used values of A = 1 and B = 1/2 were adopted^{[15] [16]}.

v_s = molar volume of toluene, $106.2 \text{ cm}^3/\text{mol}$ ^[17].

In this study, the Flory-Huggins interaction parameter, $\chi = 0.3795$ was adopted because it has been reported to be suitable for rubber-toluene systems^{[18] [19]}. The volume fraction (v_r) was calculated using equation 3.6.

$$v_r = \frac{w_2}{\left(w_2 + w_3 \frac{\rho_r}{\rho_s}\right)} \dots \dots \dots (3.6)$$

Where: w_2 = is the weight of dried rubber after swelling

w_3 = weight of the solvent in the swollen rubber (calculated as; weight of swollen sample (w_1) minus dried sample (w_2)).

ρ_s , ρ_r = density of solvent (toluene = 0.8650 g cm^{-3}) and density of rubber (0.9203 g cm^{-3}).

3.3 RESULTS AND DISCUSSION

3.3.1 UV-vis analysis of TUBALL™ SWCNT suspension

The UV-vis spectra of the two dilutions of TUBALL™ SWCNT suspension are illustrated in Figure 3.1. The absorbance observed in the range 200 – 350 nm corroborates the dispersion of SWCNT. This is because generally, dispersed individualised SWCNT are known to be active in the UV-vis region and display characteristic bands that tallies with the additional adsorption due to 1D Van Hove singularities^{[20] [21] [22]}. Undispersed or bundled SWCNT are hardly active in the UV-vis region; the quenching is thought to be due to the tunnelling charges between the bundled SWCNT^{[20] [23]}.

The dip seen at the absorbance peak at about 260 nm is likely due to the differences in SWCNT diameters and electronic type^[24]. Also, it is evident that a higher concentration of the dispersed SWCNT-suspension resulted in a significant increase in absorbance. This is in agreement with the findings from literature^{[20] [21] [25]}.

The dispersion of the otherwise hydrophobic SWCNT involves the disruption of the strong van der Waals forces of attractions, resulting from adsorbed sodium carboxymethyl cellulose (NaCMC) surfactant molecules. The molecules of the NaCMC surfactant exhibits a distinct duality that assist in the dispersion of SWCNT, this includes: the hydrophobic anhydroglucose units absorbed onto the SWCNT surfaces and the hydrophilic carboxymethyl cellulose units that is solvated^[26].

Yunhua *et al.*,^[21] employed the UV-vis spectroscopy technique to quantitatively study the concentration of dispersed SWCNT. In that particular work, the surfactant, sodium dodecyl sulfate (SDS) was used to disperse SWCNT under sonication. Minami *et al.*,^[26] reported NaCMC to be twenty times better in dispersing SWCNT compared to SDS.

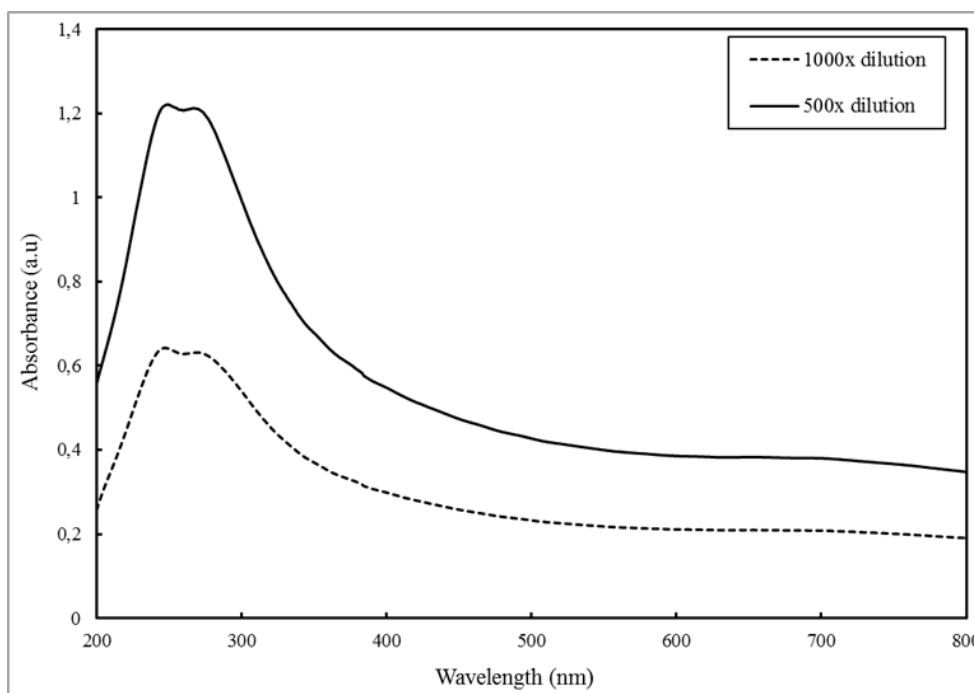


Figure 3.1: Evolution of UV-Vis spectra of 0.1 wt% TUBALL™ SWCNT suspension: the suspension was diluted 1000 (solid line) and 500 times (dashed lines).

3.3.2 ATR-FTIR analysis of TUBALL™ SWCNT suspension

The comparative ATR-FTIR spectra of NaCMC, Tuball™ SWCNT suspension, d-Tuball™ SWCNT and p-Tuball™ SWCNT are illustrated in Figure 3.2. The following transmittance frequencies are assigned to the peaks obtained for NaCMC (a); axial stretching of –OH at $\sim 3267\text{cm}^{-1}$, axial C-H and –CH₂ stretching at $\sim 2880\text{cm}^{-1}$ and symmetrical deformations of –CH₂ and –COH groups between $\sim 1320\text{--}1411\text{cm}^{-1}$. In addition, the peak at $\sim 1588\text{cm}^{-1}$ is assigned to stretching of glucose rings present in NaCMC; whereas the stretching of –CH₂ and –CH₂OH are assigned for the peak at $\sim 1015\text{cm}^{-1}$. These agree with findings from several literatures^{[27] [28] [29]}.

The position of FTIR absorbance frequencies and intensity of the transmittance bands are known to be indicative of the quality of SWCNT dispersions^[24]. Since the Tuball™ SWCNT (b) suspension contains NaCMC, one would expect to observe a similar spectrum as earlier highlighted. However, the axial stretching of –OH and axial C-H and –CH₂ stretching coalesced into a single peak. The broadening and intensification of the –OH peak could also be attributed to water molecules present in the suspension. The shifting of the glucose stretching peak to the left is also noticeable. Equally, the earlier observed activities around $\sim 1600\text{--}1015\text{ cm}^{-1}$ disappeared in the (b) spectrum. It is presumed that the peaks shifted to the

right and coalesced because of the high intensity peak observed around wavelengths below $<1000\text{ cm}^{-1}$ (Figure 3.2 b).

Subsequently, d-Tuball™ SWCNT (c) shows very similar FTIR activities when compared to those of NaCMC (a) and p-Tuball™ SWCNT (d). There is a clear decrease in the transmittance peaks of NaCMC in (c), notable around the range of wavelength $\sim 1320\text{-}600\text{ cm}^{-1}$. The evaporation of the volatile component and masking effect of SWCNT is responsible for the decrease in the size of the peak.

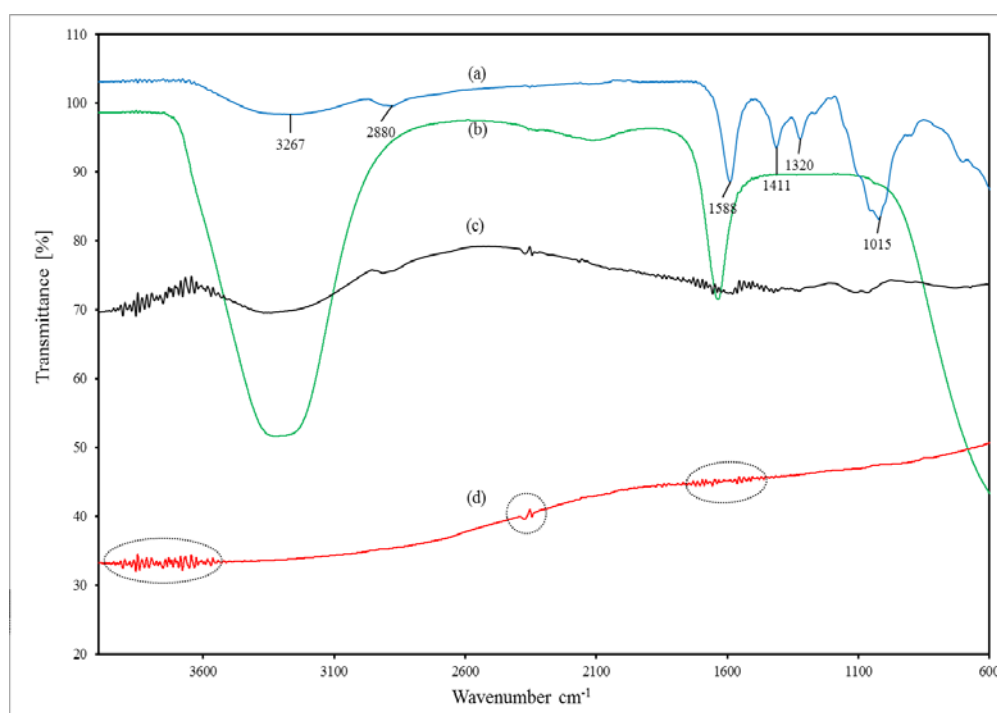


Figure 3.2: ATR-FTIR spectra of NaCMC (a), Tuball™ SWCNT suspension (b), d-Tuball™ SWCNT (c) and p-Tuball™ SWCNT (d).

There are almost no distinct absorption peaks recorded for p-Tuball™ SWCNT as illustrated in Figure 3.2 (d). All the encircled areas are thought to show weak/suppressed IR activity as seen for the signals of p-Tuball™ SWCNT in Figure 3.2 (also appear d-Tuball™ SWCNT). The activity around $\sim 1600\text{ cm}^{-1}$ likely originates from C-C stretching vibrations resulting from the phonon modes of the SWCNT^[7]. The weak peak observed between $2380\text{-}2342\text{ cm}^{-1}$ (centre circled (d)) could be due to suppressed -CO_2 stretching^[30]. The FTIR characterization technique has been widely used to identify the functional groups present in dispersion of SWCNT^{[24] [7] [30] [5]}.

3.3.3: Analysis of the concentration of PvNRL

The concentration of lattices is usually described as its total solid content (TSC) and dry rubber content (DRC). The experimentally determined average TSC and DRC of the PvNRL used in this study are illustrated in Figure 3.3. It can be seen that the measured average TSC is about 60.47 %, which is close to the average specified by the supplier of about 60.42%. Nonetheless, the measured average DRC is about 58.79%; which is not surprising because the difference between TSC and DRC is reported to be about 3%^{[31][32]}. In general, the DRC gives a better information on the concentration of PvNRL compared to TSC. This is because a larger sample mass ($\sim 10 \text{ g} \pm 1 \text{ g}$) is utilized for DRC determinations compared to TSC ($2.5 \text{ g} \pm 0.5 \text{ g}$). Again, the acetic acid coagulated DRC is less hygroscopic than the air-dried TSC; thus, a less chance of error arising from adsorbed atmospheric moisture^[32].

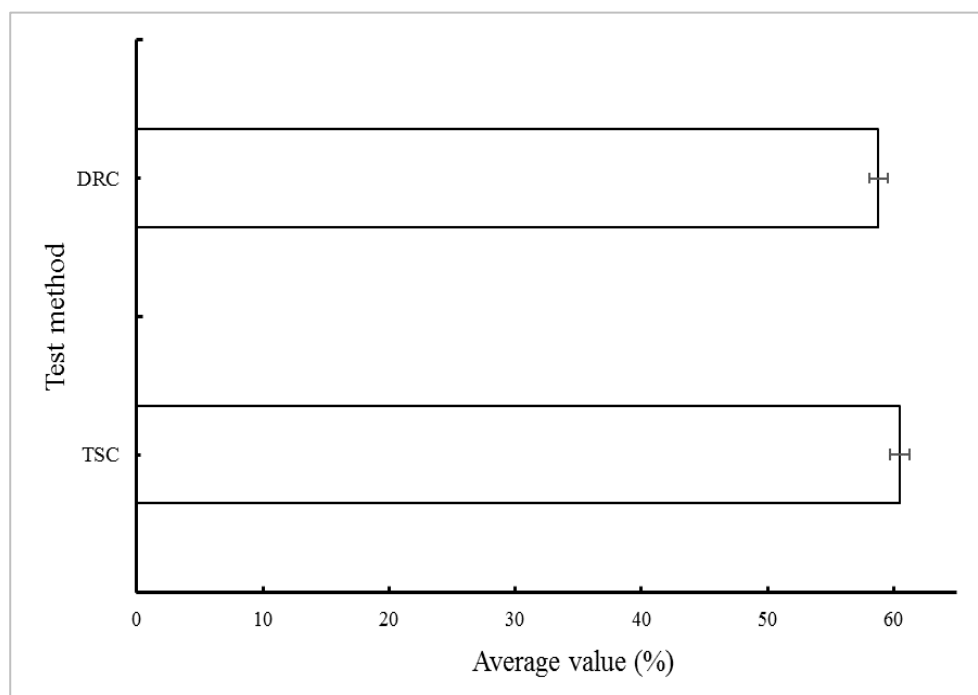


Figure 3.3: Bar graphs showing the average total solid content (TSC) and dry rubber content (DRC) of PvNRL.

3.3.4: TGA analysis of PvNRL and SWCNT reinforced PvNRL.

The thermogravimetric (TGA) and differential thermogravimetric (DTG) curves shown in Figure 3.4 illustrates the drying behaviour of PvNRL. The TGA curve represents the weight loss associated with the evaporation of the volatile components. On a closer inspection of the TG curve, it is apparent that the evaporation of the different components are overlapping. The TG curve is clearly not well resolved despite the slow heating rate ($3^{\circ}\text{C min}^{-1}$) used.

However, the DTG curve revealed the multi-component nature of the drying events. The onset of weight loss as shown by the DTG curve occurs almost immediately, and reaches a maximum around 60°C before gradually slowing down until ~90°C. This is followed by an abrupt increase in the rate of weight loss, peaking at ~105°C. The shape of the DTG curve between 30 and 160°C clearly suggests that the drying of PvNRL involves numerous evaporation events occurring together.

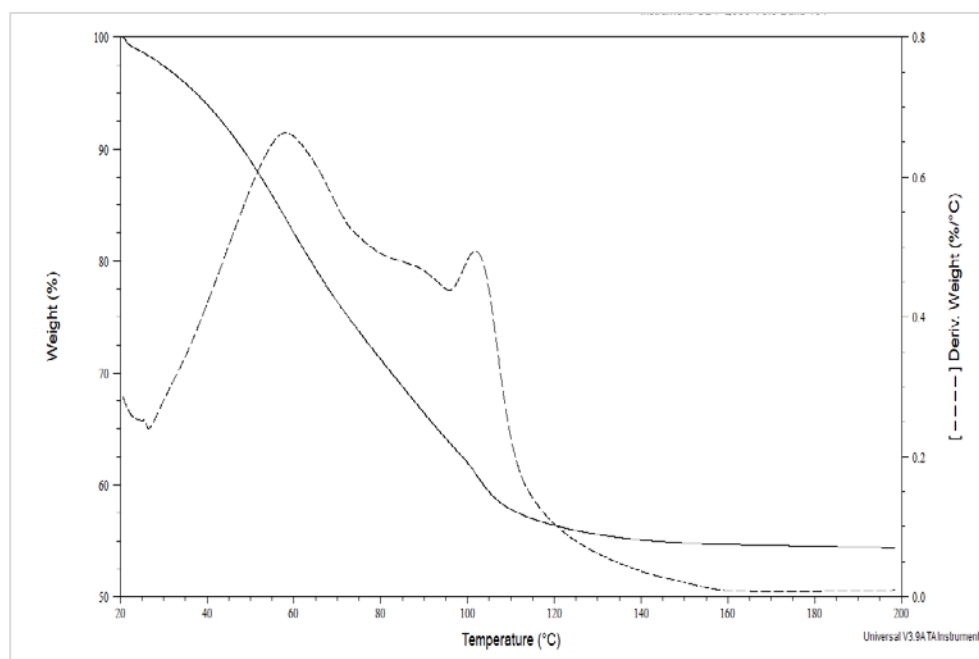


Figure 3.4: TGA (solid line) and DTA (dashed line) curves showing the evaporation of the volatile components of PvNRL.

The aqueous (continuous) phase of PvNRL is known to be highly concentrated^{[31] [32]}. The principal components are water (H₂O), ammonia (NH₃), volatile fatty acids (VFA), potassium hydroxide (KOH), carbohydrates and organic acids^{[31] [32]}. Consequently, the colligative properties (especially boiling point) of the volatile components present in the aqueous phase of PvNRL would be affected due to the interactions between the molecules of these different species.

When in solution, NH₃ forms ammonium hydroxide (NH₄OH), with a boiling point around 37.7 °C; whereas that of most VFA occur around ~117 °C^[33]. The DTG maximum at 105 °C is probably due to the increased evaporation of H₂O. In addition, desorption of H₂O molecules initially bound on the rubber interphase would also contribute to weight loss.

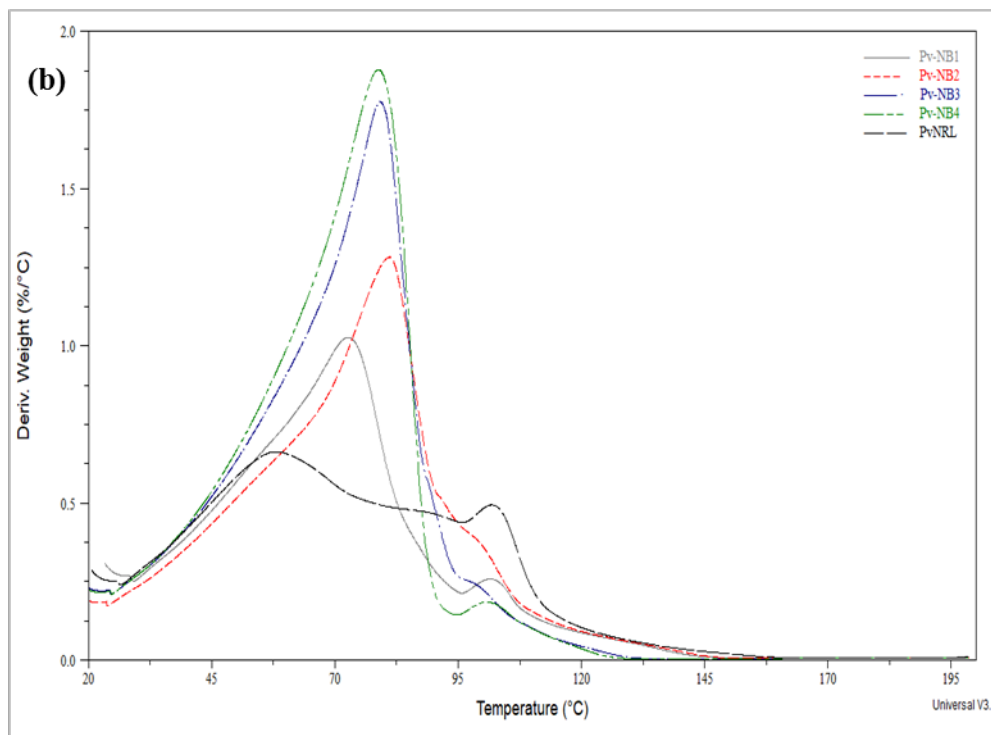
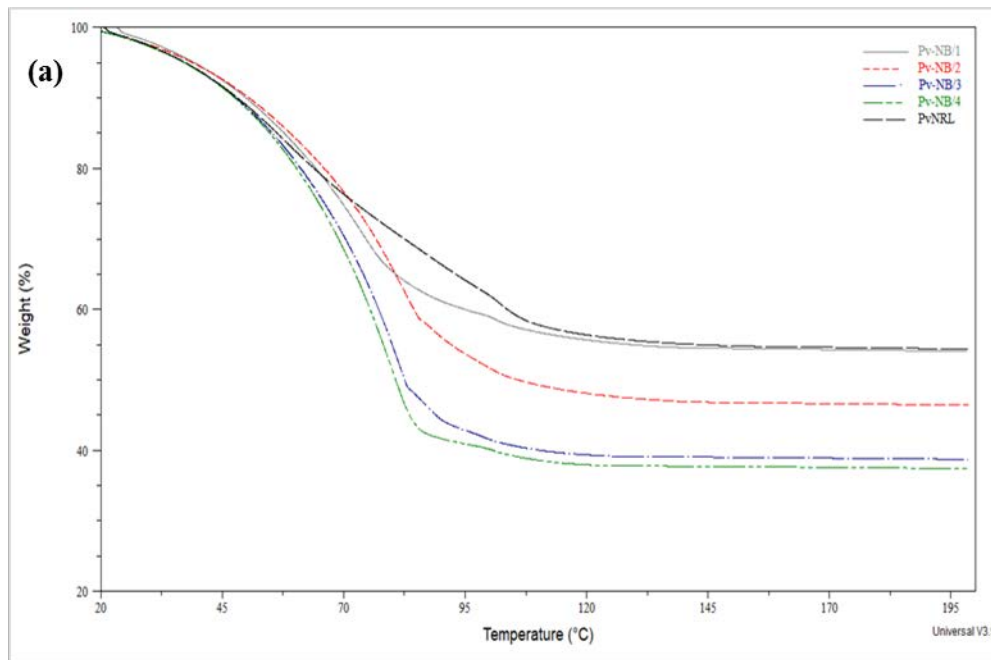


Figure 3.5: Plots of the drying behaviour of PvnRL containing varying loadings of Tuball™ SWCNT: (a) comparison of TGA curves, (b) comparison of DTG curves.

The incorporation of SWCNT nano-suspension is seen to increase the rate of drying of PvnRL as shown in Figure 3.5 (a) by the progressive shift in the TG curves from right to left. PvnRL is a poor conductor of heat, whereas SWCNT are known to possess excellent thermal conductivity^[34]. Hence, it is only apparent that the introduction of the nano-

suspension would result in an increase in thermal conductivity of PvNRL. The DTG curves in Figure 3.5 (b) also supports the above mentioned idea. The increase in the rate of weight loss resulted in the coalescing of DTG peaks, which suggests an increasing simultaneity of the evaporation events.

3.3.5: Effect of SWCNT suspension on swelling index and crosslink density of PvNRL films

The swelling of crosslinked rubbers involve the diffusion of a suitable solvent into the rubber matrix which leads to the weakening of the crosslinked molecular chains^[2]. Hence, a higher swelling index shows the ease at which the solvent molecules migrate into the crosslinked networks of rubber chains. Swelling leads to a macroscopic increase in volume as a result of the rubber-solvent and rubber-filler interactions^{[2] [35]}.

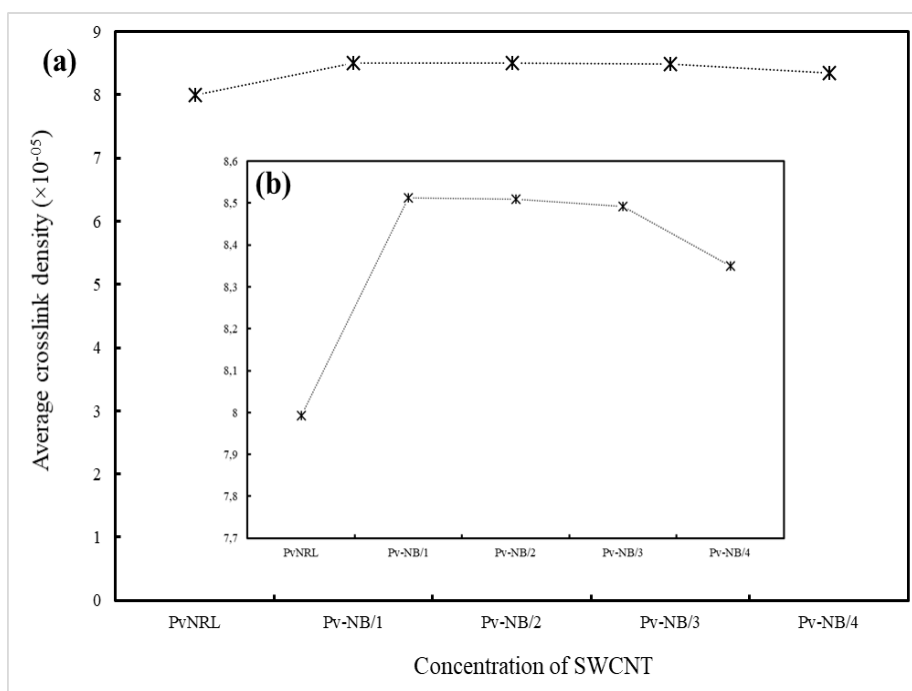
The effect of varying loadings of SWCNT nano-suspension on the swelling index of PvNRL films are illustrated in Table 3.2. PvNRL films clearly showed the highest swelling ratio compared to reinforced samples. The incorporation of nano-suspension slightly decreased swelling, probably due to the polymer-filler interactions which are known to reduce the extent of solvent adsorption^[35]. In this study, the high specific surface area of SWCNT (nano-filler) is assumed to result in significant physical adhesion (via Van der Waals forces) with the rubber chains.

Although Pv-NB/1 showed the least swelling at 470.88 %, it however has the highest statistical uncertainty at ± 6.3 %. Therefore, if the uncertainty is taken into consideration, it appears that all the nano-blends exhibit similar swelling characteristics (Table 3.2). The gel content is the fraction of the rubber that is solvent swollen, which is mainly untangled crosslinked rubber chains; whilst the sol content represent the solvent dissolved fraction^[36].

The crosslink density (XLD) of a vulcanised rubber is directly related to the average molecular weight between adjacent crosslinks^{[2] [35]}. Figure 3.6 illustrates the effect of varying loadings of SWCNT suspension on the XLD of PvNRL. A higher crosslink density was observed for the films of Pv-NB compared the PvNRL films. The blends with the higher XLD showed the least swelling index, suggesting more restricted polymer-chain mobility and dense network of crosslink^[2].

Table 3.2: Swelling index, Gel and Sol content

Sample description	Average swelling index (%)	Gel content (%)	Sol content (%)
PvNRL	480.74 (\pm 3.6)	93.75	6.25
Pv-NB/1	470.88 (\pm 6.3)	94.84	5.16
Pv-NB/2	475.43 (\pm 2.7)	95.58	4.42
Pv-NB/3	476.99 (\pm 0.9)	95.75	4.25
Pv-NB/4	477.47 (\pm 1.6)	95.09	4.91

**Figure 3.6:** (a) Plot showing the comparison of crosslink density. Insert (b) plot truncated in the y-axis for clarity of comparison.

It can be seen in Figure 3.6 that similar XLD values were observed for films of Pv-NB/1, Pv-NB/2 and Pv-NB/3; whereas the film with the highest loading (Pv-NB/4) showed a slightly lower XLD (Figure 3.6: insert b). Although the observation shows slight differences in XLD of PvNRL seemed to increase upon addition of SWCNT. The increase in XLD of

rubber upon incorporation of nano-fillers has been reported^[35]. The effective XLD of a rubber nanocomposite is taken to be a combination of the chemical crosslinks between rubber chains and the significant rubber-filler interactions^[7].

The decrease in solvent swelling due to strong rubber-filler interactions is characteristic of nanocomposites^[37]. Huge interphase layers are formed due of these interactions, mainly because of the substantial surface area of SWCNT^[35] ^[37]. Furthermore, the prospect of adsorption of unused accelerators and other vulcanizing agents on the surface of the SWCNT along these interface, is also thought to promote additional crosslinking, resulting in a higher XLD ^[35] ^[38].

3.4 SUMMARY OF OBSERVATIONS

- The TUBALL™ SWCNT suspension exhibited a characteristic absorption signal in the UV-Vis region. The intensity of the absorbance peaks was observed to be affected by concentration. Therefore, the appearance of these distinct absorbance peaks indicates the presence of individually dispersed SWCNT.
- ATR-FTIR confirmed the presence of the surfactant molecules.
- The concentration of the PvNRL have been successfully evaluated by via the determination of total solid content (TSC) and dry rubber content (DRC).
- Blends of PvNRL and TUBALL™ SWCNT have been prepared following the latex mixing technique.
- Thermogravimetric analysis revealed that the incorporation of TUBALL™ SWCNT suspension into PvNRL resulted in faster drying
- Results obtained from equilibrium swelling experiments suggests a slight increase in the crosslink density of PvNRL upon the addition of TUBALL™ SWCNT. PvNRL films exhibited the highest swelling index.

REFERENCES

- [1] N. Claramma and N. Mathew, "Studies on prevulcanization of rubber latex with special reference to influence of storage and after treatments on properties of films," Cochin University of Science and Technology, 1997.

- [2] C. Ruslimie, M. Norhanifah, M. Fatimah Rubaizah, and M. Asrul, "Effect of Pre Vulcanisation Time on the Latex Particles, Surface Morphology and Strength of Epoxidised Natural Rubber Films," 2015.
- [3] J. Fröhlich, W. Niedermeier, and H.-D. Luginsland, "The effect of filler–filler and filler–elastomer interaction on rubber reinforcement," *Composites Part A: Applied Science and Manufacturing*, vol. 36, pp. 449-460, 2005.
- [4] T. Kurian, P. De, D. Khastgir, D. Tripathy, S. De, and D. Peiffer, "Reinforcement of EPDM-based ionic thermoplastic elastomer by carbon black," *Polymer*, vol. 36, pp. 3875-3884, 1995.
- [5] Z. Peng, C. Feng, Y. Luo, Y. Li, and L. Kong, "Self-assembled natural rubber/multi-walled carbon nanotube composites using latex compounding techniques," *Carbon*, vol. 48, pp. 4497-4503, 2010.
- [6] M. D. Frogley, D. Ravich, and H. D. Wagner, "Mechanical properties of carbon nanoparticle-reinforced elastomers," *Composites Science and technology*, vol. 63, pp. 1647-1654, 2003.
- [7] A. Shanmugaraj, J. Bae, K. Y. Lee, W. H. Noh, S. H. Lee, and S. H. Ryu, "Physical and chemical characteristics of multiwalled carbon nanotubes functionalized with aminosilane and its influence on the properties of natural rubber composites," *Composites Science and technology*, vol. 67, pp. 1813-1822, 2007.
- [8] G. Sui, W. Zhong, X. Yang, and Y. Yu, "Curing kinetics and mechanical behavior of natural rubber reinforced with pretreated carbon nanotubes," *Materials Science and Engineering: A*, vol. 485, pp. 524-531, 2008.
- [9] A. Anand K, S. Jose T, R. Alex, and R. Joseph, "Natural rubber-carbon nanotube composites through latex compounding," *International Journal of Polymeric Materials*, vol. 59, pp. 33-44, 2009.
- [10] S. Hussain, P. Jha, A. Chouksey, R. Raman, S. Islam, T. Islam, et al., "Spectroscopic investigation of modified single wall carbon nanotube (SWCNT)," *J. Mod. Phys*, vol. 2, pp. 538-543, 2011.
- [11] ASTM D1076., "Standard Specifications for Rubber-Concentrated, Ammonia Preserved, Creamed, and Centrifuged Natural Latex," ed, 2006.

- [12] K. M. Z. Hossain, N. Sharif, N. Dafader, M. Haque, and A. Chowdhury, "Physicochemical, thermomechanical, and swelling properties of radiation vulcanised natural rubber latex film: Effect of Diospyros peregrina fruit extracts," *ISRN Polymer Science*, 2013.
- [13] G. Jana, R. Mahaling, and C. Das, "A novel devulcanization technology for vulcanized natural rubber," *Journal of applied polymer science*, vol. 99, pp. 2831-2840, 2006.
- [14] P. J. Flory and J. Rehner Jr, "Statistical mechanics of cross-linked polymer networks I. Rubberlike elasticity," *The Journal of Chemical Physics*, vol. 11, pp. 512-520, 1943.
- [15] P. J. Flory, "Statistical mechanics of swelling of network structures," *The Journal of Chemical Physics*, vol. 18, pp. 108-111, 1950.
- [16] F. T. Wall and P. J. Flory, "Statistical thermodynamics of rubber elasticity," *The Journal of Chemical Physics*, vol. 19, pp. 1435-1439, 1951.
- [17] W. Haynes and C. Handbook, "Chemistry and Physics," ed: CRC Press, 2010.
- [18] S. K. Mandal, N. Alam, and S. C. Debnath, "Reclaiming of Ground Rubber Tire by Safe Multifunctional Rubber Additives: I. Tetra Benzyl Thiuram Disulfide," *Rubber Chemistry and Technology*, vol. 85, pp. 629-644, 2012.
- [19] D. De, A. Das, D. De, B. Dey, S. C. Debnath, and B. C. Roy, "Reclaiming of ground rubber tire (GRT) by a novel reclaiming agent," *European Polymer Journal*, vol. 42, pp. 917-927, 2006.
- [20] D. Ponnamma, S. H. Sung, J. S. Hong, K. H. Ahn, K. Varughese, and S. Thomas, "Influence of non-covalent functionalization of carbon nanotubes on the rheological behavior of natural rubber latex nanocomposites," *European Polymer Journal*, vol. 53, pp. 147-159, 2014.
- [21] Y. Shi, L. Ren, D. Li, H. Gao, and B. Yang, "Optimization conditions for single-walled carbon nanotubes dispersion," *Journal of Surface Engineered Materials and Advanced Technology*, vol. 3, p. 6, 2013.
- [22] B. Sohrabi, N. Poorgholami-Bejarpasi, and N. Nayeri, "Dispersion of carbon nanotubes using mixed surfactants: experimental and molecular dynamics simulation studies," *The Journal of Physical Chemistry B*, vol. 118, pp. 3094-3103, 2014.

- [23] J.-S. Lauret, C. Voisin, G. Cassabois, C. Delalande, P. Roussignol, O. Jost, et al., "Ultrafast carrier dynamics in single-wall carbon nanotubes," *Physical review letters*, vol. 90, p. 057404, 2003.
- [24] C. Backes and I. Stemmler, "Absorption Spectroscopy as a Powerful Technique for the Characterization of Single-Walled Carbon Nanotubes," 2013.
- [25] J. H. Lehman, M. Terrones, E. Mansfield, K. E. Hurst, and V. Meunier, "Evaluating the characteristics of multiwall carbon nanotubes," *Carbon*, vol. 49, pp. 2581-2602, 2011.
- [26] N. Minami, Y. Kim, K. Miyashita, S. Kazaoui, and B. Nalini, "Cellulose derivatives as excellent dispersants for single-wall carbon nanotubes as demonstrated by absorption and photoluminescence spectroscopy," *Applied Physics Letters*, vol. 88, p. 093123, 2006.
- [27] D. de Britto and O. B. Assis, "Thermal degradation of carboxymethylcellulose in different salty forms," *Thermochimica Acta*, vol. 494, pp. 115-122, 2009.
- [28] J. Wang and P. Somasundaran, "Adsorption and conformation of carboxymethyl cellulose at solid-liquid interfaces using spectroscopic, AFM and allied techniques," *Journal of Colloid and Interface Science*, vol. 291, pp. 75-83, 2005.
- [29] D. S. Ruzene, A. R. Gonçalves, J. A. Teixeira, and M. T. P. De Amorim, "Carboxymethylcellulose obtained by ethanol/water organosolv process under acid conditions," in *Applied Biochemistry and Biotechnology*, ed: Springer, 2007, pp. 573-582.
- [30] D. Singh, P. Iyer, and P. Giri, "Functionalization of carbon nanotubes and study of its optical and structural properties," *Nanotrends*, vol. 4, pp. 55-58, 2008.
- [31] NOCIL LIMITED., "Technical Note : NR-Latex & Latex Products," pp. 1-56, 2010.
- [32] K. O. Calvert, *Polymer Latices and Their Applications*. Essex, England.: APPLIED SCIENCE PUBLISHERS LTD, 1982.
- [33] B. Zygmunt and A. Banel, "Formation, occurrence and determination of volatile fatty acids in environmental and related samples," in *Proceedings of the 3rd WSEAS International Conference on Energy Planning, Energy Saving, Environmental Education, Renewable Energy Sources, Waste Management, Tenerife, Spain, 2009*, pp. 476-481.
- [34] J. M. Ngoy, S. E. Iyuke, W. E. Neuse, and C. S. Yah, "Covalent functionalization for multi-walled carbon nanotube (f-MWCNT)-folic acid bound bioconjugate," *Journal of Applied Sciences*, vol. 11, pp. 2700-2711, 2011.

- [35] S. Rabiei and A. Shojaei, "Vulcanization kinetics and reversion behavior of natural rubber/styrene-butadiene rubber blend filled with nanodiamond—the role of sulfur curing system," *European Polymer Journal*, vol. 81, pp. 98-113, 2016.
- [36] E. Bilgili, H. Arastoopour, and B. Bernstein, "Pulverization of rubber granulates using the solid state shear extrusion process: Part II. Powder characterization," *Powder Technology*, vol. 115, pp. 277-289, 2001.
- [37] M. López-Manchado, J. Valentín, J. Carretero, F. Barroso, and M. Arroyo, "Rubber network in elastomer nanocomposites," *European polymer journal*, vol. 43, pp. 4143-4150, 2007.
- [38] A. De Falco, A. Marzocca, M. Corcuera, A. Eceiza, I. Mondragon, G. Rubiolo, et al., "Accelerator adsorption onto carbon nanotubes surface affects the vulcanization process of styrene–butadiene rubber composites," *Journal of applied polymer science*, vol. 113, pp. 2851-2857, 2009.

SECTION B:

**FLOW BEHAVIOUR OF PRE-VULCANISED NATURAL RUBBER LATEX
AND ITS NANO-BLENDS USING ROTATIONAL VISCOMETRY AND
POWER LAW MODEL**

3.5: INTRODUCTION

The flow behaviour of sulfur pre-vulcanised natural rubber latex (PvNRL) especially viscosity, determines its storage-stability and processability. Different grades of PvNRL are commercially available and serve as convenient raw materials in the production of latex foam, dipped goods including gloves and condoms and, as well as extruded goods^[1]. PvNRL only requires low temperature curing to give rubber articles with good properties. Additionally, increasing the drying temperature and adding extra curatives is also known to significantly improve the final properties of the cured articles ^{[2][3]}.

The pre-vulcanisation of natural rubber latex introduces crosslinks between rubber polymer chains without significant alteration of particle size or colloidal stability ^{[1][2]}. However, the dynamic manufacturing techniques which involves; pumping, agitation, dipping and casting, exposes PvNRL to different forms of shear stress that influences its flow behaviour ^[2].

Flow behaviour is a bulk material property which reveals the nature of particle (and molecular) interactions in a material, and the resultant viscosity. PvNRL is considered to have two major phases, an aqueous continuous phase (dispersion medium; mainly water) and a solid dispersed phase (mainly cross-linked cis-1,4-polyisoprene rubber particles)^[2].

Studies have shown that significant electrostatic interactions occur between the components of both phases ^{[4][5]}. Adsorbed layers of proteins and phospholipids introduce negative charges on rubber particles while the counter-charges are predominantly dissolved ammonium cations (NH_4^+) present in the dispersion medium, ^{[4][5]}.

Recent advancements in the field of nanotechnology have impacted positively in PvNRL processing. The most notable impact is the use of nano zinc oxide (ZnO) activator which is more efficient at low loadings compared to micro ZnO ^[6]. Several nanomaterials, including single walled carbon nanotubes (SWCNT), have been found to perform as excellent nano-fillers even at low loadings due to their high aspect ratio and excellent strength ^[7]. Thus, reawakening the desire to reinforce low modulus PvNRL articles such as condoms and gloves in a bid to enhance their mechanical and thermal properties ^{[7][8]}.

The preparation of PvNRL-nanoblends through latex stage mixing require careful dispersion and stabilization of the nanomaterial in a suitable solvent, preferably water, before blending ^[8]. Subsequently, the overall flow behaviour of the resulting nano-blend is also expected to match the intended manufacturing conditions whilst maintaining PvNRL's colloidal stability. This is important because the viscosity of PvNRL under varying processing

conditions goes a long way in determining the storage-stability, ease of production and quality of the end products^{[2] [5]}.

However, since sp^2 hybridized nano-materials like SWCNT are generally insoluble in water, they require special functionalisation to achieve the desired solubility^{[7] [9] [10]}. Covalent functionalisation involves the introduction of suitable functional groups on the surface of the nanomaterial to increase its solubility^[11]. However, this method comes at the expense of compromising the structure of pristine SWCNT. Non-covalent functionalisation involves either establishing hydrophobic interaction between an amphiphilic surfactant and the nanomaterial or via enthalpy-driven interactions such as π - π , CH- π , NH- π in order to promote solvation^{[7] [8] [12] [13]}.

Some of the most commonly used molecules to non-covalently disperse SWCNT includes; sodium dodecyl sulfate (SDS), sodium dodecylbenzene sulfonate (SDBS) and the water-soluble polymer sodium carboxymethyl cellulose (NaCMC). In the case of NaCMC, dispersion is attained because the hydrophobic region of the amphiphilic surfactant molecule adsorbs onto the surface of SWCNT whilst the hydrophilic component is solvated. Several studies have reported the dispersion of SWCNT in water via covalent and non-covalent functionalisation^{[7] [12] [13] [14]}. Consequently, NaCMC is also known to modify flow behaviour of rubber lattices including PvNRL^{[5] [7]}.

In this study, the flow behaviour of PvNRL/SWCNT blends prepared via the latex stage mixing method have been investigated. SWCNT non-covalently dispersed in water using NaCMC as a surfactant/dispersant was used. Varying shear rates ($0.1 - 100 \text{ s}^{-1}$) was applied using a rotational viscometer fitted with concentric cylinder geometry. To study the effect of temperature, flow behaviour was investigated at 3 isothermal temperatures (25, 30 and 35° C). This is based on the probable conditions reached during storage, handling and processing. The Power law model was successfully fitted to experimentally obtained results, and have been used to further elucidate the observed flow behaviours.

3.6: EXPERIMENTAL

3.6.1: Materials and sample preparation

Medium modulus prevulcanised natural rubber latex (PvNRL) and Tuball™ SWCNT suspension were used in this study. The PvNRL/SWCNT blends were prepared using the same loading regime described in SECTION A (Page 36).

The blends prepared have been assigned the following alphanumeric codes: Pv-NB/1, Pv-NB/2, Pv-NB/3 and Pv-NB/4. The numerical aspect of the codes signifies the increasing loading of SWCNT nano-suspension, i.e., 0.02, 0.04, 0.06 and 0.08 wt. % (Per 100g rubber weight).

The pH of the PvNRL blends were monitored using a probe pH metre (OHAUS Europe GMBH, Switzerland), and maintained at 10.7 using 0.5 M potassium hydroxide solution. The pH measurements were performed at $20 \pm 2^\circ\text{C}$.

3.6.2: Flow behaviour measurements

The flow behaviour of PvNRL, Pv-NB/1, Pv-NB/2, Pv-NB/3 and Pv-NB/4 was evaluated 72 hours after preparing them using an Anton-paar Modular Compact Rheometer (MCR-502) fitted with a coaxial cylinder (Bob and cup) geometry measuring system and a Peltier temperature control system. Samples were stirred for a few minutes before transferring precise volumes into the sample container and placed in the test-chamber to equilibrate to the programmed isothermal test temperature (25, 30 and 35°C).

The analysis sequence was pre-programmed using the RheoCompass™ software to measure the viscosity (η) and shear stress (σ) response of the samples to applied varying shear rate ($\dot{\gamma}$). Shear rate ($\dot{\gamma}$) was logarithmically ramped from $0.1 - 100\text{s}^{-1}$, a total of 30 points with 10 seconds' interval between each test point were recorded. The choice of $\dot{\gamma}$ and $T^\circ\text{C}$ were based on the probable conditions experienced during pumping, mixing and dipping.

To assess the repeatability of the result obtained, the analysis sequence was repeated thrice (runs 1, 2 & 3) on PvNRL sample with a 2 minutes' interval from the end of the first and start of the second. As represented in Figure 3.7 the overlap of the three curves from the repeated sequences at 25 and 35°C (minimum and maximum test-temperatures) confirms reproducibility of results. There is also a clear decrease in η upon raising temperature by 10°C .

It can be seen in Figure 3.8 that an inverse relationship exists between η and σ at any specific $\dot{\gamma}$. This highlights “ $\dot{\gamma}$ -dependent” η of PvNRL, more accurately referred to as an “apparent η ” which is the η of a non-Newtonian fluid at a specific $\dot{\gamma}$. Newtonian fluids on the other hand maintain a constant η value irrespective of changes to $\dot{\gamma}$ [15].

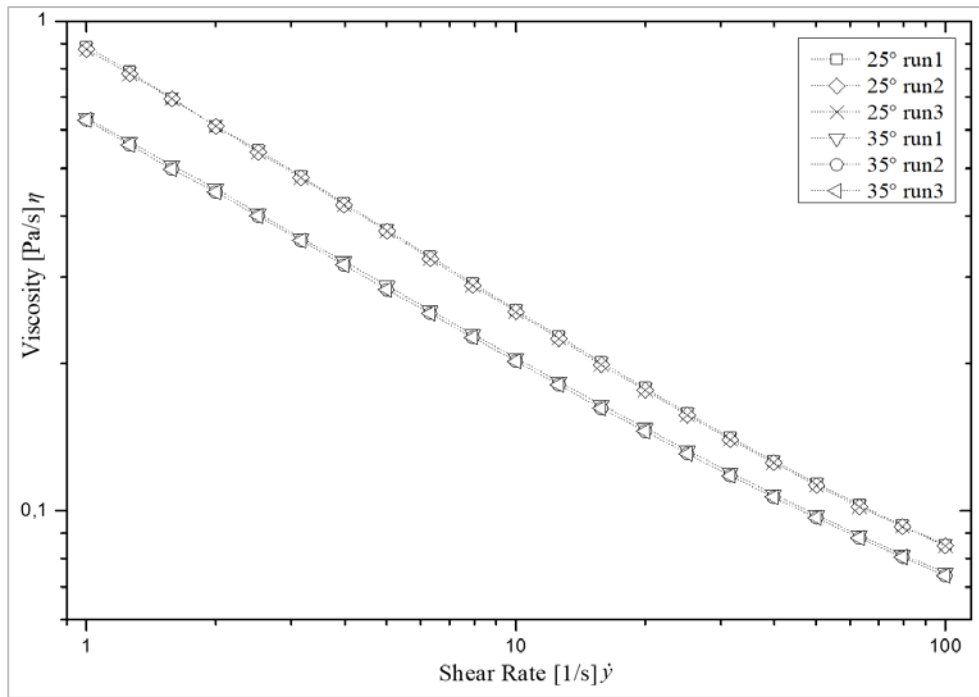


Figure 3.7: Viscosity versus shear rate of PvnRL at 25 and 35°C showing the overlay of run 1 run 2 and run 3

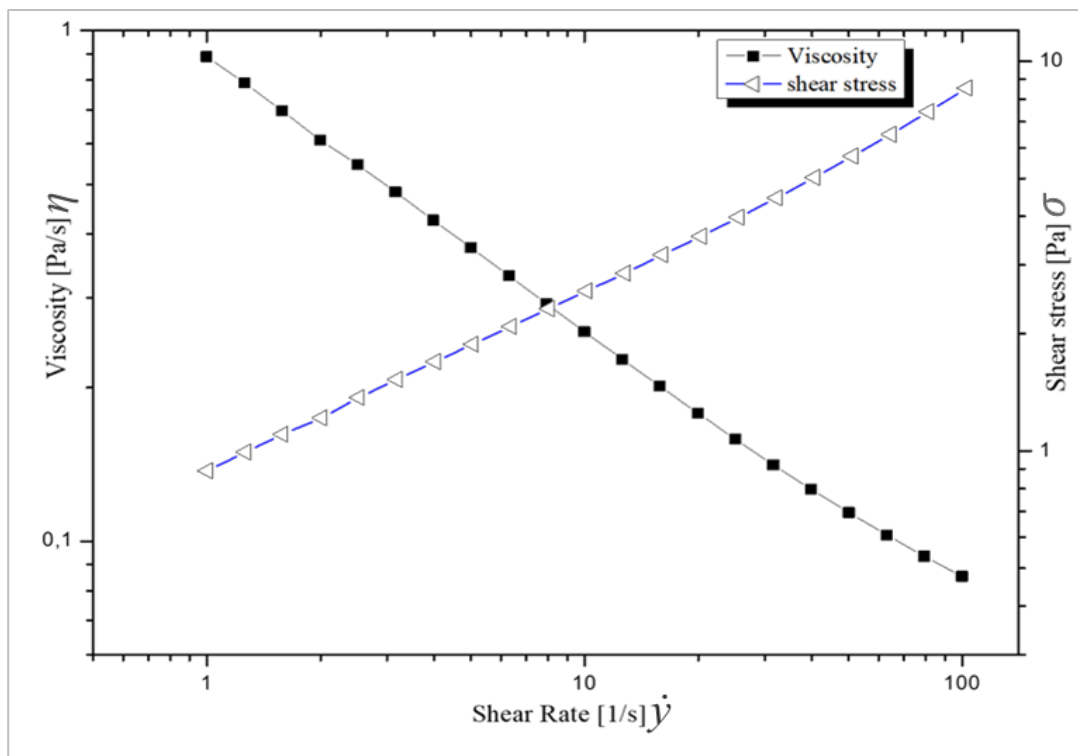


Figure 3.8: Plot showing the relationship between shear stress and apparent viscosity of PvnRL under varying shear rates.

3.6.3: Power law model

The Power Law or Ostwald de Waele as shown in equations 1 and 2, was used to mathematically represent the linear shear-thinning region. This region (dash-line in Figure 3.9) is marked by a gradual reduction in viscosity, hence referred to as “apparent viscosity” with an increase in shear rate as is observed in some controlled shear rate and temperature viscosity tests [16] [15] [17] [18].

$$\sigma = k \cdot \dot{\gamma}^n \dots \dots \dots 1 \quad \text{Or}$$

$$\eta = k \cdot \dot{\gamma}^{n-1} \dots \dots \dots 2$$

Where; σ = shear stress, $\dot{\gamma}$ = shear rate, k = consistency index, n = power law index, η = viscosity.

The power law index (n) for a shear thinning fluid is always $0 < n < 1$. Several polymeric solutions and polymer melts are known to show an n value between the range 0.3 and 0.7, whereas Newtonian fluids have n value of 1. The value of n is the slope of the linear region (dash lines) from the log-log plot of viscosity (η) or shear stress (σ) and shear rate ($\dot{\gamma}$) as shown in Figure 3.3.

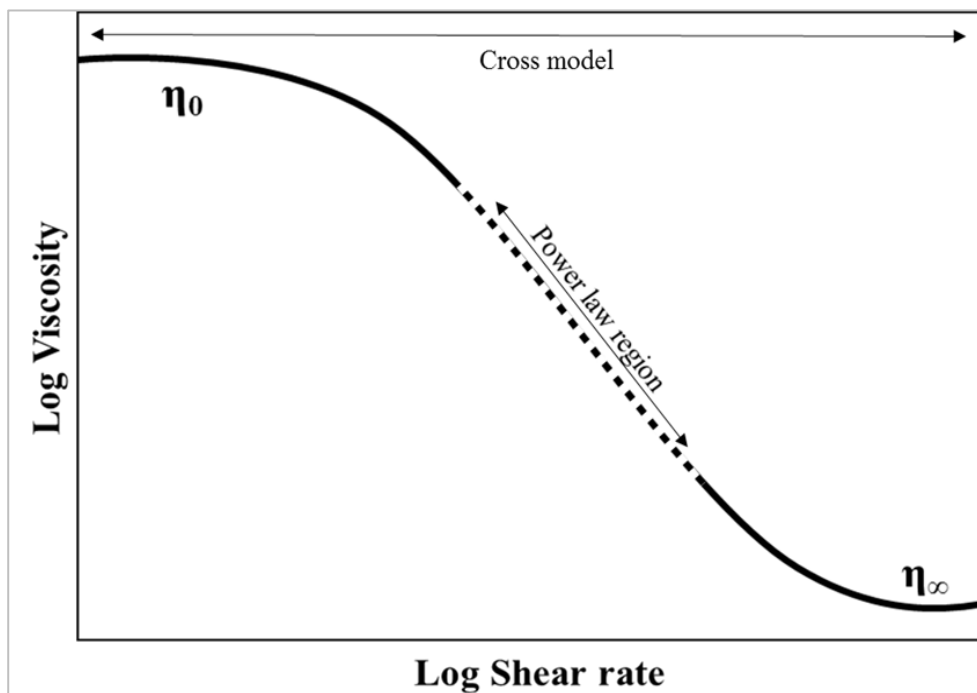


Figure 3.9: An idealised flow curve showing the power law region, zero shear and infinite shear viscosity regions; adopted from the article “Malvern Instruments Ltd”^[17].

The numerical value of the consistency index k is the viscosity measured at $1s^{-1}$ and describes the consistency of the fluid at that shear rate. Subsequently, the apparent viscosity of a fluid at any shear rate $\dot{\gamma}$ within the shear thinning region can be estimated if the values of n and k are known^{[15][17][18]}. However, the power law model is unable to predict neither the upper nor the lower Newtonian plateaus where the viscosity approaches zero ($\eta \rightarrow 0$) or infinity ($\eta \rightarrow \infty$). This limitation can easily be explained by employing the well-known Cross-WLF viscosity model.^{[15][17]}

3.7: RESULTS AND DISCUSSION

3.7.1: Effect of shear rate and Temperature on viscosity of PvNRL

The effect of shear rate ($\dot{\gamma}$) the on viscosity (η) of prevulcanised natural rubber latex (PvNRL) studied at 25, 30 and 35°C is shown in Figure 3.1.1 The measured η is an “apparent- η ” since it is seen to decrease with increasing $\dot{\gamma}$, which indicates pseudoplasticity or shear-thinning^[5]. The pseudoplastic behaviour arises from the varying contributions of the highly dissolved aqueous phase (mainly water) and the dispersed phase (mainly rubber particles) with respect to applied $\dot{\gamma}$ ^{[2][5][19]}. Several studies on rubber lattices have reported similar flow behaviour^{[2][5][16][20]}.

Two considerations are often used to explain pseudoplastic behaviour of PvNRL^{[2][5]}, namely:

- The network of asymmetric rubber particles at rest are extremely entangled and randomly orientated. However, the gradual application of $\dot{\gamma}$ begins to align particles to the direction of flow, reducing the degree of entanglement and consequently reduction in apparent η . The effects of Brownian motion could also oppose orientation of particles. Nevertheless, complete orientation may be achieved at very high $\dot{\gamma}$; this favours stronger particle-particle interactions which ultimately results in irreversible coagulation.
- Dispersed rubber particles are highly solvated at rest and the resulting effect of this interaction is a positive contribution to apparent η . However, increasing $\dot{\gamma}$ could end-up shearing away the solvated layers leading to decreasing interaction and a subsequent reduction in apparent η .

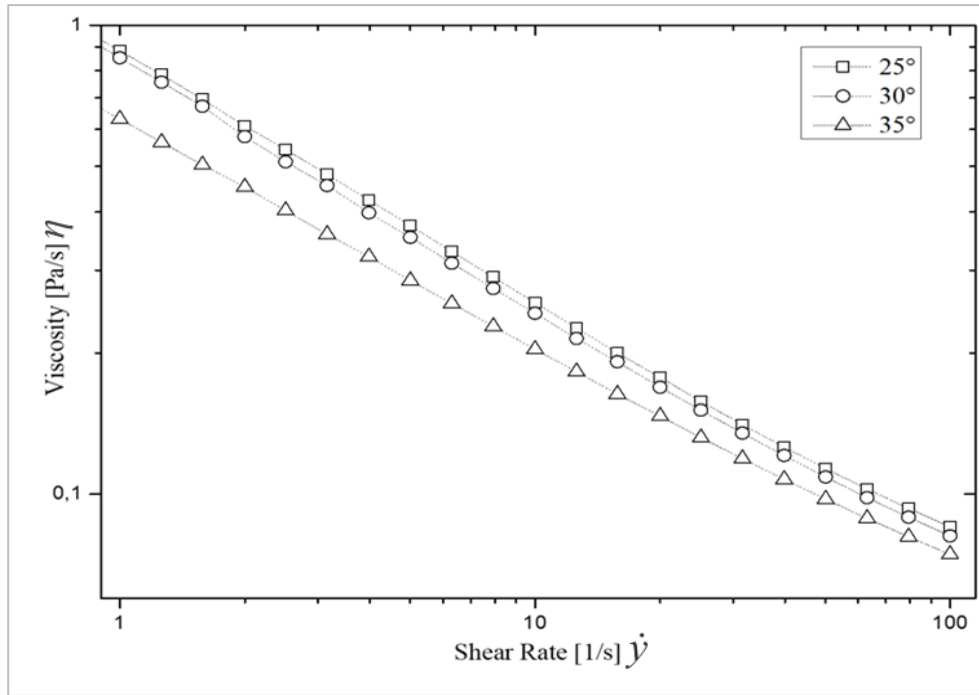


Figure 3.1.1: *Viscosity versus shear rate of PvNRL at 25, 30 and 35°C showing shear thinning behaviour*

An increase in temperature from 25 to 35°C resulted in a decrease in viscosity, especially at low shear rate ranges (between 1 – 10 s⁻¹), as shown in Figure 3.1.1. This could partly be due to an increase in free volume of the dispersion medium (aqueous phase) with increase in temperature and/or due to the removal of water molecules adsorbed to rubber particles via van der Waals forces upon raising $\dot{\gamma}$ [5].

The apparent volume (V) of colloidal latex at any temperature is the sum the volume of the individual rubber molecules (V_0) and the free volume (V_f). Therefore, raising the temperature is more likely to increase the free volume which leads to the flow unit's experiencing fewer restriction, increased energy and becoming less organized [5]. This agrees with observations reported by Sridee [20].

The decline in apparent- η or shear thinning behaviour suggests a changing colloidal structure with increasing $\dot{\gamma}$ (Figure 3.1.1). However, it is evident that the colloidal structure is quickly restored upon withdrawal of $\dot{\gamma}$, suggesting that PvNRL has no “shear-memory”, hence considered to also be pseudoplastic.

3.7.2: Effect of TUBALL™ SWCNTs suspension on viscosity of PvNRL

The effect of TUBALL™ SWCNTs suspension loadings on the viscosity (η) of PvNRL is shown in Figure 3.1.2. The blend with the least loading of the Nano-suspension exhibited the smallest apparent η , as seen for Pv-NB/1 blend at all shear rate ($\dot{\gamma}$) ranges. Although the viscosity of Pv-NB/2 matched that of PvNRL at $\dot{\gamma}$ of 1 s^{-1} , it quickly diminishes as the $\dot{\gamma}$ increases.

The decrease in η could be due to an increase in continuous phase of PvNRL upon the addition of the water based Nano-suspension. However, this is not the case for Pv-NB/3 and Pv-NB/4 blends which instead show higher apparent η compared to PvNRL. This observed modification of the bulk flow behaviour is speculated to be likely due to the effect of growing interaction between the PvNRL matrix and the surfactant stabilised SWCNT.

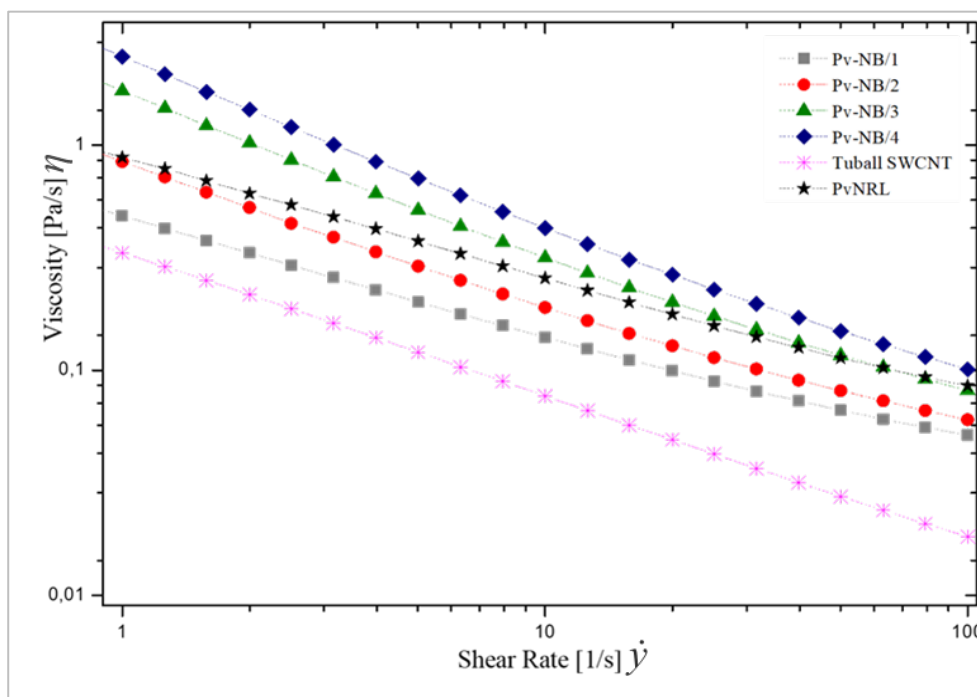


Figure 3.1.2: Plot of viscosity versus shear rate at 25°C of PvNRL, Tuball™ SWCNT and the four nanoblends.

The water-soluble anionic polymeric surfactant sodium carboxymethyl cellulose (NaCMC) is a known viscosity modifier which is extensively used in latex compounding, pharmaceuticals and food industries^{[21] [22]}. Its solubility and viscosity (η) is determined by several factors including; concentration, degree of substituted hydroxyl group (otherwise

referred to as degree of substitution), degree of polymerization and the degree of neutralisation of carboxymethyl groups (as shown in Figure 3.1.3).

The nano-suspension is also seen to exhibit shear-thinning behaviour (Figure 3.1.2). Solutions of NaCMC are known to readily show pseudoplastic behaviour as detangled polymer chains NaCMC align to the direction of flow, although low degree of polymerization would result in thixotropic flow behaviour^{[21] [22]}. Due to the amphiphilic nature of NaCMC, the hydrophilic carboxymethyl cellulose units of NaCMC become solvated in water (dispersion medium), whilst the hydrophobic SWCNT bound to the anhydroglucose units of NaCMC adsorbs onto the surface of the rubber particles^{[5] [23] [24]}.

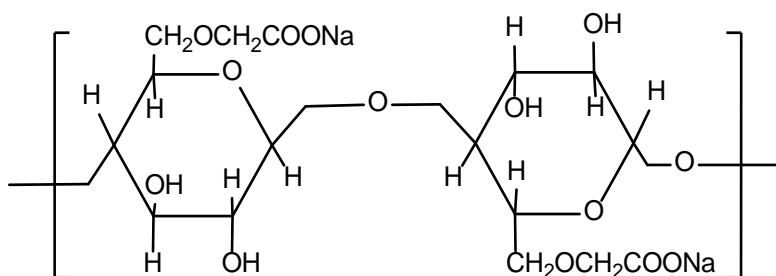


Figure 3.1.3: Chemical structure of sodium carboxymethyl cellulose showing 1 degree of substitution^[21]

Therefore, the increasing associative structure could contribute towards the observed higher apparent η of Pv-NB/3 and Pv-NB/4 as seen in Figure 3.1.2. Nevertheless, this contribution is seen to quickly diminish with increasing $\dot{\gamma}$. The extent of shear thinning is increased with higher loadings of nano-suspension, most especially for Pv-NB/3 and Pv-NB/4 where their apparent η is seen to approach that of PvNRL at $\dot{\gamma} > 10 \text{ s}^{-1}$ (Figure 3.5). A schematic showing a proposed interaction between the surfactant stabilised SWCNT present in the Nano-suspension and a rubber particle is represented in Figure 3.1.4.

Another possible explanation to the observed increase in apparent- η of Pv-NB/3 and Pv-NB/4 could arise from the increase in concentration and networks of adsorbed polyelectrolyte NaCMC onto rubber particles. This could increase the surface charge density of colloidal latex which could raise the extent of the electroviscous effect experienced during laminar shear flow, this is known to contribute to the increase in viscosity^{[25] [26]}.

The surface of colloidal rubber particles is negatively charged due to adsorbed proteins and phospholipids. The resulting van der Waals attraction between particles are counter balanced via coulombic repulsive forces resulting from dissolved cations in the aqueous phase.

Sunney and Thomas investigated the flow behaviour of low protein latex ^[5]. The study revealed that higher protein content in natural rubber latex increased the contribution of electroviscous effect which resulted in increase in apparent- η .

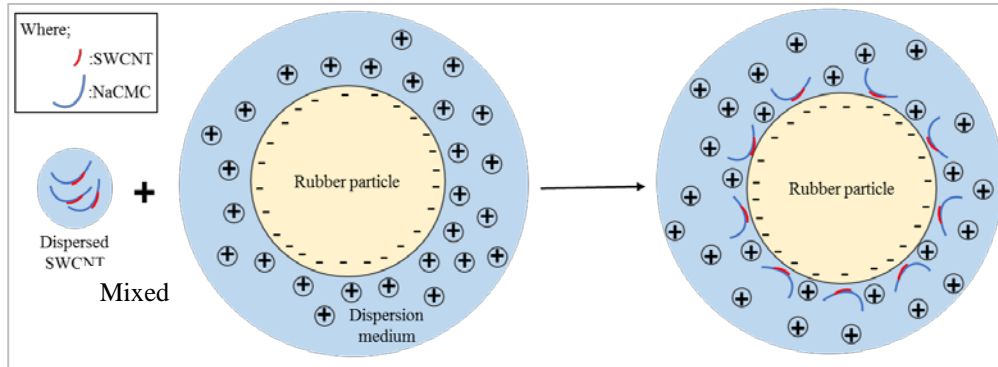


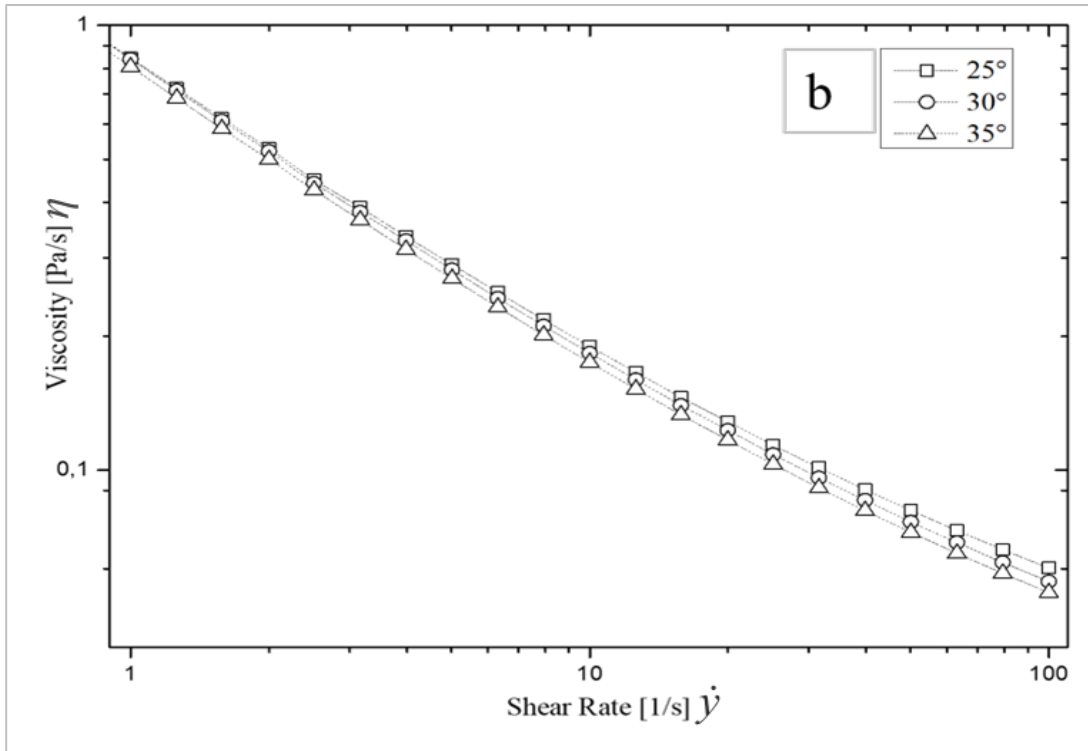
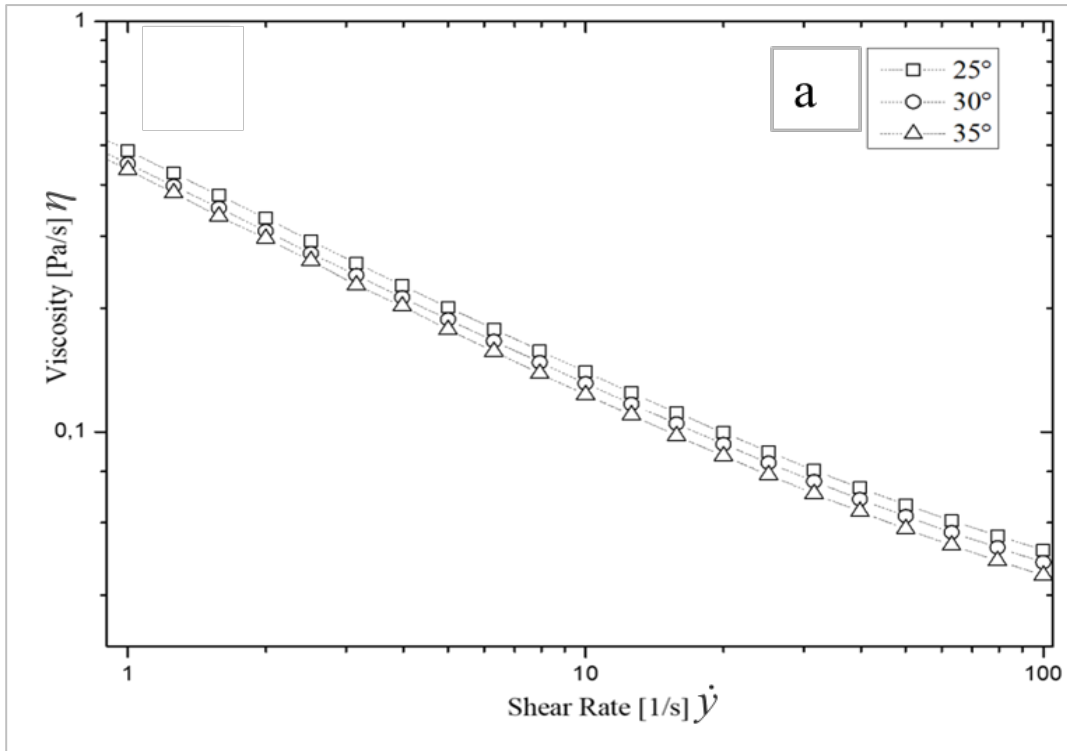
Figure 3.1.4: A schematic showing proposed interaction between surfactant (NaCMC) stabilized SWCNT and a solvated rubber particle (Note that sizes are exaggerated for clarity).

Three forms of the electroviscous effect can occur in charged colloidal systems. Firstly, when at rest, an electrical double layer (EDL) is formed around charged rubber particles by dissolved ions present in the dispersion medium. The distortion of the EDL upon shearing results to a primary electroviscous effect. Secondary electroviscous effect arises when the EDL of neighbouring particles overlap. Whereas, the probable change in shape or size of particle upon laminar shear leads to a tertiary electroviscous effect^{[5] [25] [26]}. It can be speculated that lower loadings could have disrupted the contributions of electroviscous effect, resulting in lower apparent- η of Pv-NB/1 and Pv-NB/2.

It is also evident that the earlier observed reduction in viscosity of PvNRL at 35°C gradually diminishes upon raising the loadings of the nano-suspension (see Figure 3.1.5 (a), (b), (c), and (d)). This strongly suggests a reduction in temperature sensitivity upon increasing the loading of surfactant stabilised SWCNT suspension.

This reduction in temperature sensitivity follows the order;

$$Pv-NB/4 > Pv-NB/3 > Pv-NB/2 > Pv-NB/1 > PvNRL$$



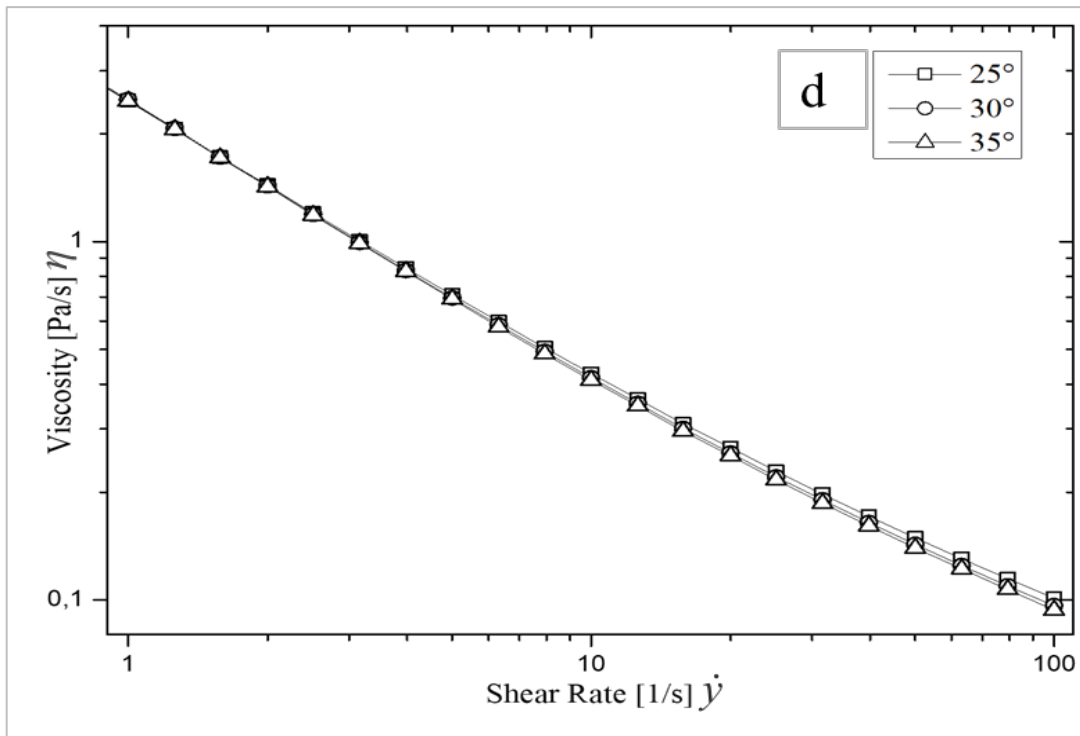
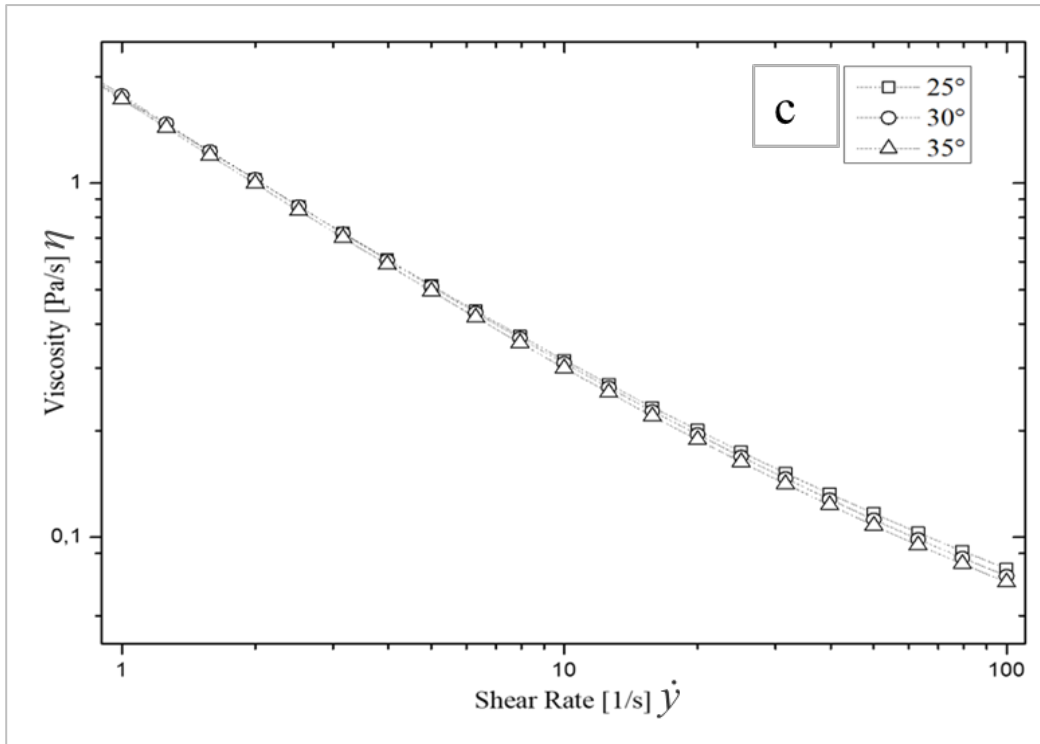


Figure 3.1.5: Viscosity versus shear rate at 25, 30 and 35°C showing shear thinning behaviour. a) Pv-NB/1, b) Pv-NB/2, c) Pv-NB/3 and d) Pv-NB/4

3.7.3: Effect of low shear rates on the flow behaviour of PvNRL and its nanoblends

The flow behaviours of PvNRL and its nanoblends at low shear rates ($\dot{\gamma}$) at 25°C are represented in Figure 3.1.6. All samples exhibited shear-thinning behaviour; however, the onset of transition from non-Newtonian to Newtonian flow is seen for Pv-NB/3 and more pronounced for Pv-NB/4 at $\dot{\gamma}$ below $\ll 1 \text{ s}^{-1}$. The appearance of a slight Newtonian plateau suggests greater equilibrium colloidal particle-interactions. This further confirms earlier suggestions that the adsorption of surfactant stabilised Nano-suspension at those loadings encouraged electroviscous effect and increased solvation of rubber particle, resulting in a slight increase in effective particle size.

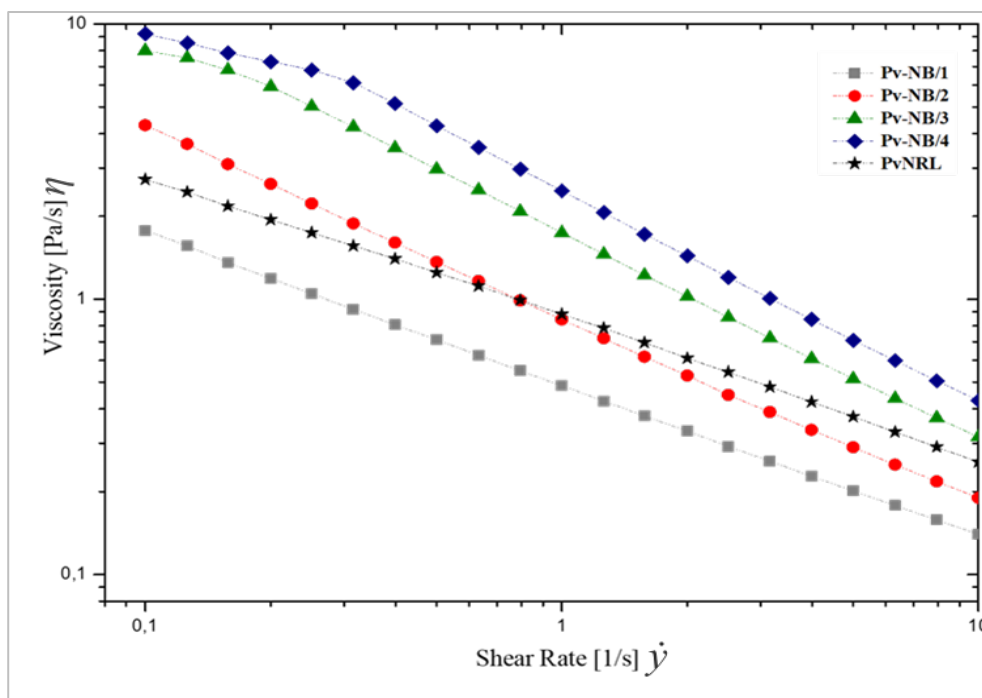


Figure 3.1.6: Viscosity versus shear rate 25°C showing the flow behaviour of PvNRL and the various nano-blends at low shear rates;

This behaviour however is not observed for PvNRL or the Pv-NB/1 and Pv-NB/2 which rather continued to shear-thin even at $\dot{\gamma}$ below $\ll 1 \text{ s}^{-1}$ suggesting that the colloidal flow units are more unevenly sheared in those respective blends. Pv-NB/2 is seen to show a higher apparent- η at shear rates below 1 s^{-1} compared to Pv-NRL. However, it begins to show significant shear-thinning as $\dot{\gamma}$ is increased.

An overlap of apparent- η of Pv-NB/2 and PvNRL can be seen around 1 s^{-1} before continuing with its downward shear-thinning trend. Pv-NB/1 remains the least viscous blend even at

low $\dot{\gamma}$ ranges. The results indicate that at higher loadings of the surfactant-stabilised nano-suspension induces more pseudoplastic behaviour to PvNRL, most likely due to the surfactant NaCMC. Claramma and Mathew^[2] also reported a similar observation in a study that compared NaCMC to other viscosity modifiers.

The instantaneous viscosity at very low shear rates is often referred to as the materials zero-shear viscosity^[15]. Figure 3.1.6 also revealed that Pv-NB/3 and Pv-NB4 possessed the highest zero-shear viscosities compared to the other blends at 0.1s^{-1} . For a colloidal system like PvNRL, a high viscosity at rest improves colloidal stability due to low occurrence of particle-particle collision that would result in irreversible coagulation^{[27] [28]}. Claramma and Mathew^[2] also reported an increase in zero-shear viscosity of PvNRL upon addition of NaCMC compared to two other common viscosity modifiers.

3.7.4 Fitting the power law model for viscosity measurements at 25°C

The correlation between shear stress (σ) and shear rate ($\dot{\gamma}$) is commonly used to demonstrate the flow behaviour of fluids like PvNRL^[16]. The results indicate that PvNRL and the nano-blends behave in a non-Newtonian manner as they show a time-independent shear thinning or pseudoplastic behaviour. The power law (Equation 1) was therefore used to model the shear-thinning region between $\dot{\gamma}$ of $1 - 10\text{ s}^{-1}$; the graphical representation is shown in Figure 3.1.7.

The power law index (n) and the consistency index (k) at 95% confidence interval was calculated from the slope of the model fittings shown in Figure 3.1.7. Fitting parameters are summarised in Table 3.3. The correlation coefficient for all the fits at 95% confidence interval are well above $R^2 \geq 0.9970$. Also, the model prediction of k which is equivalent to the measured apparent- η (at $\dot{\gamma} = 1\text{ s}^{-1}$) shows good agreement (Table 3.3). Thus, it confirms that the Power law model is able to adequately predict the flow behaviour of shear-thinning colloidal fluids like PvNRL.

An ideal Newtonian fluid has a power law of $n = 1$, deviations from this unitary value indicates shear-thinning or pseudoplastic behaviour when $n < 1$ and shear thickening or dilatant behaviour for $n > 1$ ^[15]. The value of n decreased with higher loadings of the surfactant-stabilised SWCNT (Table 3.3). This confirms that the higher loadings of the nano-suspension favours an increase in shear-thinning behaviour (since $n < 1$).

However, Pv-NB/1 is seen to be an exception, because it is observed to exhibit shear-thinning behaviour similar to that of PvNRL; as reflected by their comparable power law indices (see Table 3.3).

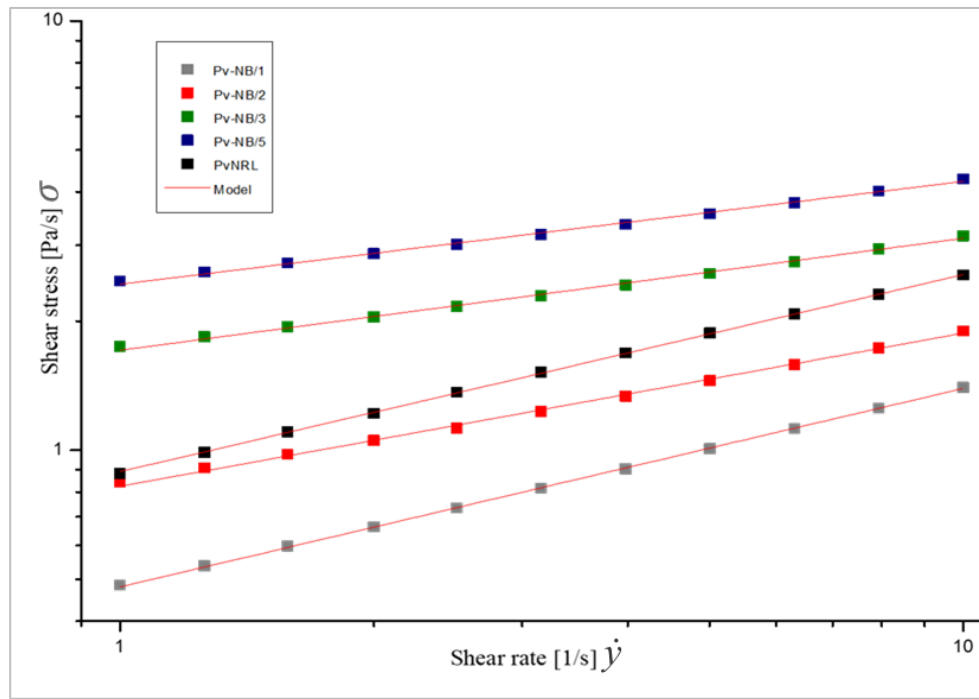


Figure 7.1.7: Shear stress [Pa/s] versus shear rate [1/s] of PvNRL and the four nano-blends at 25°C. The red-line shows the fitting of the power law model.

The consistency index (k) which is equivalent to the apparent- η at $\dot{\gamma} = 1 \text{ s}^{-1}$ reveals the consistency (or thickness) of the blends at that shear rate^[17]. Accordingly, the high apparent- η recorded for Pv-NB/3 and Pv-NB/4 at low $\dot{\gamma}$ is affirmed by their large k values. This observation infers that those blends possess higher viscosity at rest.

Consequently, Figure 3.1.8 was used to show the relationship between the power model terms k and n and the resulting significance on the flow behaviour Pv-NRL and the nano-blends. Taking a closer look at Figure 3.1.8, it is apparent that the blends with higher consistency (k) exhibited more shear thinning behaviour (n).

Again, Pv-NB/1 is an exception as it shows almost 50% decrease in consistency (k) at $\dot{\gamma} = 1 \text{ s}^{-1}$, when compared to consistency of PvNRL at the same $\dot{\gamma}$. This suggests that the concentration of the surfactant stabilised SWCNT was not significant enough to cause an increase in viscosity. Instead, the low loading of the nano-suspension leads to the dilution of PvNRL. This conclusion is supported by the observed low apparent- η and k of Pv-NB/1.

Table 3.3: A summary of the fitting parameters of the power law model for Pv-NRL and its nano-blends.

EXPERIMENTAL		MODEL PARAMETERS				STATISTICS	
Sample description	Apparent- η ($\dot{\gamma} = s^{-1}$)	k	Standard Err (for k)	n	Standard Err (for n)	Adj. R^2	Reduced Chi-Sqr
PvNRL	0.8824	0.8915	0.00271	0.4591	0.00176	0.9999	3.99301E-5
Pv-NB/1	0.4845	0.4804	0.00171	0.4625	0.00206	0.9998	1.60075E-5
Pv-NB/2	0.8441	0.8238	0.00696	0.3571	0.00511	0.9981	2.29369E-4
Pv-NB/3	1.7438	1.7105	0.01223	0.2606	0.00452	0.9971	6.2609E-4
Pv-NB/4	2.4766	2.4368	0.01525	0.2396	0.00400	0.9973	9.49175E-4

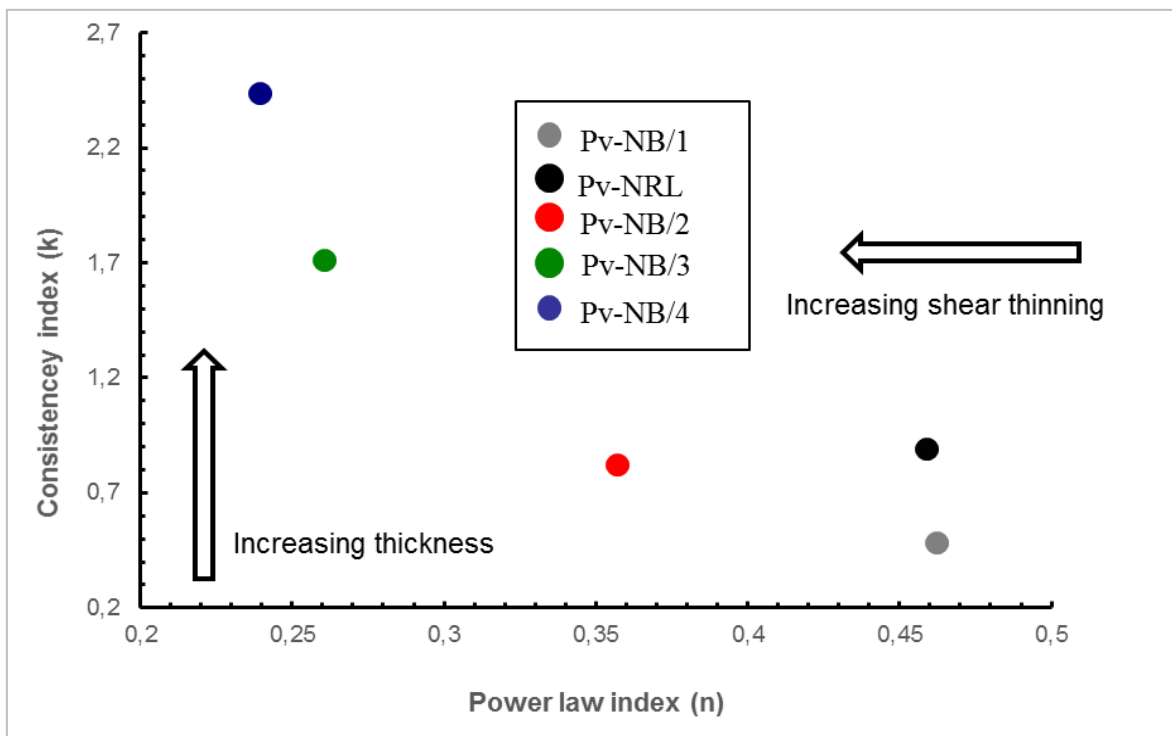


Figure 3.1.8: Interpretation of Consistency (k) versus Power law index (n) for all the samples studied.

3.8: SUMMARY OF OBSERVATIONS

- Prevulcanised natural rubber latex (PvNRL) exhibited non-Newtonian flow behaviour. This was seen with the time-independent shear-thinning when the shear rate was increased.
- It is clear that the introduction of surfactant stabilised nano-suspension influenced the flow behaviour of PvNRL. Increase in Pv-NRL viscosity with higher loadings of surfactant stabilised SWCNTs suspension was also observed. However, 0.02%/wt. loading had a dilution effect.
- The appearance of a Newtonian plateau in the limit of $\eta \rightarrow 0$ became more noticeable for Pv-NB/3 and Pv-NB/4 blends corresponding to 0.06 and 0.08 wt. % SWCNT concentration.
- A decrease in apparent- η of PvNRL at varying $\dot{\gamma}$ was observed for measurements performed at 25, 30 and 35°C. However, this observation gradually diminished with increasing loadings of the nano-suspension.
- The power law model showed good fitting and successfully predicted the flow behaviour within the modelled shear rate region.

REFERENCES

- [1] John Woon. (2013). Practical latex technology: Over 100 Questions Answered plus Many Useful Tips and Ideas (Kindle Edition ed.). 2. Available: <http://latexconsultants.blogspot.com>
- [2] N. Claramma and N. Mathew, "Studies on prevulcanization of rubber latex with special reference to influence of storage and after treatments on properties of films," Cochin University of Science and Technology, 1997.
- [3] K. O. Calvert, Polymer Latices and Their Applications. Essex, England.: APPLIED SCIENCE PUBLISHERS LTD, 1982.
- [4] NOCIL LIMITED., "Technical Note : NR-Latex & Latex Products," pp. 1-56, 2010.
- [5] S. M. Sunney and E. Thomas, "Studies on the Production, Properties and Processability of Low Protein Latex," Cochin University of Science and Technology, 2005.
- [6] K. Anand, S. Varghese, and T. Kurian, "Effect of Micro and Nano Zinc Oxide on the Properties of Pre-vulcanized Natural Rubber Latex Films," Progress in Rubber, Plastics and Recycling Technology, vol. 31, p. 145, 2015.

- [7] D. Ponnamma, S. H. Sung, J. S. Hong, K. H. Ahn, K. Varughese, and S. Thomas, "Influence of non-covalent functionalization of carbon nanotubes on the rheological behavior of natural rubber latex nanocomposites," *European Polymer Journal*, vol. 53, pp. 147-159, 2014.
- [8] O. S. N. Ghosh, S. Gayathri, P. Sudhakara, S. Misra, and J. Jayaramudu, "Natural Rubber Nanoblends: Preparation, Characterization and Applications," in *Rubber Nano Blends*, ed: Springer, 2017, pp. 15-65.
- [9] B. Mensah, H. G. Kim, J.-H. Lee, S. Arepalli, and C. Nah, "Carbon nanotube-reinforced elastomeric nanocomposites: a review," *International Journal of Smart and Nano Materials*, vol. 6, pp. 211-238, 2015/10/02 2015.
- [10] A. Mohamed, A. K. Anas, S. A. Bakar, A. A. Aziz, M. Sagisaka, P. Brown, et al., "Preparation of multiwall carbon nanotubes (MWCNTs) stabilised by highly branched hydrocarbon surfactants and dispersed in natural rubber latex nanocomposites," *Colloid and Polymer Science*, vol. 292, pp. 3013-3023, 2014.
- [11] J. M. Ngoy, S. E. Iyuke, W. E. Neuse, and C. S. Yah, "Covalent functionalization for multi-walled carbon nanotube (f-MWCNT)-folic acid bound bioconjugate," *Journal of Applied Sciences*, vol. 11, pp. 2700-2711, 2011.
- [12] T. Fujigaya and N. Nakashima, "Non-covalent polymer wrapping of carbon nanotubes and the role of wrapped polymers as functional dispersants," *Science and Technology of Advanced Materials*, vol. 16, p. 024802, 2015/04/28 2015.
- [13] S. W. Kim, T. Kim, Y. S. Kim, H. S. Choi, H. J. Lim, S. J. Yang, et al., "Surface modifications for the effective dispersion of carbon nanotubes in solvents and polymers," *Carbon*, vol. 50, pp. 3-33, 2012.
- [14] A. Anand K, S. Jose T, R. Alex, and R. Joseph, "Natural rubber-carbon nanotube composites through latex compounding," *International Journal of Polymeric Materials*, vol. 59, pp. 33-44, 2009.
- [15] R. P. Chhabra, "Non-Newtonian Fluids: An Introduction," in *Rheology of Complex Fluids*, J. M. Krishnan, A. P. Deshpande, and P. B. S. Kumar, Eds., ed New York, NY: Springer New York, 2010, pp. 3-34.
- [16] H. L. Corrêa, A. M. F. d. Sousa, and C. R. G. Furtado, "Natural rubber latex: determination and interpretation of flow curves," *Polímeros*, vol. 25, pp. 365-370, 2015.
- [17] Malvern Instruments Limited., "Using the Power Law Model to Quantify Shear Thinning Behaviour on a Rotational Rheometer," pp. 1-4, 2015.

- [18] P. Jahangiri, R. Streblow, and D. Müller, "Simulation of Non-Newtonian Fluids using Modelica," in Proceedings of the 9th International MODELICA Conference; September 3-5; 2012; Munich; Germany, 2012, pp. 57-62.
- [19] H. Lim and M. Misni, "Colloidal and Rheological Properties of Natural Rubber Latex Concentrate," *APPLIED RHEOLOGY*, vol. 26, 2016.
- [20] J. Sridee, "Rheological properties of natural rubber latex," Master of Engineering in Polymer Engineering, Polymer Engineering, Suranaree University of Technology, Thailand, 2006.
- [21] Hercules Incorporated, "Aqualon® Sodium Carboxymethylcellulose: Physical and Chemical Properties. Technical Report," pp. 3-28, 1999.
- [22] J. G. Batelaan, C. G. Van Ginkel, and F. Balk, "Carboxymethylcellulose (CMC)," *Handbook of Environmental Chemistry*, vol. 3, pp. 329-336, 1992.
- [23] I. Riou, P. Bertoncini, H. Bizot, J. Mevellec, A. Buléon, and O. Chauvet, "Carboxymethylcellulose/single walled carbon nanotube complexes," *Journal of nanoscience and nanotechnology*, vol. 9, pp. 6176-6180, 2009.
- [24] N. Minami, Y. Kim, K. Miyashita, S. Kazaoui, and B. Nalini, "Cellulose derivatives as excellent dispersants for single-wall carbon nanotubes as demonstrated by absorption and photoluminescence spectroscopy," *Applied Physics Letters*, vol. 88, p. 093123, 2006.
- [25] F. Rubio-Hernández, F. Carrique, and E. Ruiz-Reina, "The primary electroviscous effect in colloidal suspensions," *Advances in colloid and interface science*, vol. 107, pp. 51-60, 2004.
- [26] W. R. Bowen and F. Jenner, "Electroviscous effects in charged capillaries," *Journal of colloid and interface science*, vol. 173, pp. 388-395, 1995.
- [27] E. J. W. Verwey, "On the interaction of two parallel flat plates," *Theory of the stability of lyophobic colloids*, pp. 66-97, 1948.
- [28] P. B. Laxton and J. C. Berg, "Gel trapping of dense colloids," *Journal of colloid and interface science*, vol. 285, pp. 152-157, 2005.

SECTION C:
SINGLE WALLED CARBON NANOTUBES REINFORCED MALE LATEX
CONDOMS: PRODUCTION AND DETERMINATION OF DIMENSIONS.

3.9: INTRODUCTION

Since their discovery as suitable for prophylactic and contraceptive purposes in the late 19th century, male latex condoms (MLC) have steadily gained popularity and acceptability^[1]. The production of MLC involve a series of stringent procedures to ensure optimal quality^[2]. Some of these production steps include; compounding, maturation, prevulcanisation, moulding, vulcanising/curing and stripping^{[3] [4]}. Several standards including the SANS 4074:2003^[5], clearly define the design and quality specifications expected of MLC.

The MLC are moulded via the vertical dipping technique which involves the immersion of a former (mould) into a suitable liquid latex compound, followed by drying/vulcanisation^{[3] [4]}. The ability of a latex to spread uniformly over the former is critical towards obtaining quality MLC. Several factors and conditions require keen consideration to avoid irregular latex deposit. Some of which include^[4];

- Composition and viscosity of latex.
- Type of material the former (mould) is made of.
- The dipping and withdrawal rate.
- The contact angle of dipping ($\theta \sim 0^\circ$ to maximize wetting)
- Ratio of surface free energy between former and NRL (key towards achieving uniform spreading of NRL over the former).

Natural rubber latex (NRL) remains the most utilised raw material for making MLC^[2]. However, advancements in rubber technology have resulted in the production of condoms using a variety of elastomers^{[2] [6] [7]}. Generally, to improve the quality of elastomeric products, finely dispersed chemical ingredients such as vulcanising agents, accelerators, activators, fillers and stabilisers are often employed^{[4] [8] [9]}.

Unfortunately, conventional fillers like carbon black or fine particle clay are unsuitable for liquid NRL as they offer little or no form of reinforcement^{[3] [4] [10]}. The reinforcement is easily achieved during the dry compounding process because of the mastication step which creates free radical sites that interact with the reactive sites of the filler^{[9] [10]}. Conversely, the absence of the mastication step in NRL processing limits the potential of such fillers to only increasing the modulus with little or no influence on tensile and/or tear strengths^{[9] [10]}.

Nonetheless, nano-materials such as single walled carbon nanotubes (SWCNT) have shown great potential as a reinforcing filler for NRL due to their impressive strength and enormous

surface area^{[11][12][13][14]}. Although SWCNT are generally water insoluble, dispersions can be prepared through surface functionalisation which could either be of covalent, ionic or non-covalent type^{[11][15]}. This enhances uniform distribution, promotes inter-particle interaction and ultimately leads to better load-transfer between NRL and SWCNT. Even though some studies have reported on the reinforcement of NRL films with low loadings of nano-fillers like SWCNT^{[11][16][17]}, very few reported on the production of MLC using SWCNT-reinforced NRL.

Several standards have been developed which clearly specify MLC dimensions (length, width and thickness) for different target groups^{[2][18]}. For instance, wider MLC (51-54 mm) are preferred in Africa and Middle East, whereas most Asian countries prefer narrower MLC (47-50 mm)^[2]. During production, the length and width of MLC is controlled by the specifications of the glass former used. Thickness on the other hand is dependent on a number of factors including, composition and viscosity of NRL as well as the production technique^{[3][4]}. The specified thickness range of MLC according to the world health organisation (WHO) is between 0.06 – 0.08 ± 0.02 mm^[19].

In this current study, MLC were prepared from pre-vulcanised natural rubber latex (PvNRL) and PvNRL blends containing aqueous dispersion of SWCNT. A standard manufacturing process of MLC was adopted and this involved preparation of SWCNT-PvNRL blends, moulding, curing (vulcanisation), leaching and stripping. The dimensions of the MLC have also been investigated.

3.10: EXPERIMENTAL

3.10.1: List of chemicals

Ammonia solution 25 % (Sigma Aldrich, St Louis, MI, USA), propan-2-ol (Emplura® Merck, Darmstadt, Germany), Sodium chloride (SMM Instruments (Pty) Ltd, South Africa). All chemicals are of reagent grade and were used as supplied.

3.10.2: Formulation of blends

The formulation of PvNRL nano-blends was as per the formulation given in Table 3.4. The loadings of Tuball™ SWCNT and method of preparation was adopted from the specifications described in SECTION A (page 36). It can immediately be seen in Figure

3.1.9 that the introduction of SWCNT in the suspension leads to discolouration of PvNRL from the original off-white to greyish colour.

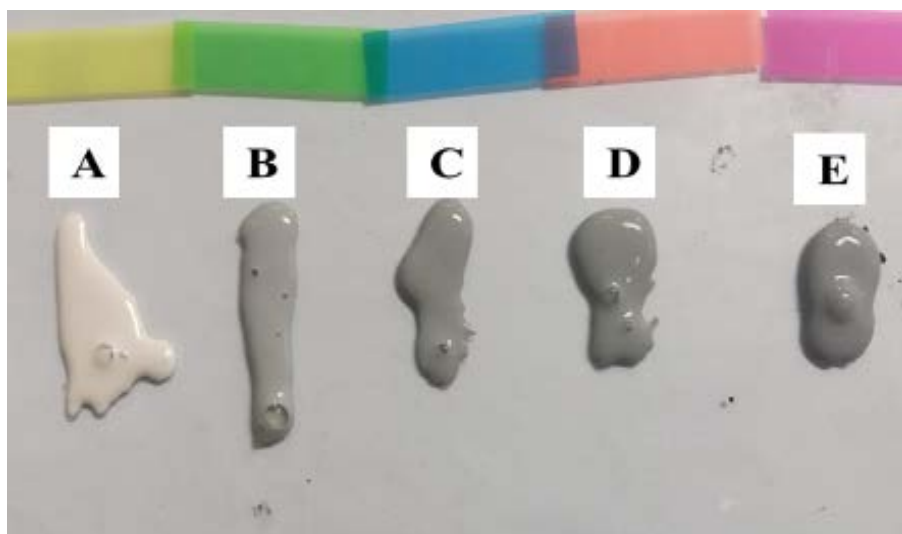


Figure 3.1.9: Image showing the discolouration of PvNRL with increasing loadings of SWCNT suspension: (A). PvNRL, (B) Pv-NB/1 (C) Pv-NB/2, (D) Pv-NB/3, (E) Pv-NB/4 .

Table 3.4: Specifications of Blend Formulation.

Blend description	Volume of PvNRL	Loading TUBALL™ SWCNTs	DRC after dilution
	(mL)	(Wt %/ DRC)	(%)
PvNRL	350	0	53
Pv-NB/1	350	0.02	55
Pv-NB/2	350	0.04	52
Pv-NB/3	350	0.06	48
Pv-NB/4	350	0.08	47

Where: Pv-NB = Pre-vulcanised natural rubber latex containing varying amounts of SWCNT; DRC = Dry rubber content.

3.10.3: Dilutions

The extent of dilution was gauged by monitoring the film thickness of MLC. In this study, 0.063 ± 0.005 mm thickness was adopted as the target thickness for MLC; this falls within WHO prescription ($0.06 - 0.08 \pm 0.02$ mm) [19]. Additionally, the narrow margin of ± 0.005 mm offset was implemented to maintain a minimal margin of error. Film thickness is a function of viscosity and dry rubber content (DRC), and the final DRC after dilution is shown in Figure 3.1.9. The method of dilution with respect to film thickness involved the following activities:

- (i) Three pieces of MLC were moulded from each blend (Table 3.5) and the thickness determined (Moulding technique and thickness determination are explained later in this section).
- (ii) A step-wise dilution was performed using 1% ammonia (NH_3) solution to adjust the DRC: predetermined volumes of 1% NH_3 was slowly added to the latex blends under low stirring (30 rpm) using an overhead stirrer (Heidolph RZR1) fitted with a gate geometry spindle. Subsequently, step (i) was repeated.
- (iii) About 1 mL of the diluted blends from step (ii) was drawn using a micro-pipette (P1000, pipetman®), then carefully dropped on a glass tray at room temperature (horizontally placed); the tray was then tilted vertically ($\sim 90^\circ$ angle) to initiate a downward flow (Figure 3.1.4).
- (iv) Time taken for the respective blends to get to the bottom of the glass tray (height $\sim 455 \pm 2$ mm) was noted.

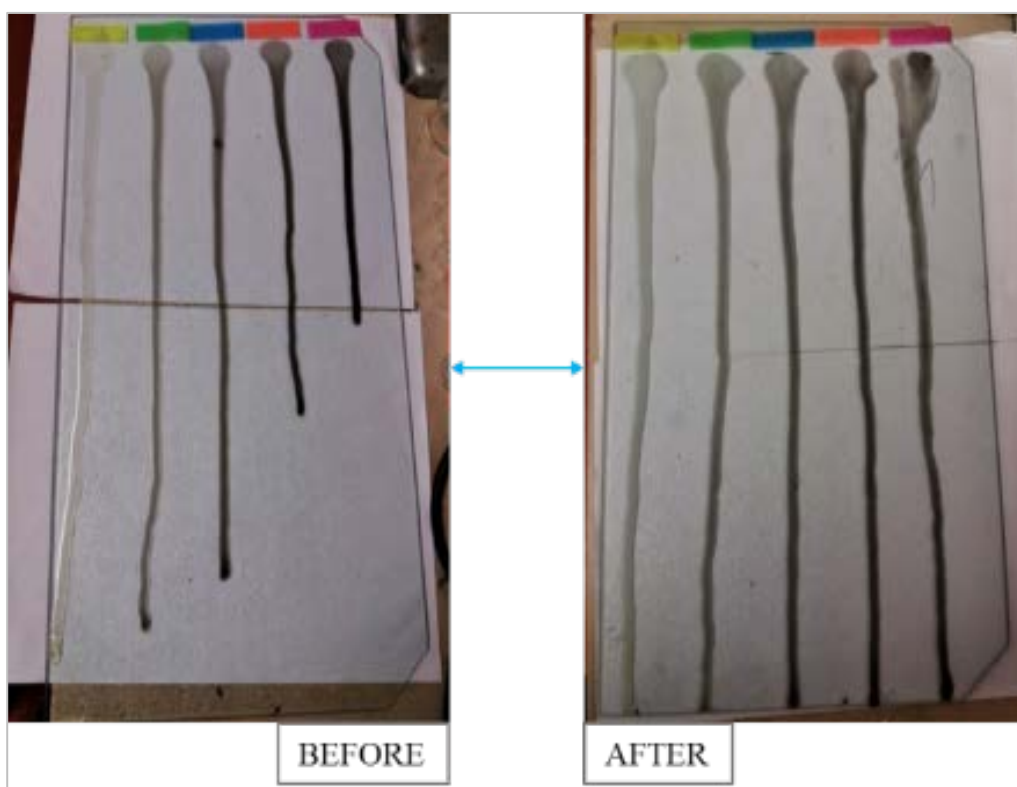


Figure 3.1.1.1: *Image showing the effect of dilution on viscosity. From left to right: PvNRL, Pv-NB/1, Pv-NB/2, Pv-NB/3 and Pv-NB/4.*

The extent of dilution in step (ii) was adjusted until all the blends achieved similar time (about 15 secs) for step (iv). The observation from step (iii) reveals the viscosity of the blend under the influence of earth's gravity (kinematic viscosity). The thickness of MLC is known to be influenced by the viscosity of latex compound used during the dipping process. Figure 3.1.1.1 shows the before and after effects of dilution.

3.10.4: Moulding

Prior to moulding, the diluted latex blends were transferred into the dipping chamber and left to deaerate in the fume hood for 24 hours. This precautionary measure is necessary to ensure the expulsion of trapped air which is known to compromise film integrity^[4]. Glass formers (Borosilicate glass former; length 290 *mm*, outside diameter 54 *mm*) were washed using soap solution, rinsed twice with distilled water, dried in an oven at 40 °C and left to cool.

Moulding of MLC was done via the vertical dipping method; a single and double dip procedure was adopted for this study. The quality of MLC film from the single dipping procedure revealed the wettability of the various PvNRL blends with respect to their viscosities. Whereas, double dipped procedure was employed to correct for any surface defect(s) that could occur from a single dip step. Figure 3.1.1.2 shows the dipping set-up where a clean glass former is carefully fastened to the attachment, is cautiously lowered into the diluted latex blend and withdrawn. The usual timing between each action in this routine was 15 seconds for lowering, 10 seconds dwelling and 25 seconds withdrawal.

The coated former was immediately detached from the attachment, inverted and rotated between angles 45° and 135°. This is to ensure even distribution of latex and for the prevention of the formation of tip blob. The inversion and rotation was done about 100 *mm* away from a hot-air fan (60 °C) to facilitate drying. For the double dipped MLC, the dried single dipped formers were let to cool before repeating the dipping process following the considerations earlier stated. The cooling of formers before performing the second dip was necessary in order to avoid heat sensitization of the latex, which is known to cause destabilisation.

The beading operation of the open end of MLC were performed by hand^[3]. This involved gentle downward strokes of the thumb around open end; the glass former was rotated clockwise after each stroke to ensure even beading.

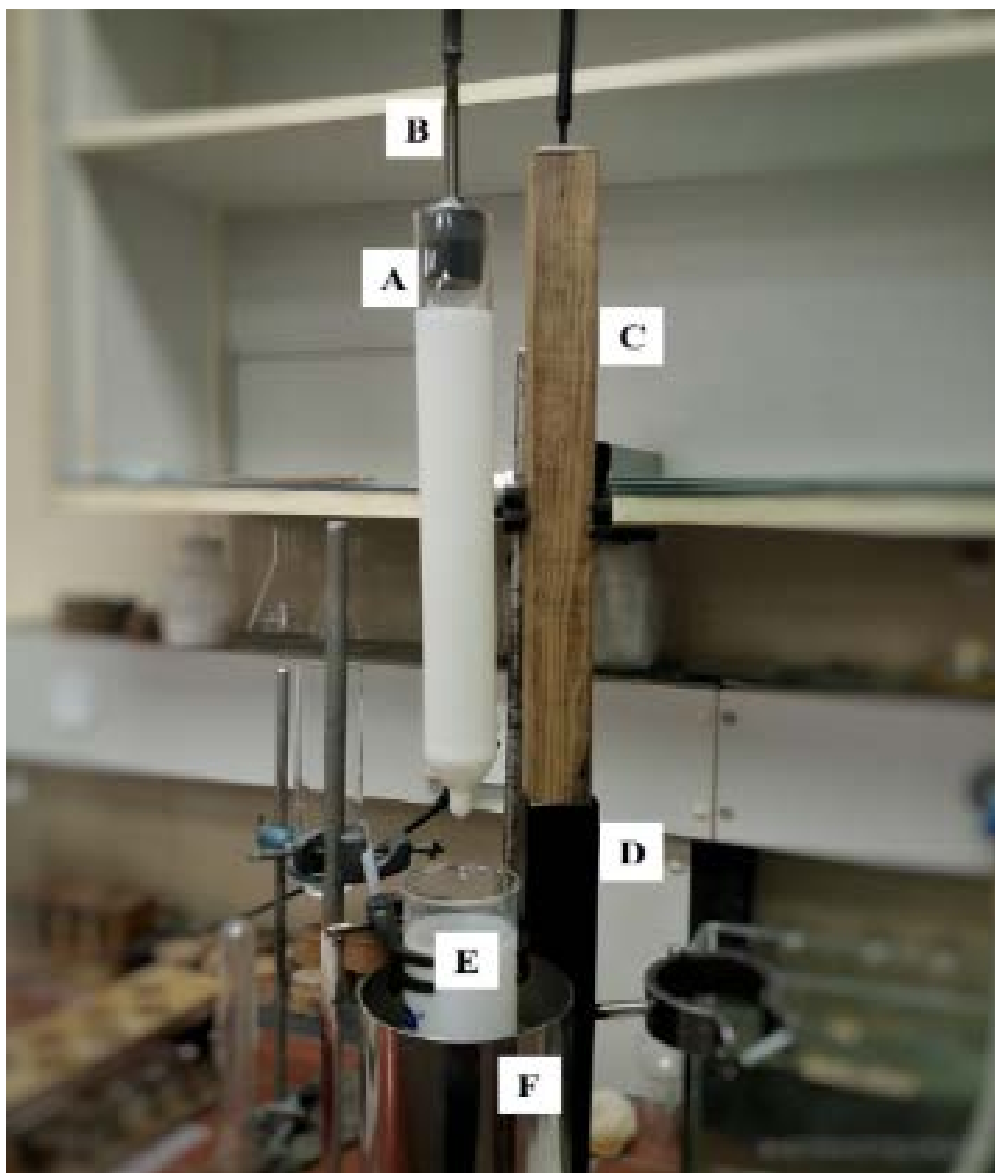


Figure 3.1.1.2: *Dipping set-up: (A) glass former, (B) former attachment, (C) wooden guide, (D) hollow steel pipe, (E) dipping chamber, (F) water jacket.*

3.10.5: Vulcanisation, leaching and stripping

The dry beaded products were vulcanised in an air oven at 70°C for a duration of 30 minutes. Afterwards, the former together with the products were leached in boiling distilled water at 90°C to expel water-soluble compounding ingredients^{[3][4]}. The surface of products was then dried using compressed air. Summarised schematic is as shown in Figure 3.1.1.3.

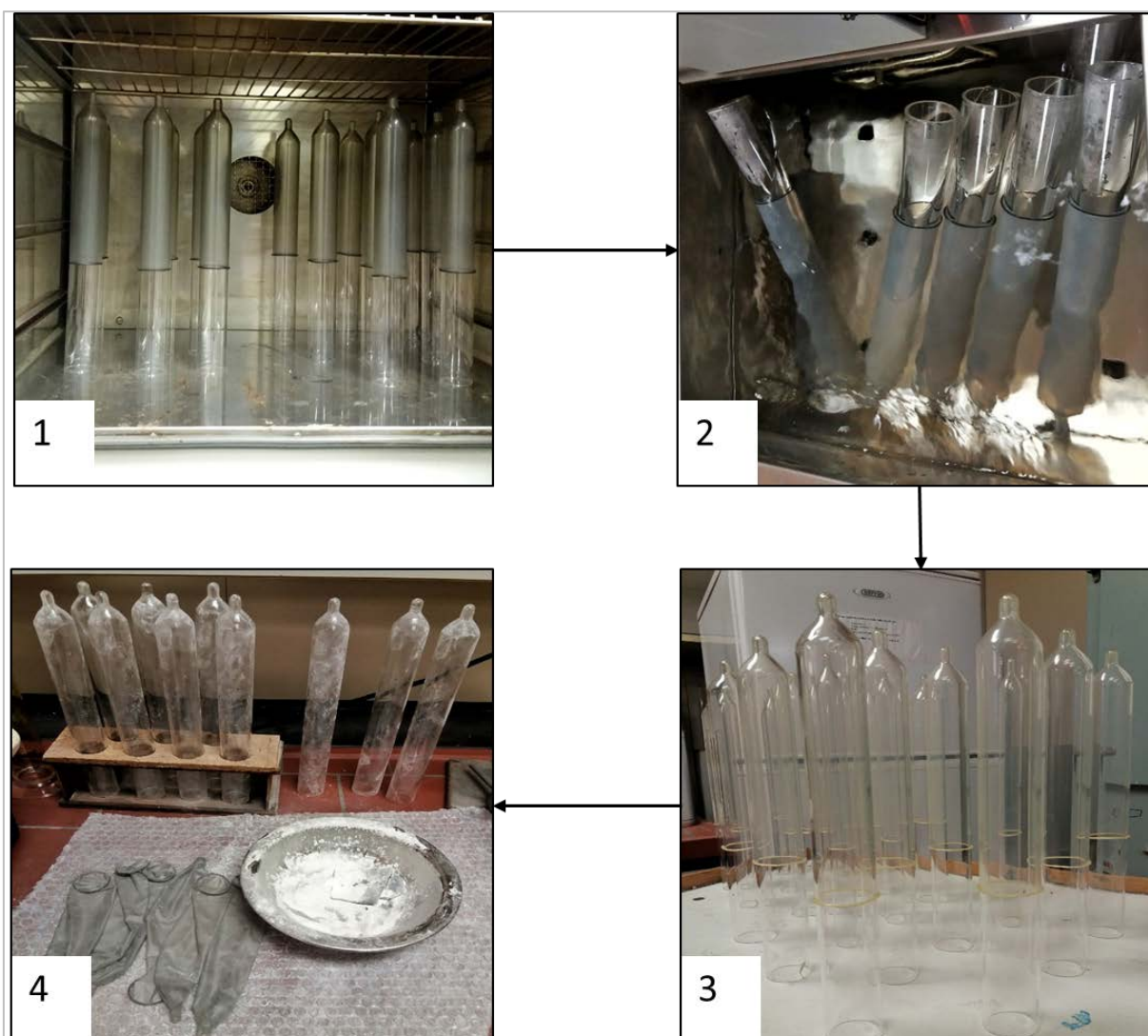


Figure 3.1.1.3: *Schematic showing various production steps; (1) vulcanisation, (2) leaching, (3) drying (4) dry stripping*

The MLC were stripped off the glass formers through the dry stripping method where talc (French chalk) was thoroughly applied on the products to eliminate tackiness^{[3] [4]}. It can be seen in Figure 3.1.1.4 that the bead at the open end is clearly visible and that the incorporation of SWCNT-suspension affected the colour of MLC. Again, the resulting discolouration clearly increases with increasing loading of the nano-suspension. The final articles were subsequently stored away from direct sunlight in airtight containers prior further analysis.



Figure 3.1.1.4: *Samples of MLC produced using the different latex blends. From left to right; PvNRL, Pv-NB/1, Pv-NB/2, Pv-NB/3 and Pv-NB/4.*

3.10.6: Determination of length and width

Both length and width measurements were done according to specifications stated in SANS 4074:2002/Cor.2:2008^[5]. The MLC were placed over a mandrel to hang freely, and stretched only by its weight. The length was measured to the nearest *mm* using a ruler. In this study, a retort stand pole of external diameter of 9.85 mm was utilised as mandrel.

For width measurements, the MLC were laid out flat, and the measurements were taken to the nearest *mm* by placing a ruler perpendicular to the MLC. The width reported here was measured from the area 30 ± 5 mm away from the open end of the MLC.

3.10.7: Determination of thickness

The determination of thickness of thin film materials such as MLC remains a challenging task. This is largely because of the difficulty posed by soft-thin nature of MLC. Theoretically, thickness is recorded as the distance between the spindle and the foot of the micrometre or caliper in contact with the specimen^[20]. In practice, micrometres and Vernier caliper are the commonly used measuring systems. However, thickness measurements of thin films using these instruments are known to give inconsistent results^{[5] [19]}. As a result,

in this study thickness was also determined by calculating the volume of Rectangular test specimens using the thickness formula as described below.

The rectangular shaped test pieces were carefully cut out from the mid-region of the MLC, using a parallel blade cutter (~8.5 mm apart). The mid-region is defined as the area 25 ± 5 mm away from the open end and 25 ± 5 mm away from the closed tip of the MLC. Test pieces were cut along the circumferential direction of the MLC. The samples were washed in propan-2-ol and dried to constant mass at 35°C. The methods used are summarised as follows:

- (i) **Micrometre Method (MMSG):** A digital micrometre screw gauge (TA IP54, Spellbound Lab. Solution. South Africa) with a resolution of 0.001 mm was used. Other specifications of the MMSG includes; a foot diameter of 6 mm and foot pressure of 25 kPa (Figure 3.1.1.5).

For measurements, test-specimen were placed on the anvil and the ratchet was turned until the spindle makes contact. A single click-sound is made by the MMSG to signify contact with test-specimen. In total, 10 rectangular MLC test pieces were analysed and the thickness of an individual test specimen was measured at the left, middle and right end. The average of the 3-measurements is reported.

- (ii) **Vernier method (VCp):** A digital Vernier caliper (ULTRA CAL VI, Fowler High precision, Massachusetts. USA) with a resolution of 0.01 mm was used (Figure 3.1.1.5).

The thickness of the same sample(s) in method (i) were then measured following the considerations stated earlier. The measurements were done using the rectangular section of the outside calliper jaws (length 10.9 mm and width 3.5 mm).

- (iii) **Thickness formula method (Fmlr):** Thickness of 10 test pieces (same samples from methods (i) & (ii)) was calculated as a ratio of the volume of the rectangular test piece to its surface area^[5].

The length and width of the test-specimen was measured using a graduated ruler, and mass determination was done on a microbalance (Mettler Toledo, UMT2. Switzerland). The mathematical expressions used are as follows:

$$t = \frac{1}{\rho} \times \frac{1}{A} \times m \dots \dots \dots (3)$$

$$A = W \times L \dots \dots \dots (4)$$

Where: t = thickness of test piece (mm)
 ρ = density of latex rubber (0.933 g/cm^3)
 A = area (mm^2) and m = mass (mg) of the test piece
 W = width and L = length (mm)

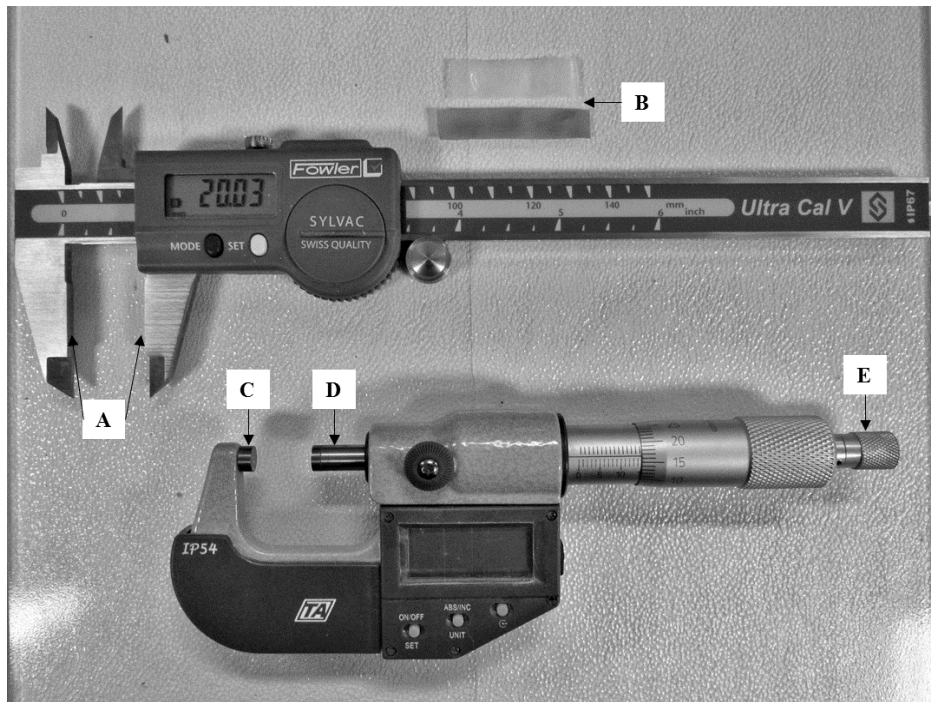


Figure 3.1.1.5: *Materials for thickness determination. (A) Vernier caliper (inside jaws), (B) rectangular test-specimens, (C) Anvil (Micrometre), (D) spindle and (E) ratchet.*

3.10.7.1: Comparison of results from thickness measurements

Statistical differences between the methods were analysed using analysis of variance (ANOVA) assuming single factor. Results obtained revealed significant statistical difference between the measured thickness and method used (ANOVA, $P < 0.003136$). This is as illustrated in Figure 3.1.1.6. Furthermore, a series of t-Test (Two-sample assuming equal variances) was used to compare the thickness measured from the 3 methods.

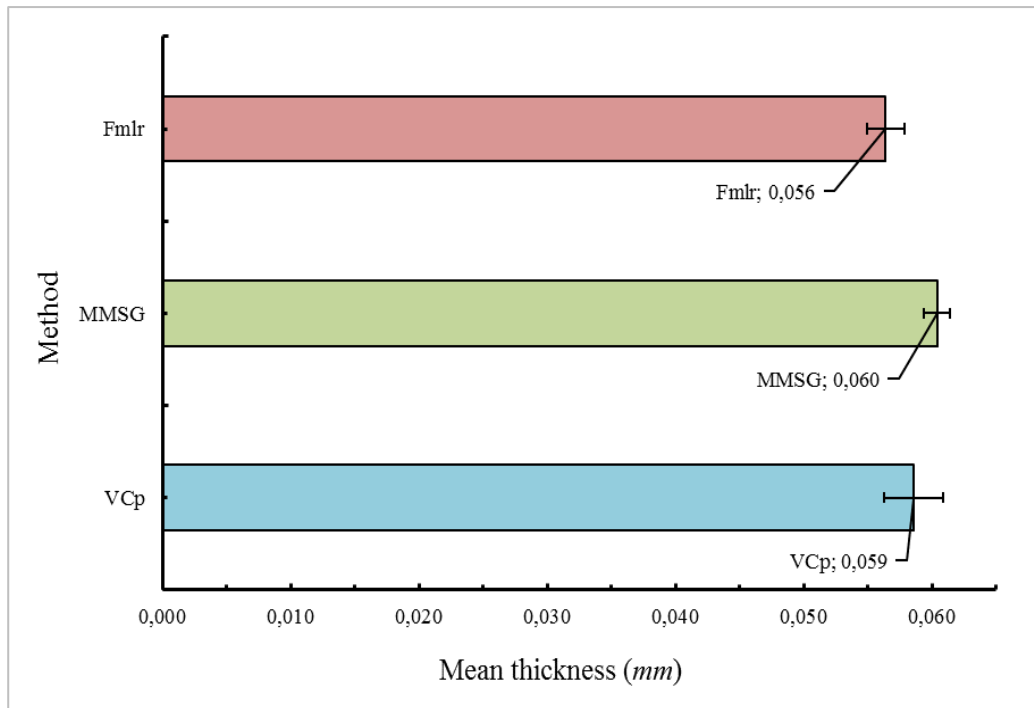


Figure 3.1.1.6: *A plot of method versus average thickness for the mid region of the male latex condoms.*

The following interpretations are put forward following the results of the t-test:

- (i) **MMSG – Fmlr:** there is a significant statistical difference in mean thickness, therefore cannot be explained by experimental error (t-test, $p < 0.0009$).
- (ii) **MMSG – VCp:** the observed difference in mean thickness can most likely be explained by experimental error (t-test, $p = 0.1236$).
- (iii) **VCp – Fmlr:** the observed difference in mean thickness could be explained by experimental error (t-test, $p = 0.08636$).

The results of mean thickness so far show some degree of discord between methods employed. The nonconforming results obtained from Fmlr method and the other two (VCp and MMSG) could most likely be due to the uneven surface (surface roughness) and the irregular thickness of the test specimens^[20]. In addition, the thickness values calculated using the Fmlr method assumes an equal volume of test specimen, which is less likely so since it doesn't account for irregular surface topography.

The slight inconsistency between the thickness measured using MMSG and VCp could be attributed to the difference in applied pressure and the resulting compression of the soft test-specimen at the contact points. The extent of compression is known to be influenced by the amount of pressure applied on the test specimen^[20].

3.11: SUMMARY OF OBSERVATIONS

- The incorporation of Tuball™ SWCNT suspension into PvNRL caused a clear discolouration.
- Dilutions of the various PvNRL blends prepared was performed before moulding the MLC. The diluted blends exhibited similar viscosities based on the result from the method of identification developed.
- The MLC were successfully made through the straight dipping technique, using a custom designed production set-up.
- Other production activities such as beading, leaching and dry stripping were successfully mastered and executed.
- Determination of dimensions (length, width and thickness) was successfully executed. The average length measured were; $\sim 191.17 \pm 5.17 \text{ mm}$ and $52.67 \pm 5.17 \text{ mm}$ respectively.
- 3 methods were employed to determine MLC thickness. Statistical analysis on the results obtained showed varying levels of agreement amongst the methods of determination.

REFERENCES

- [1] V. L. Bullough, "A Brief Note on Rubber Technology and Contraception: The Diaphragm and the Condom," *Technology and Culture*, vol. 22, pp. 104-111, 1981.
- [2] UNAIDS, "THE MALE LATEX CONDOM: 10 condom programming fact sheets," ed: WHO library, 2001, pp. http://data.unaids.org/publications/irc-pub01/jc003-malecondom-factsheets_en.pdf. Access Date: 17/08/2017
- [3] M. Jasmin and N. Mathew, "Influence of compounding and process variables on quality of condoms made from natural rubber latex," *Cochin University of Science and Technology*, 1996.
- [4] K. O. Calvert, *Polymer Latices and Their Applications*. Essex, England.: APPLIED SCIENCE PUBLISHERS LTD, 1982.
- [5] SANS 4074:2003., "Natural latex rubber condoms," in *Requirements and test methods*, ed. 1 Pretoria: SABS Standard Division, 2008.

- [6] M. Callahan, C. Mauck, D. Taylor, R. Frezieres, T. Walsh, and M. Martens, "Comparative evaluation of three Tactylon™ condoms and a latex condom during vaginal intercourse: breakage and slippage," *Contraception*, vol. 61, pp. 205-215, 2000.
- [7] M. J. Rosenberg, M. S. Waugh, H. M. Solomon, and A. D. Lyszkowski, "The male polyurethane condom: a review of current knowledge," *Contraception*, vol. 53, pp. 141-146, 1996.
- [8] D. C. Blackley, *Polymer Latices: Science and Technology Volume 3: Applications of Latices*: Springer Science & Business Media, 2012.
- [9] NOCIL LIMITED., "Technical Note : NR-Latex & Latex Products," pp. 1-56, 2010.
- [10] R. Joseph, "Latex compounding ingredients," in *Practical guide to latex technology*, Abridged edition 2013 ed: Smithers Rapra Technology, 2013, p. 122.
- [11] A. Anand K, S. Jose T, R. Alex, and R. Joseph, "Natural rubber-carbon nanotube composites through latex compounding," *International Journal of Polymeric Materials*, vol. 59, pp. 33-44, 2009.
- [12] O. S. N. Ghosh, S. Gayathri, P. Sudhakara, S. Misra, and J. Jayaramudu, "Natural Rubber Nanoblends: Preparation, Characterization and Applications," in *Rubber Nano Blends*, ed: Springer, 2017, pp. 15-65.
- [13] C. S. Yah, S. E. Iyuke, G. S. Simate, E. I. Unuabonah, G. Bathgate, G. Matthews, et al., "Continuous synthesis of multiwalled carbon nanotubes from xylene using the swirled floating catalyst chemical vapor deposition technique," *Journal of Materials Research*, vol. 26, pp. 640-644, 2011.
- [14] G. S. Simate and L. F. Walubita, "Synthesis, Properties, and Applications of Carbon Nanotubes in Water and Wastewater Treatment," *Advanced Nanomaterials for Wastewater Remediation*, p. 201, 2016.
- [15] J. M. Ngoy, S. E. Iyuke, W. E. Neuse, and C. S. Yah, "Covalent functionalization for multi-walled carbon nanotube (f-MWCNT)-folic acid bound bioconjugate," *Journal of Applied Sciences*, vol. 11, pp. 2700-2711, 2011.
- [16] S. V. Shankar and R. Dinesh, "Experimental Study on Manufacture and Analysis of Rubber Nanoclay Mwcnt Composite," *International Journal of Environmental Science and Development*, vol. 1, p. 181, 2010.

- [17] Z. Peng, C. Feng, Y. Luo, Y. Li, and L. Kong, "Self-assembled natural rubber/multi-walled carbon nanotube composites using latex compounding techniques," *Carbon*, vol. 48, pp. 4497-4503, 2010.
- [18] M. Reece, D. Herbenick, S. A. Sanders, P. Monahan, M. Temkit, and W. L. Yarber, "Breakage, slippage and acceptability outcomes of a condom fitted to penile dimensions," *Sexually Transmitted Infections*, vol. 84, pp. 143-149, 2008.
- [19] WHO/UNFPA., "Male Latex Condom: Specification, Prequalification and Guidelines for procurement," ed. Switzerland: World Health Organization, 2010.
- [20] W. Holt, "Screw micrometer gages for rubber specimens," *BS J. Research*, vol. 10, p. 575, 1932.

SECTION D

**PHYSIOMECHANICAL ANALYSIS OF SINGLE WALLED CARBON
NANOTUBES REINFORCED MALE LATEX CONDOMS**

3.12: INTRODUCTION

A reliable male latex condom (MLC) is the one that is convenient to use, impermeable to micro-organisms such as viruses, and is able to withstand the often rigorous nature of coitus. Several biomechanical analyses designed to ensure the quality and reliability of MLC have been put in place by various countries and standard organisations. The International Standards organisation (ISO) first published a series of test methods for condoms in 1990^[1]. However, earlier regulations on the quality of MLC included the 1950 Swedish standard^[2], and the 1964 British standard^[3]. Over the years, these test methods have undergone a number of revisions. For instance, the ISO standard has been revised in 1996, 2002 and most recently 2008.

The South African National Standard (SANS) published in 2009 adopted the specifications in the ISO 4074:2002/Cor.2:2008 standard^[4]. The analyses methods for MLC stipulated by SANS includes; tensile test, test for holes, inflation test, package seal, dimension specifications and lubricant quantity^[4]. MLC are tested for freedom of holes using two methods; water leakage test and electrical conductivity measurements. The burst pressure and volume of MLC are determined using a controlled air inflation test. These standardised test methods are designed to expose the MLC to extreme forms of stress/strain, so as to ensure overall mechanical integrity. However, the pseudo-static deformation of the MLC during air inflation and test for holes are in sharp contrast to the dynamic stress/strain deformations subjected on MLC during use.

A number of alternative test methods for condoms have been proposed. For instance, Torres *et al* developed a model Rheological Quality Test Systems (RQTS)^[5] designed to test for holes in condoms. The RQTS technique involves measuring the resultant conductivity after exposing condoms to a shock wave. However, RQTS technique required large quantities of water, which becomes a challenge. This proposed method was subsequently rejected by ISO after duly scrutinizing the technique, as it deemed it less feasible.

Gerofi and Wong^[1] developed a fatigue test method for male condoms by redesigning the ISO 4074 conductivity test method. The method involved applying controlled cyclic deformation via a continuous inflation and deflation of the test sample during conductivity measurements. This was maintained until the measured conductivity exceeded the specified limit as defined in ISO4074. The cyclic deformation regimen was used to simulate the probable deformation exerted on a condom during use.

The desire to produce thinner, desirable yet effective latex condoms provides a new challenge; this is because of the significant decrease in strength/modulus upon stretching, which could increase the risk of failure. It has been reported that act of donning a condom results in an estimated ~25% stretching of the material in the circumferential direction; which was established based on an average erect penile girth of ~126 mm^[6].

When a condom is donned, it experiences a constant strain/deformation stemming from the girth of the erect penis. An inward seal pressure is formed in the circumferential direction due to the resultant induced (hoop) stress, ensuring the condom stays in place as mechanical barrier^[7]. The absence of or even inadequate lubrication could also result in a build-up of additional shear stress that occurs tangentially to the condoms outer surface due to the sliding friction associated with coitus. However, such shear stresses can be minimised through adequate lubrication of the condoms^[8].

The probable decrease in elastic modulus of latex condoms, as a result of strain induced stress relaxation, could be improved upon by the incorporation of reinforcing fillers such as single walled carbon nanotubes (SWCNT). Very low loadings of SWCNT into elastomeric polymers have been shown to result in improved modulus and tensile properties^[9]. Shanmugaraj *et al*^[10] reported an increase in modulus and tensile strength of cross-linked natural rubber reinforced with aminosilane functionalised multi-walled carbon nanotubes.

In this study, Attenuated Total Reflectance-Fourier Transform Infrared Spectroscopy- (ATR-FTIR), Differential scanning calorimetry (DSC), Thermogravimetric analysis (TGA) were used to characterise samples of MLC containing varying loadings of SWCNT. The MLC samples were tested for holes using a water leak and Electrical test. Optical light microscopy were used to elucidate the surface morphology of the samples. Hardness measurements was performed using a Shore A durometer. Stress Relaxation studies were performed on a dynamic mechanical analyser to elucidate the influence of SWCNT on the Relaxation modulus of the condom samples.

3.13: EXPERIMENTAL

3.13.1: Condom production and description.

The male latex condoms (MLC) were moulded as earlier described in SECTION C, and are as summarised in Table 3.5. The current experimental scope was limited to analysing single-films. Therefore, only MLC samples moulded via the single dip procedure was analysed in

this SECTION. The dimensions of the MLC were determined according to the procedures earlier described in SECTION C. The average length, width and thickness were; $\sim 191.17 \pm 5.17 \text{ mm}$, $52.67 \pm 5.17 \text{ mm}$ and $0.063 \pm 0.005 \text{ mm}$, respectively.

Table 3.5: Description of condoms

Condom sample description	Loading of SWCNTs (Wt./%)
PvNRL	0
PvNB1	0.02
PvNB2	0.04
PvNB3	0.06
PvNB4	0.08

Where: PvNRL = Pre-vulcanised natural rubber latex; SWCNT = single walled carbon nanotubes; PvNB = PvNRL containing varying amounts of SWCNT

3.13.2: Fourier-transform infrared spectroscopy (FTIR)

The mid-infrared spectra (IR) of PvNRL and PvNB condoms were recorded using a BRUKER TENSOR II FTIR spectrophotometer (BRUKER, Billerica, MA. USA) equipped with a platinum Attenuated Total Reflectance (ATR) accessory. The spectrophotometer was operated between $3500 - 500 \text{ cm}^{-1}$ range; and was programmed to perform 100 scans at 1 cm^{-1} resolution on an OPUS data collection program. A background spectrum measurement was performed before analysing each sample. Afterwards, the sample was placed on the diamond crystal and held in place using the pressure arm of the ATR accessory.

3.13.3: Differential scanning calorimetry (DSC)

A Q200 differential scanning calorimeter fitted with a Refrigerated Cooling System (RCS 90) was used to perform this analysis (TA instruments, New Castle, USA). About 4.3 mg of the condom specimen was accurately weighed and sealed in a DSC aluminium standard pans. The specimen was cooled from ambient temperature down to -80°C at a cooling rate of $20^\circ\text{C}/\text{min}$, and held isothermal for 10 min. The glass transition (T_g) temperatures of the condom specimen were determined by heating the sample from -80°C to 0°C at a heating rate of $10^\circ\text{C}/\text{min}$ in a nitrogen atmosphere. ^[11]

3.13.4: Thermogravimetric analysis (TGA)

The effect of SWCNT on the thermal stability of the condoms produced was elucidated on a Q600 (TA instruments, New Castle, USA) simultaneous differential scanning calorimetric and thermogravimetric analyser (SDT). Platinum sample and reference pans were used for this experiment. About ~10 mg of the condom specimen was heated at a rate of $10\text{ }^{\circ}\text{C min}^{-1}$ from ambient temperature ($\sim 20^{\circ}\text{C}$) to $600\text{ }^{\circ}\text{C}$. This experiment was conducted under a nitrogen atmosphere at a gas flow rate of 100 mL min^{-1} . [11]

3.13.5: Testing for holes

The water leak and electrical assessment techniques were used to test for holes in condoms. The methods used are according to the specification in SABS^[4] SANS4074:2002/Cor.2:2008, and are as stated below:

3.13.5.1: Water Leak test

The water leakage test was performed by filling a condom mounted at its open ends with about $300 \pm 10\text{ mL}$ of water at $25\text{ }^{\circ}\text{C}$. The condom was then physically inspected to identify any leaks. Afterwards, the condom was sealed by twisting the area about 25 mm from the open end, by 2 revolutions. The close end of the sealed condom was secure on one hand and placed onto an absorbent paper. With the length of the condom parallel to the paper, the condom was gently rolled back and forth, whilst applying a gentle pressure with the fingers of the other hand. After about 5 revolutions, the paper was inspected for any sign of water marks as a result of leakage^[4]. This test was performed in a low humid environment to avoid condensation at the surface of the condom being inspected.

3.13.5.2: Electrical test

The set-up for electrical test was assembled according to the specifications outlined in SABS^[4] SANS4074:2002/Cor.2:2008. The condom was mounted on its open ends, and filled with about 200 mL electrolyte solution (10 g/L NaCl solution). It was then submerged into a glass trough filled with the same electrolyte solution maintain at $25\text{ }^{\circ}\text{C}$. A saturated calomel electrode was inserted into the condom, and a graphite electrode into the trough filled with electrolyte solution. A 10 V stabilized continuous voltage in series with a $10\text{ k}\Omega$ resistor was applied between the electrode in the condom and glass trough. Voltage was generated using a 30V XYTRON regulated DC power supply. The voltage at the resistor was recorded after $10 \pm 2\text{ s}$, using a digital multimeter.

In this current study, voltage readings were taken at two positions; (1) When just about $\frac{1}{2}$ of MLC length is immersed in the electrolyte solution and (B) when $\frac{3}{4}$ is immersed. This was done to map out the position of holes. The MLC is deemed to have failed if a voltage ≥ 50 mV is recorded; such MLC is subjected to a water-leak test to verify the position of the holes. The Electrical test set-up is as illustrated in Figure 3.1.1.7.

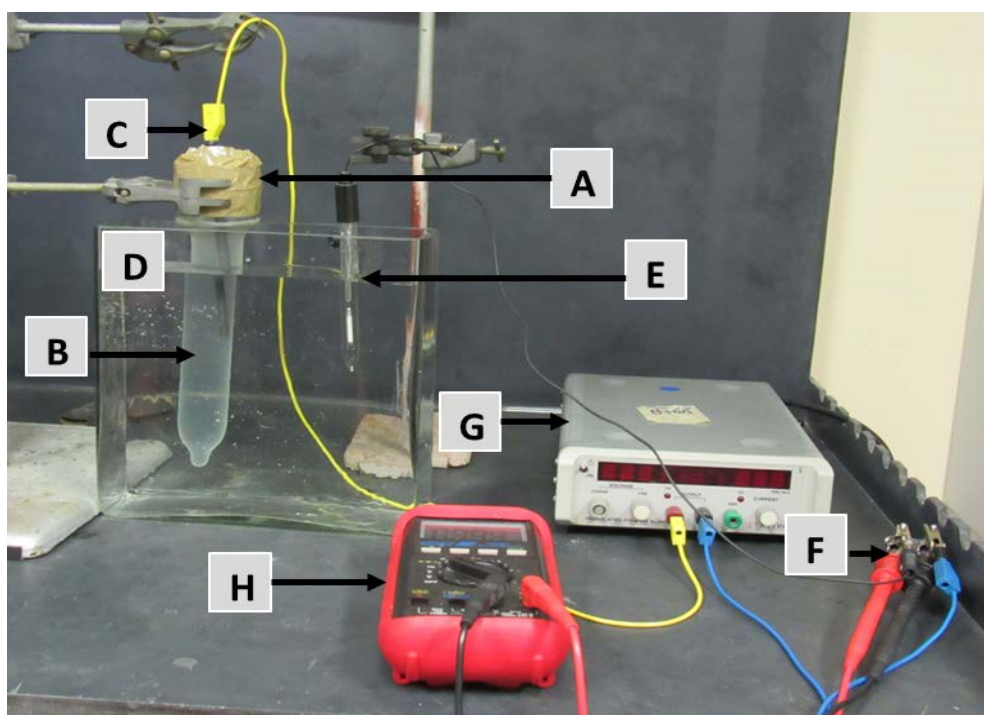


Figure 3.1.1.7: *Electrical conductivity set-up: (A) Condom support, (B) condom filled with electrolyte, (C) Electrode, (D) trough with electrolyte, (E) Electrode, (F) 10 kΩ resistor, (G) 10 V constant DC supply.*

3.13.5.2.1: Calibration of electrical test set-up

An internal method was developed in calibrating the electrical test set up. The principle of this technique infers that a condom without pinholes would act as an insulator and would not allow the flow of current; whereas the flow of current would suggest the presence of holes. Therefore, only condoms that passed the water leak test were analysed using this electrical test. An over the counter male latex condom (MLC) was used as the reference standard. The following operation(s) and considerations were conducted to elucidate the detection capabilities of the test set-up, and are summarised as follows:

- The maximum permissible voltage (MPV) of the electrolyte solution was measured before the condom was mounted. This was performed by determining the voltage after immersing both electrodes into the glass tough filled with electrolyte solution.

The measured voltage was approximately 5.56 ± 2 V; this was noted as the maximum permissible voltage of the electrolyte solution.

- The reference condom was mounted on the set-up and tested in accordance to the sequence earlier highlighted. (0.000 mV).
- A series of holes were then punctured on the reference condom using a syringe (~ 0.494 mm external diameter).
- The combination of position and number of holes were varied each time. The position of the hole was grouped into mid and low; indicating punctured positions on the condoms. The electrical tests were performed in triplicates for each combination. The measured voltages and uncertainty (\pm) are as summarised in Table 3.6.

Table 3.6: Calibration table.

Number of holes	Position of holes	Voltage reading (V)
0	-	0.000
1	mid	2.820 (\pm 0.063)
2	1 mid, 1 low	3.415 (\pm 0.013)
3	2 mid, 1 low	3.707 (\pm 0.056)
4	2 mid, 2 low	3.931 (\pm 0.017)
3	3 mid	2.965 (\pm 0.016)
3	3 low	4.910 (\pm 0.063)

From the voltage results stated in Table 3.6, it is observed that the measured voltage differed with the various combinations. However, none of the measured voltages exceeded the MPV of the electrolyte solution (earlier determined as 5.56 ± 2 V). The possible reasons behind the observed differences between the combinations are postulated as follows; (1.) position of the holes and (2.) concentration gradient due to the sedimentation of the dissolved NaCl. However, the electrolyte solution was stirred regularly to decrease the likelihood of the build-up of concentration gradient.

Again, it is pertinent to point out that SWCNT are known to increase the electrical conductivity of polymeric materials at a certain percolation threshold^[9]. This threshold is thought to occur when adequate network of SWCNT is formed within the polymer matrix. Since the MLC analysed in this study contains SWCNT, it is therefore proposed that voltage measurements that exceeds the MPV would be due to the contributions from the SWCNT.

3.13.6: Optical microscopy

The surfaces of the MLC samples was examined under a Leica S6D light microscope (Leica Microsystems, Germany). The MLC films were placed on a glass slide prior examination. Images were captured using a 3.1 Megapixel Leica EC3 colour camera (Leica Microsystems, Germany) at 6.5× magnification, under normal light condition. A colour contrast was performed before the images were taken.

3.13.7: Hardness test

Sample preparation involved obtaining a number of square specimens ($\sim 35 \times 35 \text{ mm}$) from each batch of the condom samples. The square specimens were carefully stacked on each other in such a way to avoid the trapping of air, until a thickness of $\sim 6 \text{ mm}$ was attained. Thickness was confirmed using a digital Vernier caliper (ULTRA CAL VI, Fowler High precision, Massachusetts, USA) with a resolution of 0.01 mm .

The measurements were performed according to SANS 7619-1:2009^[12] using a model HD3000 Shore A dial durometer (Hildebrand, Germany). The HD3000 features a spherical presser foot (18 mm in diameter) and a truncated indenter cone. Hardness measurements were performed by holding the durometer vertically above the specimen, then carefully lowered until the entire presser foot made full contact with the specimen. The dial reading was taken after 1 s to minimise creep contributions^[13]. All measurements were performed at ambient temperature condition and in triplicates.

3.13.8: Stress relaxation analysis

3.13.8.1: Sampling

Test specimens required for this experiment were collected from the mid-region of the MLC; the mid-region (**B**) is defined as the area $25 \pm 5 \text{ mm}$ away from the open end (**A**) and $25 \pm 5 \text{ mm}$ away from the closed tip (**C**) of the MLC (see Figure 3.1.1.8). For stress relaxation studies, rectangular shaped test pieces were carefully cut along the circumferential direction of the MLC, using a parallel blade cutter ($\sim 8.5 \text{ mm}$ apart).

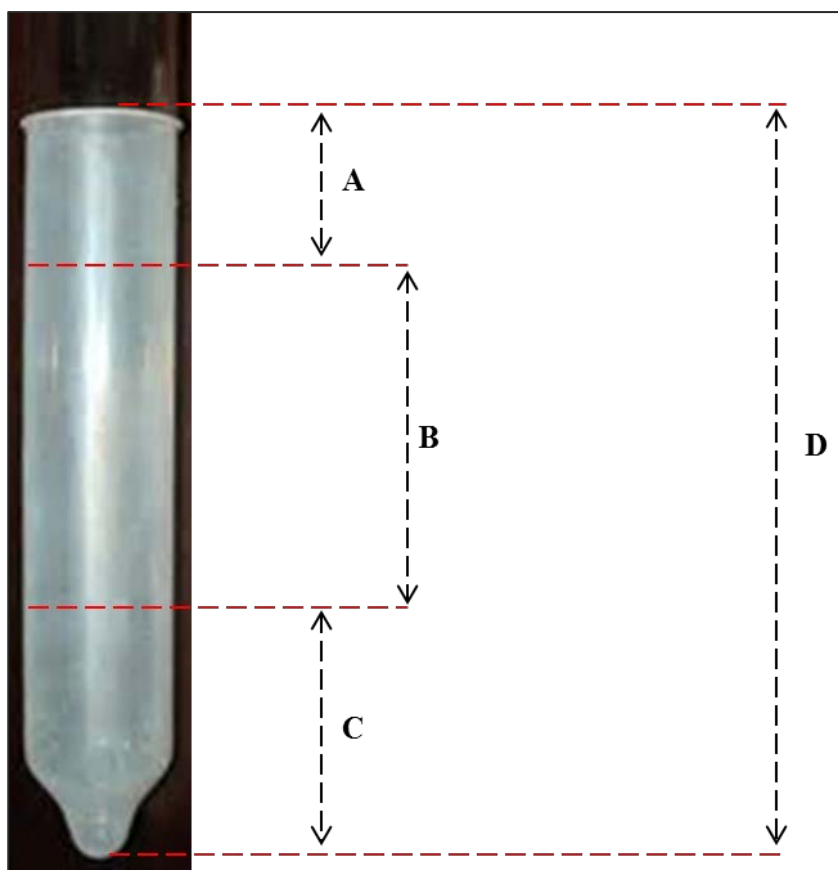


Figure 3.1.1.8: *Condom sampling description: (A) the area 25 ± 5 mm away from the open end, (B) mid-region, (C) the area 25 ± 5 mm away from the closed tip, (D) overall condom length $\sim 191.2 \pm 5.2$ mm.*

3.13.8.1: Test method

A Q800 (TA instruments, New Castle, USA) Dynamic Mechanical Analyser (DMA) fitted with a film tension clamp was used to study stress relaxation of the rectangular MLC test specimens. Stress relaxation was monitored at 0.02 N preload force and 25 % step strain. The strain was applied along the circumferential direction of the test MLC specimen. The tests were conducted at 37 °C and ambient humidity^[7]. The choice of temperature was based on the average internal temperature of humans^[14]. All tests were performed in triplicates.

3.14: RESULTS AND DISCUSSION

3.14.1: ATR-FTIR analysis of PvNRL and Pv-NB condoms

The ATR-FTIR spectra of PvNRL and the various Pv-NB condoms are as represented in Figure 3.1.1.9. It is apparent that the SWCNT loading had very little effect on the FTIR spectra of PvNRL. The spectra obtained are characteristic of the crosslinked cis-1,4-polyisoprene

rubber chains^{[15][16]}. Consequently, the transmittance peaks are assigned as follows; axial stretching of –C-H bond and –CH₃ groups at 2960.37 cm^{-1} .

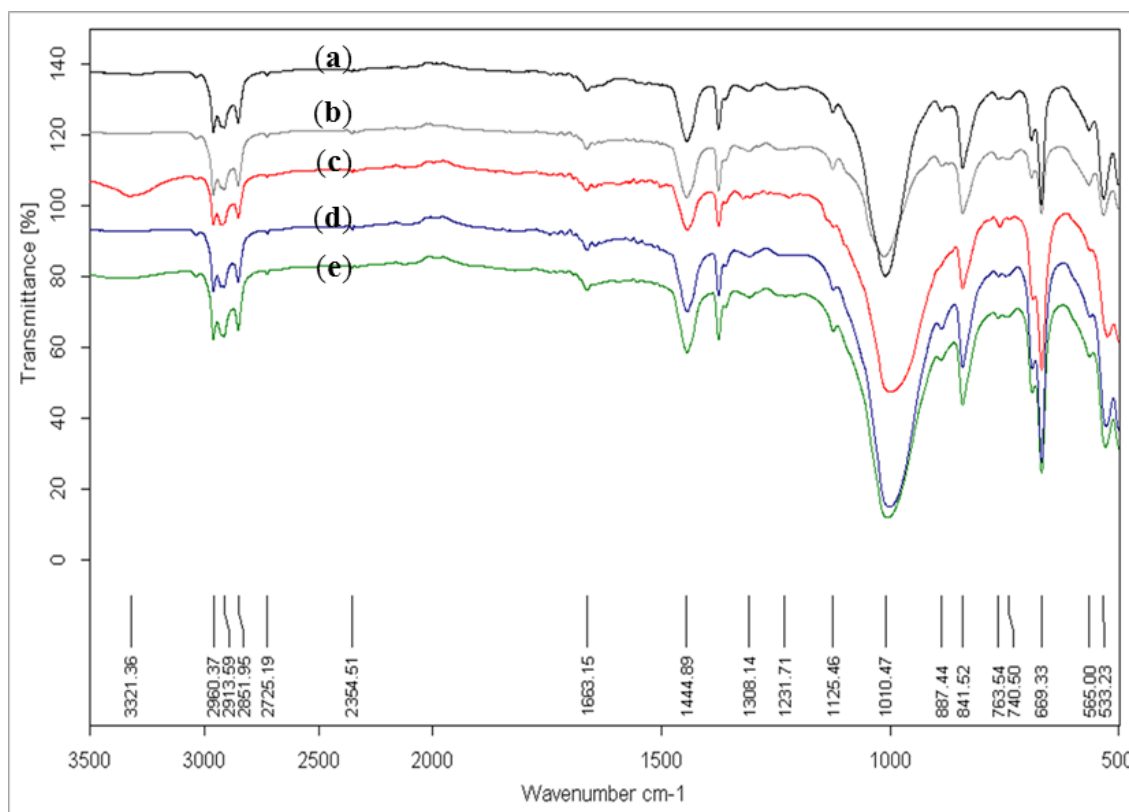
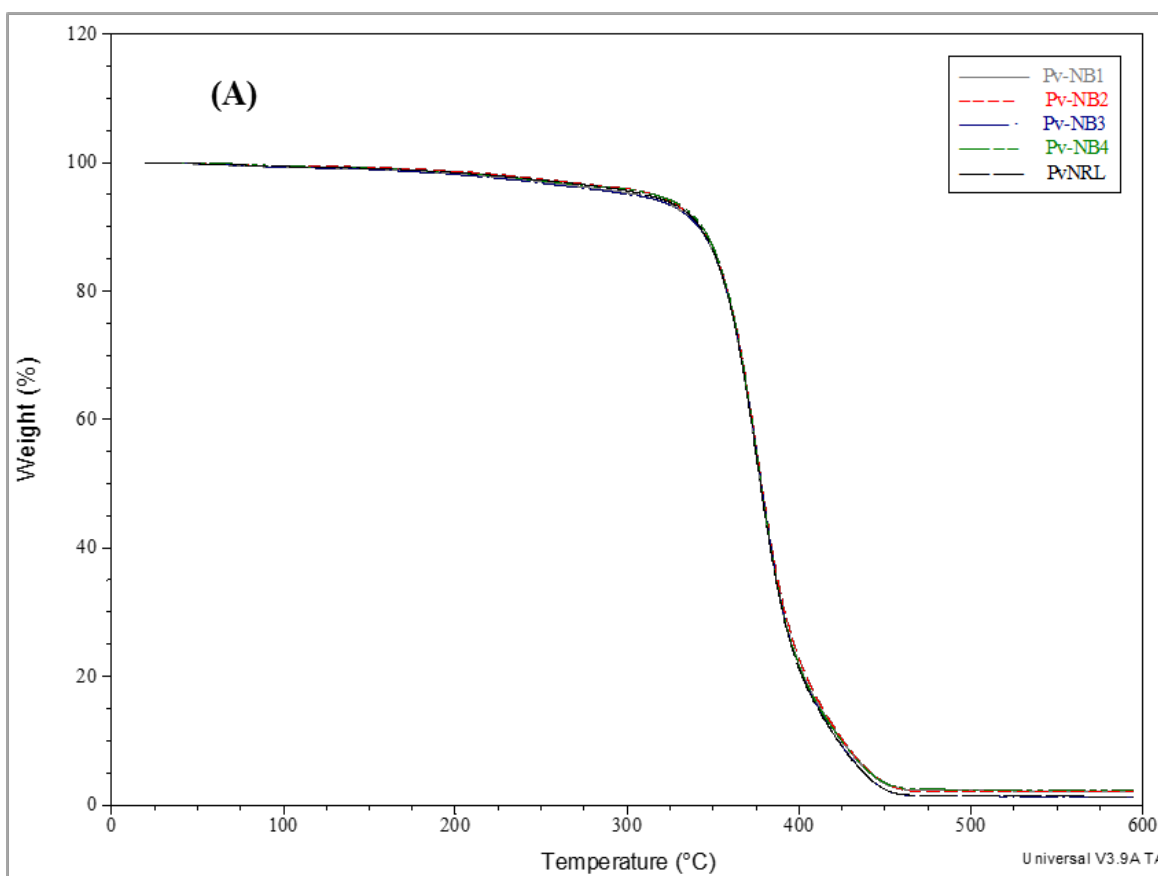


Figure 8.1.1.9: FTIR spectra of PvNRL and Pv-NB condoms: (a.) PvNRL condom, (b.) Pv-NB1 condom, (c.) Pv-NB2 condom, (d.) Pv-NB3 condom, and (e.) Pv-NB2 condom.

The peaks at 1444.89 cm^{-1} and 1374.24 cm^{-1} are assigned to symmetric and asymmetric deformation of –C-H bond and –CH₃ groups, respectively. The symmetric and asymmetric stretching of C-H bond and –CH₂ corresponds with the peak at 2913.59 cm^{-1} and 2851.95 cm^{-1} . The peak at 3321.36 cm^{-1} for sample (c.) is assigned to –O-H stretching vibrations, which suggests possible oxidation of the sample or could also be due adsorbed water molecules. The peak at 740.50 cm^{-1} is assigned to N-H vibration from the proteins present in latex. 887.44 cm^{-1} and 841.52 cm^{-1} are assigned to the –CH₃ wagging and =CH₂ out-of-plane bending respectively. The asymmetric and symmetric stretching vibrations of C-O-C are assigned to the peaks at 1231.71 cm^{-1} and 1040.47 cm^{-1} . The –C-S stretching vibration arising from the C-S crosslinks is assigned to the peak at 669.33 cm^{-1} .^{[15][16][17][18]}

3.14.2: Effect of SWCNT on thermal stability

The thermogravimetric (TGA) and derivative thermogravimetric (DTG) curves shown in Figure 3.1.1.1.1 (A and B) illustrates the thermal decomposition of PvNRL and Pv-NB condoms. The results show that there was no significant effect on the thermal degradation behaviour between the condoms with and without SWCNT. This agrees with reports from literature^[9]. The two DTG peaks (2 and 3) reveals a two staged decomposition of the rubber matrix. The first major decomposition of PvNRL at ~300°C onset temperature (marked as 1) is likely due to primary depolymerisation/condensation. The second stage decomposition at ~400°C onset temperature (marked as 4) results from the secondary evolution of condensed products.



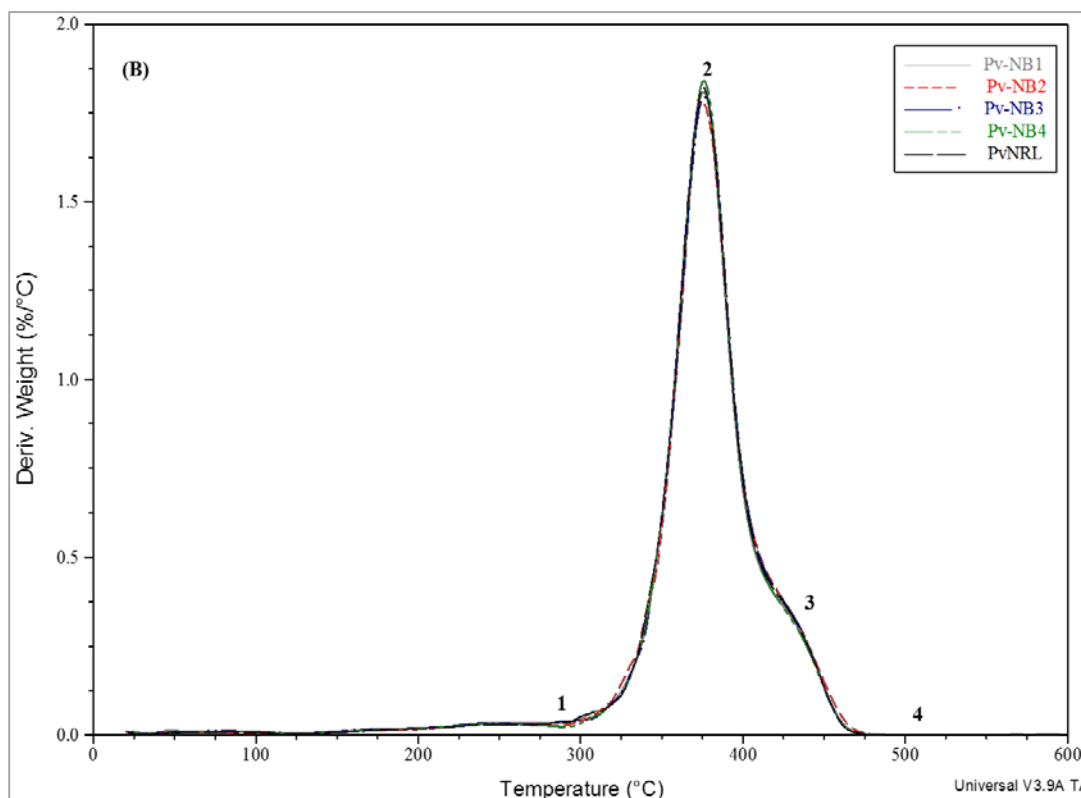


Figure 3.1.1.1.1: (A) TGA and (B) DTA plots of PvNRL and Pv-NB condoms: (1) onset temperature, (2) and (3) two staged decomposition of the rubber matrix, (4) complete decomposition

3.14.3: Effect of SWCNT on the calorimetric glass transition temperature (T_g)

The DSC technique monitors the change in heat flow during the phase transition of a material as a function of temperature and time. The overlay of the DSC thermograms of PvNRL and PvNB condoms shows a half-height glass transition temperatures (T_g) of about ~ -65.40 °C as illustrated in Figure 3.1.1.1.2. It is clear that T_g and heat capacity (ΔC_p) remained fairly the same within the range of SWCNT loadings. The addition of nanofillers such as SWCNT have been reported to have no effect on the T_g determined by static DSC method^{[19] [20]}. Some of the factors that can affect the T_g of a material includes; degree of crystallinity, molecular chain structure and chain arrangements^[20].

Chemically crosslinked elastomeric materials such as natural rubber exist above their glass transition (T_g) temperature. Nevertheless, they are known to undergo a T_g at very low temperatures (B region); below the T_g (A region), polymers become glassy and rigid due to restricted molecular movements, but becomes soft and rubbery above T_g (C region)^[21]. The

difference in the heat flow between regions **C** and **D** is attributed to the increasing molecular motions (Figure 3.1.1.1.2).

The change in T_g is marked by a change in heat capacity (Δc_p), the insert in Figure 3.1.1.1.2 shows only a minimal fluctuation in Δc_p . It is suggested that Δc_p represents the amount of polymer chain undergoing T_g ^[22]. The high Δc_p value below T_g is attributed to decrease in entropy, thus corresponds to fewer molecular motions within polymer chains. Consequently, an increase in entropy results in to the decrease in Δc_p . Calorimetrically measured T_g have been used to investigate the changes in molecular dynamics of polymer nanocomposites^[22].

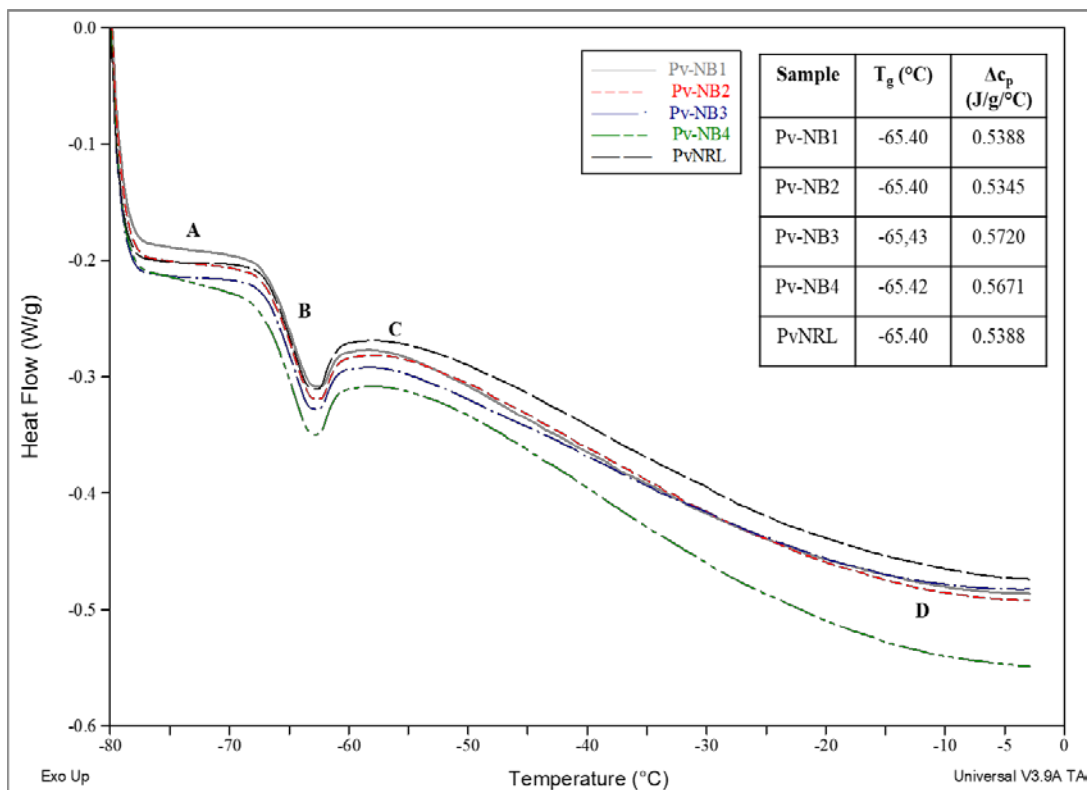


Figure 3.1.1.1.2: DSC Thermograms showing the glass transition of PvNRL and Pv-NB condoms: (A) rigid and glassy region, (B) glass transition region, (C) and (D) soft rubbery region.

It has been proposed that the restricted movements in a rubber chain of a nanocomposite material is likely to extend only within nanometres of the polymer-filler interphase^[23]. Fragiadakis *et al*^[22] reported a decrease in heat capacity of natural rubber upon addition of variable quantities of silica nanoparticles, which they attributed to immobilisation of polymer chains by nearby filler particles.

3.14.4: Surface morphology of MLC films

The images of PvNRL and Pv-NB condoms obtained from the optical microscope are as shown in Figure 3.1.1.1.3. Relatively smoother surfaces were observed for PvNRL, Pv-NB1 and Pv-NB2 condoms as compared to those of Pv-NB3 and Pv-NB4. This observation suggests that film formation could have been influenced by increasing loadings of the SWCNT. The process of latex film formation can be simplified to three distinct stages; (i.) initial linear loss of the aqueous phase, (ii.) deformation and coalescence of rubber particles and (iii.) particle-particle interdiffusion of rubber chains^[24].

The first two film formation stages are more likely to be influenced by a change in rate of evaporation and viscosity. Earlier results from drying and flow behaviour studies revealed that the drying rate and viscosity of PvNRL increased with higher loadings of SWCNT (see SECTION A and B). Hence, it is suggested that their combined effect could have contributed to increased surface undulation. Ho and Khew^[24] studied the film formation and surface morphology of natural rubber using atomic force microscopy and found that . Ruslimie *et al*^[25] reported increased surface roughness of epoxidised natural rubber films after protracted prevulcanisation time.

3.14.5: Effect of SWCNT on the occurrence of holes

The results obtained from the analysis of holes from the water leak and electrical tests are as represented in Table 3.7. It is apparent that although water leak tests could not visibly detect the presence of holes, the electric test on the other hand confirmed the presence of holes in all the condoms tested. It is seeming that the nature of the holes present in the MLC were sufficient to allow the migration of the Ionic species (Na^+Cl^-) present in the electrolyte solution. This suggests that visible analysis of holes alone is not efficient enough and should always be augmented with Electrical test.

Although PvNRL condoms always showed the least voltage reading, there are no obvious correlation in the results obtained that suggests that the presence of SWCNT contributed to the increase in voltage. There are several factors that could contribute to the formation of holes in MLC, some of which include; production technique, presence of air bubbles in the latex compound, irregular deposition of latex on the mould, and contamination of condom moulds by dust and/or hard water^[26]. Nevertheless, several standard organizations and manufacturers have instituted stringent conditions a bid to limit the presence of holes. For

instance, most condom manufactures employ the double or multi-dipping technique; thus ensuring that the initial holes are covered by successive layers of latex. [26] [27]

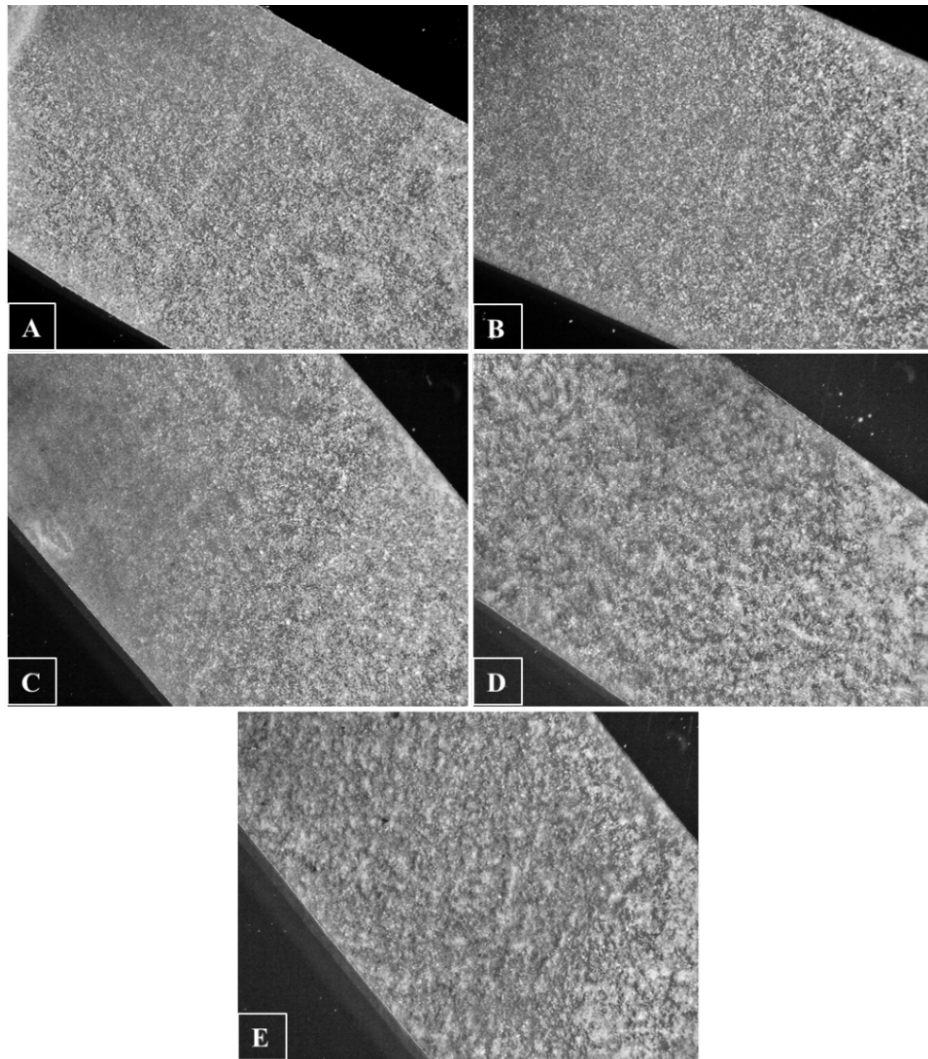


Figure 3.1.1.1.3: *Optical micrographs of condoms specimens at 6.5× magnification; (A) PvNRL condom, (B) PvNB1 condom, (C) PvNB2 condom, (D) PvNB3 condom, and (E) PvNB4 condom.*

Table 3.7: Table showing results of the water leak and electric tests

Sample description	Water leak test (6 samples)	Electrical test	
		½ immersion	¾ immersion
PvNRL	passed	2 of 6 passed	6 of 6 failed ^a
Pv-NB1	passed	1 of 6 passed	6 of 6 failed ^b

Table 3.7 *Continued.*

Pv-NB2	passed	6 of 6 failed	6 of 6 failed ^c
Pv-NB3	passed	6 of 6 failed	6 of 6 failed ^d
Pv-NB4	passed	6 of 6 failed	6 of 6 failed ^e

Average voltage measured: ^a = 2.3 ± 2.8 V, ^b = 3.7 ± 4.6 V, ^c = 4.2 ± 4.6 V, ^d = 4.2 ± 5.2 V, ^e = 3.9 ± 3.6 V.

3.14.6: Effect of SWCNT on Shore A hardness.

The results from Shore A or indentation hardness test revealed that the SWCNT had no visible effect on the hardness of the condoms (Table 3.8). The scale of shore hardness is reported as 0 – 100, the minimum value represent completely soft materials and the maximum for completely hard ones^[28]. The information obtained from this particular Shore hardness analysis serve only for comparison between the samples. This is because the analysis was performed on stacked specimens and not on a single film.

Table 3.8: Result from Shore A hardness analysis

Condom sample description	Shore A hardness (\pm @95% CI)
PvNRL	18.0 (0.72)
PvNB1	18.2 (0.84)
PvNB2	18.0 (0.72)
PvNB3	18.1 (0.82)
PvNB4	18.1 (0.92)

Nonetheless, the stacking of the specimen was necessary, as studies have shown that Shore hardness of samples with thickness smaller than 6 mm would give erroneous results. Siddiqui et al^[13] developed a theoretical treatment that reasonably predicted the dependence between Shore hardness and sample thickness of elastomers. Additionally, the Shore hardness of elastomers have been reported to have a direct relationship with its Young's modulus (E) and shear (rigidity) modulus^[13]. Gent^[29] studied this relationship and established a semi-empirical equation of obtaining relatively accurate values. Meththanani et al^[28] suggested a

satisfactory relationship between Shore hardness and Young's modulus, on the condition of minimal viscoelastic creep during the analysis.

3.14.7: Stress relaxation analysis of PvNRL and Pv-NB condoms

The results from stress relaxation analysis of PvNRL and Pv-NB condom specimens are expressed as relaxation modulus versus time, as illustrated in Figure 3.1.1.1.4. The plots reveal a general trend in the relaxation modulus under fixed strain/deformation; initially, a maximum relaxation modulus is attained, followed by the rapid decay in the relaxation modulus within the first ~5 min. This decay trend slows down after ~10 min, and a minimum relaxation modulus is attained at ~30 min (Figure 3.1.1.1.4).

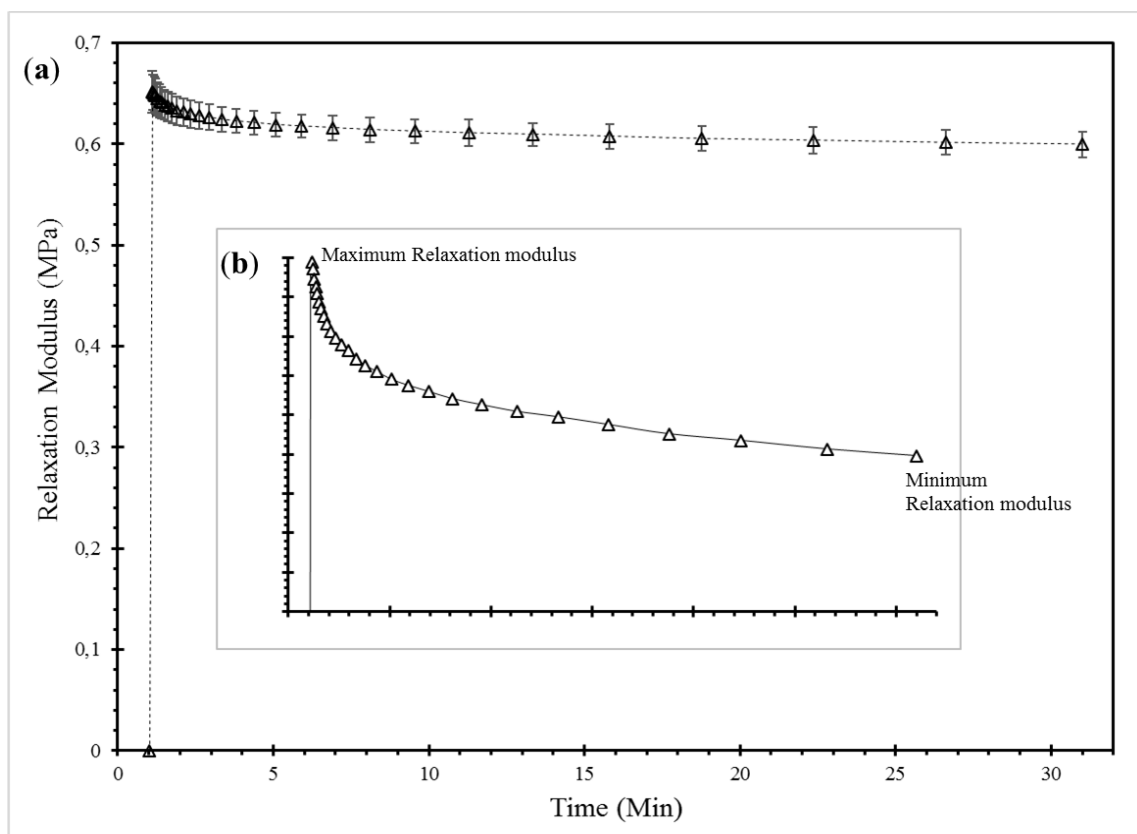


Figure 3.1.1.1.4: (a) Stress Relaxation behaviour of PvNRL condoms over 30 minutes of constant 25% strain, with error bars; (b) plot truncated in the y-axis to show min and max relaxation modulus.

This behavioural trend under constant strain conditions reveals a characteristic behaviour of amorphous elastomeric materials. The initial alignment of the elastomers molecular chains in the direction of the applied strain results in a sudden increase in material elastic modulus. The upsurge in internal stress is due to the pseudo-crystallization of the otherwise

amorphous molecular chains. Conversely, the incidence of an almost rapid entropic molecular chain rearrangement leads to the decrease in internal stress and elastic modulus.^[1] The desire to develop thinner, desirable and effective MLC can be achieved if the significant reduction in modulus associated with decrease in thickness of latex MLCs is addressed. The curves illustrated in Figure 3.1.1.1.5 shows slower decay in relaxation modulus, corresponding to the MLCs containing $\geq 0.04\%$ SWCNT. This is despite the fact that all the samples exhibited similar initial Maximum relaxation modulus. The progressive reduction in the decay of relaxation modulus at 25% strain follows the order; Pv-NB4 > Pv-NB3 > Pv-NB2.

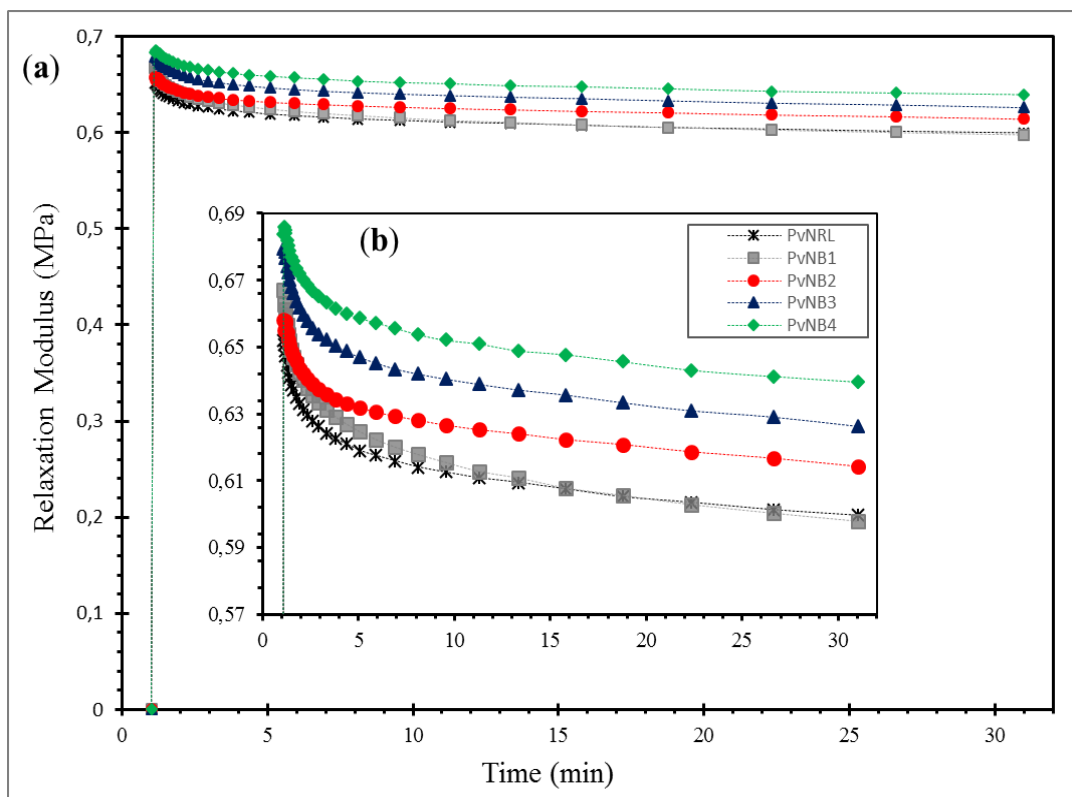


Figure 3.1.1.1.5: (a) An overlay of the stress relaxation analysis of PvNRL and Pv-NB condoms; (b) insert shows a truncated y-axis of the plot.

Table 3.9 shows the resultant change in relaxation modulus at different time periods. The PvNRL and Pv-NB1 MLC specimens both showed similarly decay in modulus. It is suggested that the presence of SWCNTs most probably is responsible for the above mentioned observation. Studies have shown that the alignment of nano fibres in the direction of the applied strain could contribute to better reinforcement^[30]. The reorientation of nanotubes have been studied using polarized Raman spectroscopy^{[31] [32] [33]}. However, the

modification of physical dynamics could also be due to the change in crystallinity, molecular weight and degree of crosslinking that occur in the presence of SWCNT^[22]. Frogley, Ravich and Wagner^[30] suggested that the strain induced reorientation of nanotubes could be responsible for the increase in modulus.

The challenge associated with the decrease in seal pressure of MLCs due to the reduction in the internal (tensile) stress that can be directly related to the significant decay in the materials modulus. Conversely, excessive modulus is counter intuitive as it would likely lead to discomfort associated with excessive pressure on the erect penis^[34]. However, the specification of minimum or maximum pressure required to maintain a secured seal and comfort is yet to be established. Sakar Das *et al* studied the stress relaxation of condoms in the presence of a variety of lubricants. The report revealed an increase in the rate of relaxation during the swelling process.

Table 3.9: Results from Stress Relaxation analysis of PvNRL and Pv-NB condoms under a 25% constant strain.

Sample description	SWCNT loading (Wt.%)	Relaxation Modulus [MPa (\pm)]			
		Max.	@ 5min	@ 15min	Min
PvNRL	0	0.6518 (0.021)	0.6190 (0.011)	0.6075 (0.012)	0.5996 (0.013)
Pv-NB1	0.02	0.6670 (0.019)	0.6247 (0.032)	0.6079 (0.033)	0.5979 (0.031)
Pv-NB2	0.04	0.6580 (0.015)	0.6319 (0.017)	0.6224 (0.018)	0.6144 (0.019)
Pv-NB3	0.06	0.6795 (0.050)	0.6469 (0.043)	0.6357 (0.038)	0.6263 (0.036)
Pv-NB4	0.08	0.6837 (0.105)	0.6587 (0.088)	0.6478 (0.080)	0.6386 (0.077)

\pm uncertainty at 95% confidence interval

3.15: SUMMARY OF OBSERVATIONS

- The peaks obtained from ATR-FTIR analysis were characteristics of crosslinked cis-1,4-polyisoprene rubber chains. There was no significant impact of SWCNT on the FTIR activity.
- DSC experiments revealed a single step glass transition temperature for all the condoms samples.
- There was significant change between the thermal stability of the PvNRL and those of Pv-NB condoms.
- Optical light microscopy revealed an increase in surface roughness for Pv-NB3 and Pv-NB4 condoms.
- Majority of the condom samples that passed the visual test for water leakage were found to register voltage readings far above the pass/fail criteria of Electrical test for holes.
- Results from Shore A hardness revealed no significant difference between the indentation hardness of the PvNRL Pv-NB condoms.
- The observation from Stress relaxation studies suggest a steady increase in the modulus of the condoms containing higher loadings of SWCNT.

REFERENCES

- [1] J. P. Gerofi and P. M. Wong, "Fatigue testing of condoms," *Polymer Testing*, vol. 28, pp. 567-571, 2009.
- [2] S. Linde, "Inspection and control of contraceptives at Apotekens centrallaboratorium," *Sartryck ur Svensk Farmaceutisk Tidskrift*, vol. 77, pp. 588-594, 1973.
- [3] BS 3704., "British Standard Specification for Rubber Condoms," ed: British Standard Institute, 1964.
- [4] SANS 4074:2003., "Natural latex rubber condoms," in *Requirements and test methods*, ed. 1 Pretoria: SABS Standard Division, 2008.
- [5] J. Torres., H. Anabitarte., R. Usieto., and E. Noguera., "RQTS, quality standard of condoms based on a rheological model,," *International Conference on AIDS*, vol. 5, p. 1042, 1989.

- [6] R. Harding and S. E. Golombok, "Test-retest reliability of the measurement of penile dimensions in a sample of gay men," *Archives of sexual behavior*, vol. 31, pp. 351-357, 2002.
- [7] S. S. Das, J. C. Coburn, C. Tack, M. R. Schwerin, and D. C. Richardson, "Exposure of natural rubber to personal lubricants—swelling and stress relaxation as potential indicators of reduced seal integrity of non-lubricated male condoms," *Contraception*, vol. 90, pp. 86-93, 2014.
- [8] M. Gabbay and A. Gibbs, "Does additional lubrication reduce condom failure?," *Contraception*, vol. 53, pp. 155-158, 1996.
- [9] A. Anand K, S. Jose T, R. Alex, and R. Joseph, "Natural rubber-carbon nanotube composites through latex compounding," *International Journal of Polymeric Materials*, vol. 59, pp. 33-44, 2009.
- [10] A. Shanmugharaj, J. Bae, K. Y. Lee, W. H. Noh, S. H. Lee, and S. H. Ryu, "Physical and chemical characteristics of multiwalled carbon nanotubes functionalized with aminosilane and its influence on the properties of natural rubber composites," *Composites Science and technology*, vol. 67, pp. 1813-1822, 2007.
- [11] Stuart von Berg., "The characterization of and formulation development using novel tyre devulcanizate," *Magister Scientiae*, Chemistry department, Nelson Mandela Metropolitan University, Port Elizabeth, 2016.
- [12] SANS 7619-1:2009., "Rubber, vulcanized or thermoplastic - Determination of Indentation hardness," in *Part1: Durometer method (Shore hardness)*, ed. 1 Pretoria: SABS Standard Division, 2009.
- [13] A. Siddiqui, M. Braden, M. P. Patel, and S. Parker, "An experimental and theoretical study of the effect of sample thickness on the Shore hardness of elastomers," *dental materials*, vol. 26, pp. 560-564, 2010.
- [14] D. Fiala, K. J. Lomas, and M. Stohrer, "Computer prediction of human thermoregulatory and temperature responses to a wide range of environmental conditions," *International Journal of Biometeorology*, vol. 45, pp. 143-159, September 01 2001.

- [15] P. Devi, "Low temperature prevulcanisation of natural rubber latex using Kiact/ZDC accelerator systems," Doctor of Philosophy, Chemistry Department, Mahatma Gandhi University, 2013.
- [16] P. Nallasamy and S. Mohan, Vibrational Spectra of Cis-1, 4-Polyisoprene vol. 29, 2004.
- [17] E. Abraham, B. Deepa, L. Pothan, M. John, S. Narine, S. Thomas, et al., "Physicomechanical properties of nanocomposites based on cellulose nanofibre and natural rubber latex," Cellulose, vol. 20, pp. 417-427, 2013.
- [18] M. A. Da Silva, M. G. A. Vieira, A. C. G. Maçumoto, and M. M. Beppu, "Polyvinylchloride (PVC) and natural rubber films plasticized with a natural polymeric plasticizer obtained through polyesterification of rice fatty acid," Polymer Testing, vol. 30, pp. 478-484, 2011.
- [19] P. S. Thomas, A. A. Abdullateef, M. A. Al-Harhi, A. Basfar, S. Bandyopadhyay, M. A. Atieh, et al., "Effect of phenol functionalization of carbon nanotubes on properties of natural rubber nanocomposites," Journal of Applied Polymer Science, vol. 124, pp. 2370-2376, 2012.
- [20] K. Subramaniam, A. Das, D. Steinhauser, M. Klüppel, and G. Heinrich, "Effect of ionic liquid on dielectric, mechanical and dynamic mechanical properties of multi-walled carbon nanotubes/polychloroprene rubber composites," European Polymer Journal, vol. 47, pp. 2234-2243, 2011.
- [21] L. Sperling, "Introduction to Polymer Science," Introduction to Physical Polymer Science, Fourth Edition, pp. 1-28, 2005.
- [22] D. Fragiadakis, L. Bokobza, and P. Pissis, "Dynamics near the filler surface in natural rubber-silica nanocomposites," Polymer, vol. 52, pp. 3175-3182, 2011.
- [23] A. Sargsyan, A. Tonoyan, S. Davtyan, and C. Schick, "The amount of immobilized polymer in PMMA SiO₂ nanocomposites determined from calorimetric data," European Polymer Journal, vol. 43, pp. 3113-3127, 2007.
- [24] C. Ho and M. Khew, "Low glass transition temperature (T_g) rubber latex film formation studied by atomic force microscopy," Langmuir, vol. 16, pp. 2436-2449, 2000.

- [25] C. Ruslimie, M. Norhanifah, M. Fatimah Rubaizah, and M. Asrul, "Effect of Prevulcanisation Time on the Latex Particles, Surface Morphology and Strength of Epoxidised Natural Rubber Films," 2015.
- [26] K. O. Calvert, *Polymer Latices and Their Applications*. Essex, England.: APPLIED SCIENCE PUBLISHERS LTD, 1982.
- [27] NOCIL LIMITED., "Technical Note : NR-Latex & Latex Products," pp. 1-56, 2010.
- [28] I. M. Meththananda, S. Parker, M. P. Patel, and M. Braden, "The relationship between Shore hardness of elastomeric dental materials and Young's modulus," *Dental materials*, vol. 25, pp. 956-959, 2009.
- [29] A. N. Gent, "On the relation between indentation hardness and Young's modulus," *Rubber Chemistry and Technology*, vol. 31, pp. 896-906, 1958.
- [30] M. D. Frogley, D. Ravich, and H. D. Wagner, "Mechanical properties of carbon nanoparticle-reinforced elastomers," *Composites Science and technology*, vol. 63, pp. 1647-1654, 2003.
- [31] H. Gommans, J. Alldredge, H. Tashiro, J. Park, J. Magnuson, and A. Rinzler, "Fibers of aligned single-walled carbon nanotubes: Polarized Raman spectroscopy," *Journal of Applied Physics*, vol. 88, pp. 2509-2514, 2000.
- [32] R. F. Landel and L. E. Nielsen, *Mechanical properties of polymers and composites*: Crc Press, 1993.
- [33] R. Saito, T. Takeya, T. Kimura, G. Dresselhaus, and M. Dresselhaus, "Raman intensity of single-wall carbon nanotubes," *Physical Review B*, vol. 57, p. 4145, 1998.
- [34] J. Gerofi, F. Deniaud, and P. Friel, "Interaction of condom design and user techniques and condom acceptability," *Contraception*, vol. 52, pp. 223-228, 1995.

CHAPTER FOUR

OVERALL SUMMARY AND RECOMMENDED FUTURE WORK

The study investigated the potential use of single-walled carbon nanotubes (SWCNT) as reinforcing filler for male natural rubber latex (NRL) condom. Therefore, four objectives as represented in the various sections of CHAPTER 3 were successfully deployed, they include; the physio-chemical analysis of SWCNT/NRL blends, the study flow behaviour of each blend, condom production and physio-mechanical analysis of condoms. This section contains a brief summary of the outcomes of each research objective and also recommendations for future work.

SECTION A:

The activities in this section were aimed towards characterizing the pre-vulcanised natural rubber latex (PvNRL) and the single walled carbon nanotube (SWCNT) suspension. Results from the various analysis are summarised as follows;

- UV-vis and FTIR spectroscopic techniques were successfully used to analyse the SWCNT suspension. UV-vis result revealed activity signals characteristic to additional absorption owing to 1D Van Hove singularities. This observation does suggest the presence of dispersed SWCNT. This was based on literature, as several reports showed that bundled SWCNT are highly inactive within that UV-vis range.
- Although the comparative FTIR analysis confirmed the presence of the surfactant (NaCMC) molecules. However, their intensity of was observed to be repressed in the presence of SWCNT. Conversely, no distinct transmittance peak could be attributed to the SWCNT, although a seemingly suppressed –CO₂ stretch vibration was identified, thus suggesting the presence of surface defects.
- The composition of the PvNRL was successfully characterised and reported in terms of dry rubber content (DRC) and total solid contents (TSC). Results showed an average DRC and TSC of about ~58.79% and ~60.42% respectively. Subsequently, blends of PvNRL and SWCNT suspension were successfully prepared; the varying loadings of SWCNT were loaded on the basis of *Wt. %* DRC.
- The drying rate of PvNRL/SWCNT composite blends were studied using Thermogravimetric analysis; results revealed that drying rate increased with higher loadings of SWCNT suspension. Equilibrium swelling analysis suggest an increase in crosslink density for films containing higher loadings of SWCNT.

SECTION B:

The flow behaviour of the blends of PvNRL/SWCNT were studied using rotational viscometry. Results from the various analysis are summarised as follows;

- The analysis was performed under variable shear rates (at 3 isothermal temperatures (25, 30 and 35° C)); the choice of shear rate range and temperature was based on the probable conditions reached during storage, handling and processing. The results from this analysis revealed a non-Newtonian Flow behaviour; as the PvNRL and the respective nanocomposite blends all exhibited time-independent shear thinning.

- Furthermore, an increase in the apparent viscosity of PvNRL/SWCNT blend was observed, especially for the blends containing 0.04, 0.06 and 0.08 wt. % SWCNT loadings. This increase was attributed to a number of reasons, two of the most likely includes; (i.) increased associative interactions between the surfactant stabilised SWCNT and the colloidal components of PvNRL, (ii.) Electroviscous effect arising from the adsorption of the polyelectrolyte surfactant (NaCMC) onto the rubber particles.
- However, the 0.02 wt. % loading resulted to an observable decrease viscosity of PvNRL. This suggests the 0.02 wt. % loading was perhaps not sufficient to effect an increase viscosity; thus hinting a possible viscosity-percolation threshold. The reduced viscosity suggest a dilution effect; likely to be as a result of the increase in free volume of PvNRL.
- Results from low shear rate ($0.1 - 10 \text{ s}^{-1}$) analysis exhibited an onset transition from non-Newtonian to Newtonian flow behaviour forPvNB3; this observation was more pronounced for low shear-rate analysis of PvNB4 blends.
- The power law model was successfully fitted to the acquired experimental results between $1 - 10 \text{ s}^{-1}$ shear rate ranges. Interestingly, the results from the calculated values of consistency index (n), it is apparent that the thickness of PvNRL increases with increasing loading of SWCNT. In contrast, the values of the power index (n) suggests an increase in shear thinning.

SECTION C:

The section was dedicated towards execution of condom production from PvNRL and PvNRL/SWCNT blends. The steps towards condom production are summarised as follows;

- An in-house dilution method developed was successfully utilised towards preparing the latex samples for moulding. The viscosity of a latex compound is known to affect film forming ability, Hence It was necessary to perform some controlled dilutions to correct the viscosity differences.
- The condoms were moulded via the straight dipping method, using custom made glass moulds (formers) and production mechanism. Two sets of condoms were prepared; the first involved a single-dip operation aimed achieving a single coating of latex, and the second involved a double-dip. The post production steps executed

included; beading, curing, leaching and dry stripping. Due to the tacky nature of cured rubber films, Talc was generously applied to serve as anti-tack before stripping the condoms from the glass moulds.

- The incorporation of SWCNT resulted in a visible discolouration of the condoms. The colours ranged from; pale-Yellow for PvNRL to dark-Grey for Pv-NB condoms. Length and width measurements were according to methods stipulated in SANS4071. The average length and width of condoms produced was found to be $\sim 191.17 \pm 5.17 \text{ mm}$ and $52.67 \pm 5.17 \text{ mm}$ respectively.
- Finally, to determine the thickness, 3 methods were adopted, which included: (1) micrometre method (**MMSG**), (2) Vernier caliper method (**VCp**) and (3) Thickness formula method (**Fmlr**). Analysis of variance (ANOVA) of the results of these 3 methods suggested a significant statistical difference between the mean variance of the results obtained by the 3 methods (ANOVA, $P < 0.003136$). A series of t-test revealed that the differences in the thickness determination methods; VCp – Fmlr (t-test, $p = 0.08636$) and MMSG – VCp (t-test, $p = 0.1236$) could be explained by experimental errors.

SECTION D:

In this section, condoms produced by means of the single-dip process were characterized using FTIR and thermal analysis techniques. The condoms were tested for holes and their surface morphology was captured using an optical light microscope. Hardness was elucidated using a Shore A durometer. Finally stress relaxation analysis was performed on a DMA. Results from the various analysis are summarised as follows;

- FTIR analysis established that the incorporation of SWCNT showed no significant influence on the overall chemical structure of the condom films. Additionally, the FTIR spectrum could not confirm any chemical interaction between the SWCNT and the crosslinked rubber. Hence, it is proposed that physical interactions were predominantly established.
- Thermal analyses experiments on all condom samples revealed a single step glass transition temperature and no significant change between the thermal stability of the PvNRL and those of Pv-NB condoms. This means that the overall quantity of the nano-materials in latex samples is very low and does not affect the homogeneity and

thermal stability of samples. Similarly, hardness experiments revealed no significant difference between the indentation hardness of the PvNRL and Pv-NB condoms.

- Majority of the condom samples that passed the visual test for water leakage were found to register voltage readings far above the pass/fail criteria of Electrical test for holes. This suggested that a visual leakage test alone is not sufficient enough in the detection of pinholes for single-dip condoms. Additionally, there was no concrete evidence that suggested the presence of SWCNT influenced voltage measurements during the electrical test.
- Optical light microscopy revealed an increased in surface roughness for Pv-NB3 and Pv-NB4 condoms. This is in-line with stress relaxation findings which showed a steady increase in the modulus of the condoms containing higher loadings of SWCNT.

It is therefore proposed that, the increase in surface roughness could be a consequence of increased drying rate (see SECTION A); faster evaporation of water from the rubber latex is anticipated to encourage irregular coalescence of rubber particles. This ultimately could have either promoted the nature of the physical interaction between the rubber chains and the SWCNT or resulted in a change in crystallinity or degree of crosslinking (as was observed during crosslink density analysis in SECTION A).

RECOMMENDED FUTURE WORKS

A variety of materials and experimental techniques were utilised in this research. However, the following ideas which were deemed surplus for the current scope are recommended for future studies:

- The covalent functionalisation of singlewalled carbon nanotubes (SWCNT) prior to compounding is recommended; this would be in a bid to promote better interfacial interaction between the rubber chains and SWCNT.
- It is also pertinent to develop a nanosuspension that would impart minimal changes to the viscosity of latex. Hence in moving forward, it is required that SWCNT suspensions using different surfactants/stabilisers at varying loadings be prepared and investigated.

- Electron microscopic Imaging is recommended to better elucidate the morphology and the nature of interaction between SWCNT and natural rubber latex (NRL).
- Further mechanical analysis of the condoms using the O-ring tensile tester is recommended to complement the results obtained from DMA analysis. Also, solid state nuclear magnetic resonance spectroscopy (NMR) is recommended to support the results obtained from FTIR analysis.
- A comparisomal study using Post-vulcanised NRL as opposed to the prevulcanised NRL used in this current study is also recommended. However, this would involve an optimization of the NRL's compounding recipe.